Characterizing the roles of ADAM10 and 15 disintegrins in prostate biology and disease

by

Magdalena M. Grabowska

A dissertation submitted in partial fulfillment
of the requirements for the degree of
Doctor of Philosophy
(Cellular and Molecular Biology)
in The University of Michigan
2011

Doctoral Committee:

Professor Mark L. Day, Chair
Professor James T. Elder
Professor Robert S. Fuller
Professor Jill A. Macoska
Professor Benjamin L. Margolis

To my parents for their unending support

Acknowledgements

I would like to extend a tremendous thank you to my family and friends without whose support this doctoral process would not have been possible. I would also like to thank Derek for being a constant source of support in all aspects of my life. I would like to thank Mark for taking me on as a graduate student and my committee for their commitment to my training. Thank you to the faculty members and administrators of the Cellular and Molecular Biology and the Cancer Biology Programs for your willingness to help with training, letters, funding, and graduate student business as a whole. Finally, I would like to thank collaborators who have provided reagents, resources, expertise, and lab equipment without which my research would not have been possible. Thank you.

Table of Contents

List of Figures

List of Tables

Abstract

During the progression of prostate cancer, the adhesion molecule epithelial (E)-cadherin can be lost from the cell surface by ADAM15 proteolytic processing, generating an extracellular 80kDa fragment referred to as soluble E-cadherin (sE-cad). Contrary to observations in cancer, the generation of sE-cad appears to correlate with ADAM10 activity in benign prostatic epithelium. The ADAM10-specific inhibitors INCB008765 and proA10 inhibit sE-cad generation, downstream signaling, and cell proliferation. Addition of EGF or amphiregulin to benign prostatic hyperplasia cells (BPH-1) or immortalized prostate epithelial cells (PrEC) increases the amount of sE-cad shed into the conditioned media and bound to EGFR. EGF-associated shedding appears to be mediated by ADAM10 as shRNA knockdown of ADAM10 results in reduced sE-cad generation.

To examine the physiologic consequence of sE-cad on prostatic epithelium, we treated cells with a sE-cad analog (Fc-Ecad), which resulted in phosphorylation of EGFR, signaling through ERK, and cell proliferation. Pre-treating cells with cetuximab, a therapeutic antibody against EGFR, decreased the ability of Fc-Ecad to induce EGFR phosphorylation, downstream signaling and proliferation. These data demonstrate that ADAM10-generated sE-cad may have a role in EGFR signaling independent of traditional EGFR ligands.

In order to better characterize the role of ADAM10 in normal prostate biology, we generated prostate specific knockout mice utilizing probasin (Pb) driven Cre. Preliminary analysis of *Adam10* $^{loxP/loxP}$ *Pb-Cre* mice indicates an unexpected epithelial hyperplasia into the luminal space and areas of continued ADAM10 expression. However, cell lines generated from *Adam10* $^{loxP/loxP}$ *Pb-Cre* mouse prostates express no ADAM10.

Because of our interest in targeting ADAM15 in prostate cancer, we initiated studies investigating potential inhibitors and domain requirements for E-cadherin cleavage. In these preliminary studies, the EGF-like domain of ADAM15 appears to be critical for sE-cad generation. We have also observed that the ADAM10 inhibitor, INCB08765, can inhibit ADAM15 activity during *in vitro* and CD23 peptide cleavage assays. Furthermore, ADAM15 and ADAM10 co-immunoprecipitate as a catalytically active unit. These studies suggest a novel role for the EGF-like domain of ADAM15 and present an interesting observation of functional interaction between ADAM10 and ADAM15.

Chapter 1: Introduction

Benign and malignant prostatic disease

The human prostate is a walnut sized organ, which sits at the base of bladder and surrounds the urethra. The gland is comprised of epithelial cell acini which are separated by fibromuscular stroma (1). Each acinus is comprised of secretory luminal cells, surrounded by basal cells and the basement membrane. The two most common diseases of the prostate gland are benign prostatic hyperplasia (BPH) and prostate cancer.

BPH is characterized by lower urinary tract symptoms (LUTS), which manifest as difficult and painful voiding (1). The causes of BPH remain poorly characterized, although androgen receptor (AR) and epithelial-stromal interactions appear to play a critical role in disease pathology (2, 3). Alpha blockers, which target $alpha_1$ adrenergic receptors on smooth muscle cells, inhibit contraction of the fibromuscular stroma, and provide symptom relief but no reduction in prostate volume; conversely, 5-alpha-reductase inhibitors target the conversion step of testosterone to dihydrotestosterone (DHT), resulting in low tissue levels of DHT, inducing prostate epithelial cell death and reductions in prostate volume (2).

Unlike BPH, which is characterized as a benign disorder and limited to the prostate gland, prostate cancer is capable of migrating through the prostatic capsule and metastasizing to distant sites. Because prostate cancer retains AR, and is initially dependent on AR signaling, AR ablation therapy is the first line of treatment for metastatic disease. While successful for a time, eventually the majority of metastatic prostate cancer patients will relapse and develop castration resistant prostate cancer (CRPC) (4). Although CRPC is no longer sensitive to androgen ablation therapy, AR signaling continues through a variety of mechanisms including increased AR expression, splice variants, ligand-independent activation, and increased androgen and DHT synthesis from weak adrenal androgens (5). Because CRPC is no longer sensitive to androgen ablation therapy, but still dependent on AR signaling, efforts continue to therapeutically target the AR pathway. For example, abiraterone treatment targets CYP17A1, which contributes to the turnover of adrenal androgens to DHT (6). Conversely, other researchers are focusing on alternative pathways which may drive CRPC.

Epidermal growth factor receptor family

The epidermal growth factor receptor (EGFR) family is an emerging area of CRPC research and targeted therapy. The EGFR family is comprised of four transmembrane tyrosine kinase members: EGFR (ErbB1, HER1), HER2 (ErbB2, Neu), HER3 (ErbB3), and HER4 (ErbB4) (7). The EGFR family members contain a cysteine-rich ligand binding domain, a transmembrane domain, and a

cytoplasmic tyrosine kinase domain. Signaling is achieved by an EGF-like ligand binding to a single receptor, which can then homo- or hetero-dimerize with an adjacent EGF-like ligand bound receptor via a “dimerization loop” generating the functional complex (8). Complex formation allows for transautophosphorylation of the kinase domain, which allows for the docking of Src homology (SH2) domain or phosphotyrosine binding (PTB) containing proteins, such as Src, Grb2, and phosphoinositol 3-kinase, which mediate further downstream signaling events (9).

The binding affinities of ligand to receptor depend on the receptors existing as dimers. EGFR binds EGF, transforming growth factor alpha (TGFalpha), amphiregulin (AREG), epiregulin (EPR), betacellulin (BTC), heparin binding EGF (HB-EGF), and biregulin (BiR), an engineered chimera of EGF and heregulin (HRG) (10). HER2 has no reported direct ligand, but its active conformation (11) allows it to be a preferred heterodimerization partner with other EGFR family members (12). Conversely, HER3 can bind HRGbeta, HRGalpha, and BiR (10), but has a catalytically dead kinase domain, so it must heterodimerize with EGFR, HER2, or HER4 in order to transduce signals (13). Interacting with HER2 allows HER3 to also bind neuregulin-2beta (NRG2beta) and EPR (10). HER4 binds BTC, HRGbeta, BiR, NRG2beta, HRGalpha, NRG3, but in association with HER2, it can also bind EGF, EPR, HB-EGF, and TGFalpha (10). The ability of each heterodimer to bind different ligands results in signaling diversity, which has implications in development and disease (7).

In the normal adult prostate, EGFR is expressed in basal cells and is localized in the lateral membrane junctions between the basal and luminal epithelium, while in BPH patients, EGFR staining expands to include moderate staining in a portion of luminal epithelium (14). 36% of BPH samples over-express EGFR (1.7-9.0 fold over controls) and 63% over-express HER2 (15), with increasing levels of EGFR expression correlating with BPH grade (16). Some studies have even reported that by immunohistochemistry, BPH samples express more EGFR than prostate cancer samples (14, 17). These results suggest that EGFR may be a component of a regulatory pathway involved in epithelial hyperproliferation in the prostate gland (18) and a potential target for therapy.

In prostate cancer, expression of EGFR, HER2, and HER3 correlates with more advanced disease and poor clinical outcome. EGFR staining is strongly associated with CRPC and EGFR family member signaling may contribute to androgen independence (19). Whether this is due to the suppression of AR by EGFR and HER2 signaling (20) or the failure of androgens to suppress EGFR expression in prostate cancer (21) remains to be determined. HER2 expression in prostate cancer has been associated with androgen-independent AR signaling, poor survival in CRPC, and may promote prostate cancer cell growth in bone (22-24). HER3 is also over-expressed in prostate cancer, has been observed in the nuclei of sections and cell lines, and high expression correlates with poor clinical outcome (25). Unlike the other family members, HER4 expression is a positive prognostic marker for hormone-sensitive tumors (23). These data

suggest that some EGFR family members support CRPC and patients could benefit from direct targeting of EGFR family members or metalloproteases, such as the ADAM family, which promote EGFR family signaling.

A disintegrin and metalloprotease (ADAM) family

ADAM10 and ADAM15 are members of the disintegrin family of zinc-dependent metalloproteases which, in humans, is composed of 25 members, of which 13 members (including ADAM10 and 15) are catalytically active (26). Family members are characterized by five extracellular domains: prodomain, metalloprotease, disintegrin, cysteine-rich, and EGF-like. The multiple domains of ADAMs allow for a myriad of functions including proteolysis, integrin binding, and signal transduction (26). ADAM10 is predominantly a sheddase, which is known to cleave EGF-like ligands from the cell-surface, thus promoting EGFR family member signaling (27). ADAM10 also plays a critical role in the regulated intramembrane proteolysis (RIP) of Notch, CD44, and Fas ligand, whereby sequential processing of the pro-form of the protein by ADAM10 then gamma-secretase complex allows the intramembrane fragment to enter the nucleus, bind DNA, and induce transcription of target genes (28). The catalytic domain of ADAM10, therefore, plays a critical role in cellular signaling.

The cytoplasmic domain of ADAM10 is predominantly a regulatory component, with a proline-rich portion being required for correct baso-lateral localization of ADAM10 to the membrane (29). This process may be mediated by Src homology 3 (SH3) domain containing proteins, such as Lck, MAD2, SAP97,

Eve-1, and PACSIN3 which bind the ADAM10 cytoplasmic tail PXXP motif (26). Additionally, the catalytic activity of ADAMs can be controlled by the phosphorylation status of the cytoplasmic tail. In the prostate, the G-protein coupled receptor (GPCR) CXCR4 can respond to the chemokine CXCL12 by activating Src, which can in turn activate ADAM10, thus mediating amphiregulin shedding and EGFR signaling (30).

Frequent disregulation of ADAM10 in inflammation and disease has made the protein's catalytic domain a target for therapy (31-35). In the prostate, membranous ADAM10 expression is high in BPH patient samples, while prostate cancer patients lose membranous expression and gain nuclear staining of an ADAM10 cytoplasmic domain fragment (36). *In vitro,* the ability of the ADAM10 cytoplasmic domain to translocate into the nucleus is dependent upon DHT, which allows AR to bind processed ADAM10 and translocate into the nucleus (36). Interestingly, DHT treatment of these cells also increases ADAM10 expression (37). The nuclear translocation of ADAM10 requires that it undergo RIP, which has been reported to be mediated by ADAM9 and 15, as well as gamma-secretase (38). These data suggest that while ADAM10 may play a role in benign proliferative disorders, its catalytic activity on the cell surface will likely be diminished in diseases where ADAM15 is over-expressed and shedding ADAM10 from the cell surface. It is worthy of note that this cleaved soluble ADAM10 retains its catalytic activity to some degree (38), an observation that may have clinical implications and warrants further investigation.

The expression of ADAM15 is widespread in human tissues, but it is the highest in mesenchymal stem cells and the urogenital system (26). It is also significantly over-expressed in breast, prostate, ovarian, gastric, and lung cancer (39). Unlike ADAM10, ADAM15 only has five reported substrates: CD23, pro-amphiregulin, pro-HB-EGF, and E- and N-cadherin (40-44), but its unique RGD sequence in the disintegrin domain, also allows interactions with $alpha_v beta_3$, $alpha_5 beta_1$, and $alpha_9 beta_1$ integrins (45-47). Interestingly, while $alpha_v beta_3$ and $alpha_5 beta_1$ integrins require the RGD sequence for ADAM15-integrin binding (45, 46), $alpha_9 beta_1$ binding occurs independently of this motif (47). The extracellular domain of ADAM15, therefore, can serve as an adhesive or catalytic unit, depending on the circumstance.

The cytoplasmic tail of ADAM15 can associate with the Src family tyrosine kinases Lck, Hck, Abl, and Src, as well as MAD2, Grb2 (48). While the associations between Lck and Hck are potentiated by ADAM15 cytoplasmic tail phosphorylation, both kinases are able to phosphorylate the tyrosine residues of ADAM15 themselves (48). Splice variants of ADAM15 occurring in the cytoplasmic tail have varying affinities for Hck and Lck (49), which may have clinical implications in breast cancer, where certain splice variants correlate with dramatic decreases in patient survival (50). *In vitro,* these splice variants alter cell adhesion, motility, migration and association with intracellular effectors such as Src (50) which mediates the catalytic activity of ADAM15 (51). The association between the cytoplasmic tail of ADAM15 and the Src family members suggest that these interactions may mediate proteolysis and have implications in

adhesion, migration, and disease progression (48, 50, 51). ADAM15 has also been shown to be an effecter of GPCR signaling whereby it responds to lysophosphatidic acid (LPA) and promotes EGFR signaling (42).

In the prostate, ADAM15 expression is much higher in localized and metastatic cancer than in BPH or normal tissue (39), and our previous studies have implicated ADAM15 in the malignant progression of breast and prostate cancer (43, 44). The catalytic and disintegrin activity of ADAM15 has also been reported to mediate inflammation (52, 53) and platelet aggregation (54). The ability ofADAM15 to promote tumor growth and support metastasis in prostate cancer (43), makes ADAM15 a therapeutic target of interest.

Unlike the *Adam10 -/-* mouse which is embryonic lethal at embryonic day 9.5, with defective central nervous system and heart developments (55), the *Adam15 -/-* mouse is viable, demonstrating that ADAM15 does not play a critical role in development (56). Studies of tissue specific *Adam10-/-* mice have also indicated a critical role for ADAM10 in brain, cardiovascular, thymocyte, skin, and marginal zone B cell development (57-61), suggesting ADAM10 may also play critical roles in adult tissues. Conversely, studies of adult *Adam15-/-* mice have indicated that ADAM15 plays homeostatic roles in cartilage and bone (62, 63), and only under pathological conditions such as hypoxia-induced proliferative retinopathy or implantation of melanoma xenografts do *Adam15-/-* mice exhibit defects in angiogenesis and tumor growth (56). These studies suggest that targeting ADAM15 in cancer would most likely produce limited side effects to the

patient, as compared to targeting ADAM10 which appears to play a critical and active role in adult tissues.

Epithelial (E) -cadherin

E-cadherin is a homophilic, calcium-dependent, adhesion protein, which is expressed at adherens junctions between epithelial cells. E-cadherin has an extracellular region comprised of five domain repeats, each one containing a set of seven beta-sheets arranged in an immunoglobulin fold (64). Adhesion is achieved by lateral dimerization between E-cadherin molecules on the same cell, creating a homodimer which can then interact with an adjacent E-cadherin homodimer on a neighboring cell via cadherin repeat 1 (EC1) (65).

Although E-cadherin is predominantly a homophilic adhesion molecule, it also exhibits heterophilic interactions. Of particular interest, E-cadherin can associate with CD103, killer cell lectin receptor G1 (KLRG1), and EGFR (66-68). The E-cadherin receptor, CD103 or $alpha_E beta_7$ integrin, is located on T lymphocytes and helps to target T cells to epithelial cells, where it binds extra cellular domains EC1 and EC2 of E-cadherin (66). Another receptor for E-cadherin, KLRG1, is expressed on T cells and natural killer (NK) cells, where the binding of KLRG1 to E-cadherin-expressing cells prevents the lysis of epithelial targets (68) and is responsible for controlling the activation threshold of NK and T cells and thereby suppressing immune response (69).

E-cadherin can also interact with receptor tyrosine kinases, such as EGFR. E-cadherin interaction with EGFR is dependent upon the extracellular

domain of E-cadherin and independent of beta-catenin and p120 binding (70). Moreover, the re-expression of E-cadherin in deficient cell lines inhibits ligand-dependent activation of EGFR (70). Work in diffuse gastric type carcinoma with an E-cadherin mutant lacking exon 8, which lies in the extracellular domain, demonstrated that mutant E-cadherin bound EGFR less efficiently and this retarded EGFR internalization in response to EGF (71). The association of EGFR with E-cadherin, therefore, can provide an inhibitory signal for EGFR.

Within the cell, E-cadherin interactions support adhesion established through homodimerization. The cytoplasmic tail of E-cadherin associates directly with beta-catenin, p120, and indirectly with alpha-catenin. Beta-catenin binding to E-cadherin provides structural support and aids in transport of E-cadherin to the baso-lateral plasma membrane (72). The formation of this ordered structure allows for binding of alpha-catenin, which can bind actin, stabilizing and coordinating actin dynamics at the adherens junction (73, 74). p120 binding to E-cadherin also stabilizes the complex and maintains high E-cadherin levels (75). Regulation of E-cadherin adhesion can occur by altering the composition of the cadherin-catenin complex, the presence growth factors, tyrosine phosphorylation of the cadherin-catenin complex, p120 binding to E-cadherin, and the activity of small GTPases and proteins which aid in cell polarity determination (76), as well as cleavage in the extracellular or cytosolic domains.

The disruption of E-cadherin function by proteolytic cleavage can occur in the extracellular domain or cytosolic tail of E-cadherin. The initial observation of E-cadherin cleavage was reported by Wheelock *et al* who observed an 80kDa

soluble E-cadherin in the conditioned media of MCF-7 breast cancer cells (77). This fragment, containing the five extracellular domains of E-cadherin and referred to as sE-cad, could disrupt adherens junctions of mouse mammary tumor cells (77). To date, members of the A Disintegrin and Metalloprotease (ADAM) family (ADAM10 and 15), matrix metalloprotease (MMP) family (MMP-2, 3, 7, 9, and 14), Kallikrein-7, and plasmin have all been implicated in the generation of sE-cad (44, 78-92).

Previous studies in our laboratory have focused on ADAM15 dependent cleavage of E-cadherin to sE-cad. Initial studies by Kuefer *et al* identified ADAM15 as the most highly over-expressed protease in prostate cancer progression (39) and later studies demonstrated that ADAM15 was critical for tumor maintenance, cancer cell-endothelial cell interaction, and metastasis (43). Najy *et al* also demonstrated that serum withdrawal from breast cancer cells induced E-cadherin cleavage by ADAM15, and the generation of sE-cad could be abrogated by shRNA knockdown of ADAM15 or increased by ADAM15 over-expression (44). Our unpublished observations suggest this is also the case in prostate cancer cells.

The observation that ADAM15 is not highly expressed in BPH (93) and our early studies suggested that in normal prostate biology ADAM10 is a more likely E-cadherin sheddase. E-cadherin and ADAM10 co-localize at the adherens junction (29), and ADAM10 has been implicated in E-cadherin cleavage in keratinocytes and gastric cancer cell lines (83, 84). Moreover, the high

membranous expression pattern of ADAM10 in BPH patients (36), suggests it might play a role in normal or proliferative disorder prostate biology.

The presence of sE-cad in patient fluids is a negative prognostic factor in multiple disease states (reviewed in Chapter 2). The loss of E-cadherin by promoter hypermethylation, gene deletion or mutation (94) and proteolytic cleavage (77), results in the liberation of beta-catenin, which can then translocate into the nucleus and promote the transcription of pro-epithelial to mesenchymal transcription (EMT) factors (95). In conjunction with constitutive activation of receptor tyrosine kinases, loss of E-cadherin can cement the mesenchymal phenotype in cancer cells (96). Moreover, sE-cad can induce cell migration, invasion, and signaling (reviewed in Chapter 2).

The process of EMT in tumor progression allows epithelial cells to lose their differentiated non-migratory state and instead become motile and metastasize. Once colonized in a new organ, these cancer cells can undergo the reverse process of MET (96). In prostate cancer cell lines, xenograft studies of EMT allowed prostate cancer cells to metastasize to bone (97). The process of EMT and MET can also be observed in prostate cancer patients, where E-cadherin expression is reduced in localized cancer progression, but when the tumors metastasize there is a degree of E-cadherin re-expression in the bone metastasis (98). In recent years, EMT has also become a point of interest for BPH research. Alonso-Magdalena *et al* demonstrated that BPH sections contained an increased amount of EMT transcription factors such as Slug and Snail, suggesting EMT may be contributing to the pathogenesis of BPH (99).

Scope of dissertation

This dissertation will cover four related topics. First, it will provide a review of the literature pertaining to sE-cad generation, presence in patient fluids, and the consequences of sE-cad presence in disease (Chapter 2). From there, the role of ADAM10-mediated E-cadherin cleavage in untransformed prostate biology is examined. These studies utilize two immortalized prostate cell lines and demonstrate the role of ADAM10 in E-cadherin cleavage, as well as the consequences of sE-cad stimulation on prostate cell lines (Chapter 3). Studies in Chapter 3 have defined a novel ADAM10-mediated sE-cad/EGFR signaling axis in the prostate (Figure 1-1).

We also initiated *in vivo* studies to determine the role of ADAM10 in normal prostate biology by generating a prostate specific ADAM10 knockout mouse, which has provided *Adam10* $^{-/-}$ cell lines and preliminary observations regarding consequences of ADAM10 loss in the mouse prostate (Chapter 4). Chapter 5 includes preliminary studies pertaining to ADAM inhibitors, the role of the ADAM15 EGF-like domain in substrate cleavage, and ADAM10 and 15 interactions. These studies, although preliminary, provide interesting insight into the role of ADAM10 in normal prostate biology, propose a novel function for the EGF-like domain of ADAM15, and suggest ADAM10 and 15 exist in a functional complex that may have biological significance in benign and malignant prostatic disease.

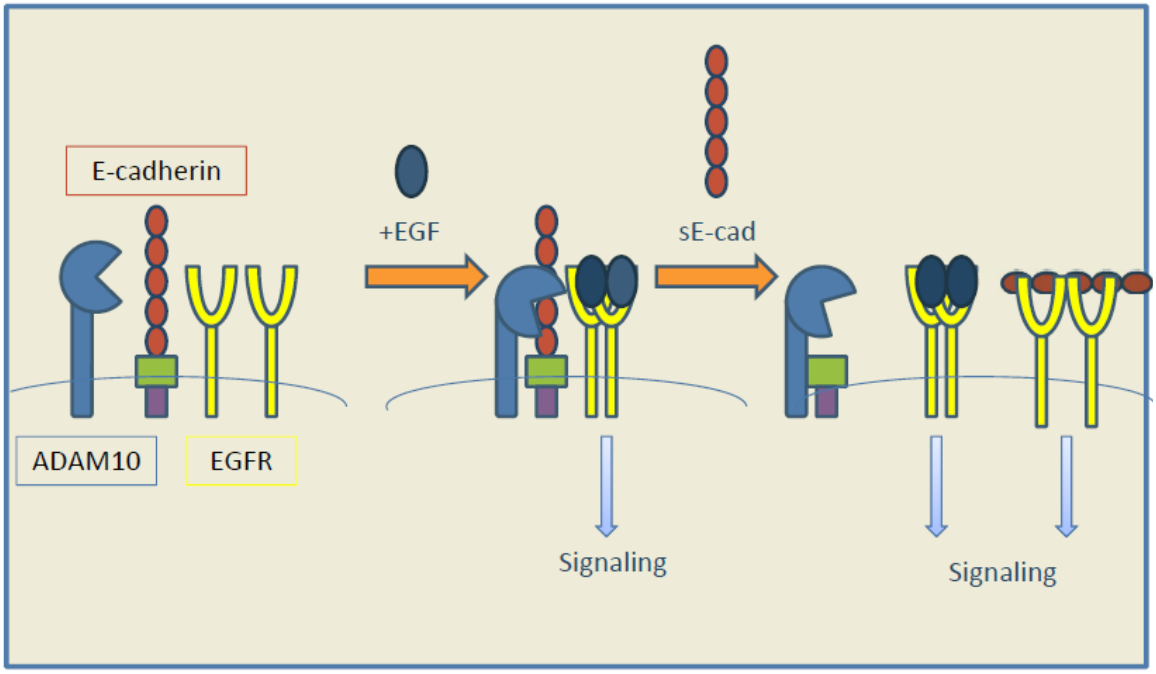

Figure 1-1: The ADAM10-mediated sE-cad/EGFR signaling axis.

Chapter 2: Soluble E-cadherin: More Than a Symptom of Disease

Abstract

Epithelial (E)-cadherin is a homophilic adhesion molecule which is responsible for maintenance of baso-lateral cell adhesion and polarity. E-cadherin can be lost from the cell surface by proteolytic cleavage, resulting in the generation of an 80kDa fragment referred to a soluble E-cadherin (sE-cad). Although originally discovered in the conditioned media of breast cancer cells and later verified in the fluids of cancer patients, today sE-cad has been recorded in patients with viral and bacterial infections, organ failure, and benign disease. The proteases implicated in this cleavage event include members of the disintegrin family (ADAM10 and 15), bacterial proteases (gingipains and BFT), cathepsins (B, L, S), matrix metalloproteases (MMP-2, 3, 7, 9, and 14), KLK7, and plasmin. Stimulus that induces sE-cad generation by ADAMs, MMPs, Kallikrein-7 and plasmin *in vitro* ranges from serum withdrawal to pro-inflammatory cytokines to growth factors. The cellular or physiologic consequences of sE-cad accumulation include the disruption of adherens junctions, cellular migration and invasion, induction of MMPs, as well as cell signaling, suggesting that sE-cad may contribute to disease progression

Introduction

Epithelial cadherin

E-cadherin is a homophilic, calcium-dependent, adhesion protein, which is expressed at adherens junctions between epithelial cells. E-cadherin has an extracellular region comprised of 5 domain repeats, each domain containing a set of seven beta-sheets arranged in an immunoglobulin fold (64). Adhesion is achieved by lateral dimerization between E-cadherin molecules on the same cell, creating a homodimer which can then interact with an adjacent E-cadherin homodimer on a neighboring cell via cadherin repeat 1 (EC1) (65).

Although E-cadherin is predominantly a homophilic adhesion molecule, it also exhibits heterophilic interactions. Of particular interest, E-cadherin can associate with CD103 and Killer cell lectin receptor G1 (KLRG1) (66, 68, 100). The E-cadherin receptor, CD103 or $alpha_E beta_7$, is located on T lymphocytes and helps to target T cells to epithelial cells, where it binds extra cellular domains EC1 and EC2 of E-cadherin (66). Another receptor for E-cadherin, KLRG1, is expressed on T cells and natural killer (NK) cells, where the binding of KLRG1 to E-cadherin-expressing cells prevents the lysis of epithelial targets (68). The interaction between KLRG1 and E-cadherin is mediated by the homodimeric interface on EC1, suggesting that monomeric E-cadherin at epithelial cell surfaces is responsible for controlling the activation threshold of NK and T cells and thereby suppressing immune response (69). E-cadherin, therefore, can serve as an adhesion molecule or a targeting molecule, depending on binding partner. Within the cell, E-cadherin interactions support adhesion established

through the homodimerization. The cytoplasmic tail of E-cadherin associates directly with beta-catenin, p120, and indirectly with alpha-catenin. Beta-catenin binding to E-cadherin provides structural support and aids in transport of E-cadherin to the baso-lateral plasma membrane (101). The formation of this ordered structure allows for binding of alpha-catenin, which can bind actin, stabilizing and coordinating actin dynamics at the adherens junction (74, 102). p120 binding to E-cadherin also stabilizes the complex and maintains high E-cadherin levels (75). From the cytoplasmic side, regulation of E-cadherin adhesion can occur by altering the composition of the cadherin-catenin complex, the presence growth factors, tyrosine phosphorylation of the cadherin-catenin complex, p120 binding to E-cadherin, and the activity of small GTPases and proteins which aid in cell polarity determination (76). Additionally, E-cadherin adhesion can be disrupted by E-cadherin cleavage in the extracellular or cytosolic domains.

E-cadherin cleavage

The disruption of E-cadherin function by proteolytic cleavage can occur in the extracellular domain or cytosolic tail of E-cadherin. The initial observation of E-cadherin cleavage was reported by Wheelock *et al* who observed an 80kDa soluble E-cadherin in the conditioned media of MCF-7 breast cancer cells (103). This fragment, containing the five extracellular domains of E-cadherin and referred to as sE-cad, could disrupt adherens junctions of mouse mammary tumor cells (103). To date, members of the A Disintegrin and Metalloprotease

(ADAM) family (ADAM10 and 15), bacterial proteases (gingipains and BFT/fragilysin), cathepsins (B, L, S), matrix metalloprotease (MMP) family (MMP-2, 3, 7, 9, and 14), Kallikrein-7, and plasmin have all been implicated in the generation of sE-cad (44, 78, 80-83, 85-87, 89-92, 104-109).

The extracellular cleavage of E-cadherin can also have implications for the intracellular domains. The generation of sE-cad allows the remaining membrane-bound fragment to undergo further processing by presenilin-1/ gamma-secretase complex at the membrane/cytosol interface, which results in the disassembly of the adherens junction (110). Additionally, p120, which is critical for the association between E-cadherin and gamma-secretase (111), can aid the C-terminal fragment of E-cadherin in entering the nucleus and binding DNA to promote gene transcription (112). This tightly regulated sequential degradation of E-cadherin and resulting disassembly of adherens junctions and nuclear translocation of the C-terminal fragment, however, is not required for all E-cadherin cytoplasmic domain processing.

Apoptosis-induced cleavage of the intracellular domain of E-cadherin by calpain and caspase-3 occurs independently of extracellular processing. Calpain cleavage of E-cadherin results in a 100kDa E-cadherin fragment which can no longer bind beta-catenin and diminishes the survival of prostate cancer cells (113). Conversely, caspase-3 can generate a 24kDa cytosolic fragment of E-cadherin, but requires other metalloproteases to generate the 29kDa fragment and sE-cad (114). The generation of sE-cad, however, is not limited to

apoptosis, and there are a variety of stimuli which can induce E-cadherin cleavage.

Generation of sE-cad

Membrane sheddases

The proteases capable of extracellular E-cadherin cleavage, referred to as sheddases, are a diverse group. While many of these sheddases are misregulated or overexpressed in disease, the author has limited her descriptions to cell systems and diseases where sE-cad is present in conditioned media of cells or patient fluids. To date, no sheddase unique to E-cadherin has been identified, and the sheddases described below are also responsible for cleavage and shedding events beyond sE-cad generation (Table 2-1).

ADAM family

The human ADAM family consists of 25 members whose expression varies across tissues. Functionally, the ADAMs play roles in adhesion and substrate cleavage. To that end, ADAMs are made up of an inhibitory prodomain, a zinc-dependent metalloprotease domain, a disintegrin domain, a cysteine-rich domain, an EGF-like domain, a transmembrane domain and a cytoplasmic tail. Within the ADAM family, only ADAM10 and 15 have been implicated in E-cadherin shedding (44, 83, 85, 104).

ADAM10 can be found in mesenchymal stem cells, placenta, blood, myeloid cells, bladder, and bone marrow myeloid cells, where it is predominantly

a sheddase with a substrate list featuring 27 proteins, including E-cadherin (26). In terms of E-cadherin cleavage in the skin, ADAM10 has been implicated in generating sE-cad in normal keratinocytes as well as melanoma cell lines. In keratinocytes, Maretzky *et al* examined the soluble 80kDa form and 37kDa C-terminal fragment (CTF) associated with the membrane and determined that ADAM10 constitutively sheds sE-cad (104). ADAM10-dependet shedding of E-cadherin could be induced by the pro-inflammatory cytokines IL-1 beta, TNF-alpha, IFN-gamma, TGF-beta, and lipopolysaccharide (LPS). Additionally, biopsies from eczema patient lesions revealed elevated levels of ADAM10 and CTF (104). ADAM10 also exists in its active form in melanoma cell lines (85), but to date, no inhibitor or loss of function studies of ADAM10 in melanoma cell lines in terms of sE-cad generation have been undertaken. However, ADAM10 is up-regulated in metastatic melanoma compared to primary melanoma (115), and it is possible that it is the sheddase responsible for E-cadherin cleavage.

ADAM10 has also been implicated in shedding E-cadherin in response to *Helicobacter (H.) pylori* infection of gastric cancer cell lines (83). Previously, *H. pylori* infection was found to correlate with increased ADAM10 expression in gastric cancer patient samples and to induce ADAM10 expression in gastric cancer cell lines (116). Indeed, chemical inhibition or shRNA mediated knockdown of ADAM10 resulted in decreased sE-cad generation in response to *H. pylori* infection, suggesting that induction of ADAM10 by *H. pylori* in the gut promotes E-cadherin cleavage (83).

Recent work in our lab has determined that in benign prostatic hyperplasia (BPH) cells, epidermal growth factor (EGF) can induce sE-cad generation in response to EGF in ADAM10-dependent manner (manuscript submitted to Cellular Signaling, Chapter 3). In a paper by Arima *et al*, the authors demonstrated that ADAM10 is highly expressed on the cell surface of BPH patient samples versus cancer samples where ADAM10 resided predominantly within the nucleus (36). This suggests that based on location alone, ADAM10 is likely a major sheddase of E-cadherin in BPH, but not in prostate cancer.

Unlike ADAM10, ADAM15 has only four reported substrates, but it also has three integrin binding partners (26). The expression of ADAM15 is widespread in the human tissues, but it is the highest in mesenchymal stem cells and the urogenital system (26). It is also significantly over-expressed in breast, prostate, and lung cancer (44). Najy *et al* demonstrated that serum withdrawal from breast cancer cells induced E-cadherin cleavage by ADAM15, and the generation of sE-cad could be abrogated by shRNA knockdown of ADAM15 or increased by ADAM15 over-expression (44). Our unpublished observations also suggest that prostate cancer and bladder cancer cells shed sE-cad in response to serum withdrawal in an ADAM15- dependent manner as well. Additionally, in untransformed mouse cells, ADAM15 knockout prostate cell lines fail to shed appreciable amounts of sE-cad as compared to wild-type control cell lines, suggesting ADAM15 can also cleave E-cadherin in mouse prostate epithelial cells (unpublished observations).

Bacterial proteases (Gingipains, BFT/fragilysin)

Gingipains (HRgpA, RgpB, and Kgp) are secreted cysteine proteases which are encoded in the genome of *Porphyromonas gingivalis* (*P. gingivalis*). *P. gingivalis* has been reported to contribute to adult periodontitis in two ways. First, by infecting epithelial cells, *P. gingivalis* can influence signal transduction and innate immune response (117). Independent of epithelial cell infection, *P. gingivalis* can disrupt adherens junctions, allowing for infection of underlying tissues (118). The disruption of the adherens junction is believed to be mediated by Kgp cleavage of E-cadherin (105). Although HRgpA and RgpB can also cleavage of immunoprecipitated E-cadherin, they are unable to process E-cadherin from the cell surface of Madin-Darby canine kidney (MDCK) cells (105).

Another bacterial protease which has been implicated in E-cadherin cleavage is from *Bacteroides fragilis (B. fragilis*). *B. fragilis* produces an enterotoxin referred to as *B. fragilis* toxin (BFT) or fragilysin. Treatment of HT29/C1 colorectal adenocarcinoma cells with BFT results in the generation of the 33kDa and 28kDa cytoplasmic E-cadherin fragments (106). Although the authors demonstrated that BFT did not enter the cells and hence could not generate the cytoplasmic fragments, they were unable to observe BFT-mediated cleavage of their recombinant E-cadherin and generation of sE-cad (106). These studies suggest that E-cadherin cleavage may be an important step in bacterial infection.

Cathepsins

Cysteine cathepsins are intracellular proteases which are responsible for protein degradation in the lysosome and play critical roles in apoptosis, autophagy, and necrosis (119). Although located within the lysosome under normal conditions, an emerging body of evidence suggests cathepsins can be mislocalized or released from the cell. For example, release of active cathepsin B has been demonstrated in mechanically injured mouse gut (120), and procathepsin B can interact and localize with annexin II tetramer on the extracellular surface of human breast cancer and glioblastoma cells (121). These studies suggest that in the context of disease, cathepsins may be a viable candidate for extracellular cleavage of E-cadherin.

Interest in cathepsin cleavage of E-cadherin originated with the observation that pancreatic tumors from cathepsin B, L, or S knockout mice on the background of the RT2 pancreatic cancer mouse model retained expression of E-cadherin, suggesting E-cadherin processing was deficient (107). Indeed, when Gocheva *et al* combined recombinant E-cadherin with active cathepsins B, L, or S, E-cadherin was cleaved to a 64kDa extracellular fragment (107). Because cathepsins B and L are upregulated during pancreatic cancer progression (107) and high cathepsin B expression is an independent prognostic marker for pancreatic cancer recurrence (122), it is likely that the mislocalized cathepsins play a role in E-cadherin cleavage in pancreatic cancer.

Kallikrein-7

Kallikerein-7 (KLK7) is serine proteases which is normally expressed in the salivary gland, nervous system, kidney, mammary gland and skin and to a lesser extent in the uterus, thymus, thyroid, placenta, and trachea (123). It is not expressed in the normal pancreas, but it is dramatically over-expressed in pancreatic cancer (86). In pancreatic cancer cell line cultures, recombinant KLK7 was capable of cleaving E-cadherin *in vitro* and from the cell surface of pancreatic cancer cell lines (86). Because of its dramatic upregulation in pancreatic cancer, it is likely that KLK7 is a responsible protease for E-cadherin cleavage in pancreatic cancer patients.

MMP family

Like the ADAM disintegrins, the MMPs are zinc dependent proteases (26, 124). While the majority of the MMP family are secreted, a subset of the MMP family, the membrane type (MT) MMPs remain associated with the cell membrane (124). MMP activity is tightly controlled by MMP gene transcription, pro-enzyme activation, and MMP inhibition (124). In E-cadherin cleavage, five MMPs have been implicated: MMP-2, MMP-3, MMP-7, MMP-9 and MT1-MMP (MMP-14).

In prostate cancer, MMP-2 is an independent predictor of patient survival. Early immunohistochemical studies of MMP-2 in prostate cancer patients demonstrated that epithelial expression of MMP-2 in prostate tumors correlated with a decrease in patient survival (125). *In vitro,* MMP-2 has been implicated in

sE-cad generation in prostate cancer cells which have been transfected with protein kinase D1 (PKD1) (82). The *in vitro* data and the over-expression of MMP-2 in prostate cancer suggest MMP-2 is a possible candidate for E-cadherin shedding in prostate cancer.

MMP-3 shedding of E-cadherin has been reported in mouse and human mammary cells. Early studies by Lochter *et al* revealed that an auto-activating MMP-3 mutant transfected into mouse mammary cells resulted in the shedding of sE-cad from their cell surface (81, 87). Later analysis of MMP-3 and 7 by Noe *et al* demonstrated that E-cadherin can be cleaved *in vitro* by these metalloproteases in breast cancer cells as well (87). In patients, MMP-3 is over-expressed and activated in breast cancer samples versus normal tissue (126, 127), suggesting MMP-3 could be an E-cadherin sheddase in breast cancer.

MMP-7 generation of sE-cad has been reported in prostate, gastric, and breast cancer cells, as well as in a mouse model of lung injury (80, 87, 89, 108). In prostate cancer and gastric cancer cell lines, treatment of cells with hepatocyte growth factor/scatter factor (HGF/SF), results in the release of MMP-7 and cleavage of E-cadherin (80, 108). When MMP-7 levels are decreased by short hairpin (sh) RNA against MMP-7, sE-cad generation is lost (80, 108). Prostate cancer patients with advanced disease have more active MMP-7 in their serum (128), while for gastric patients, expression of MMP-7 correlates with a decrease in patient survival and more advanced stage (129) . In breast cancer cell lines, E-cadherin can be cleaved *in vitro* by MMP-7 (87), and in patients MMP-7 positive tumors by immunohistochemistry correlate with a worse prognosis (130).

Because MMP-7 is over-expressed in breast, prostate, and gastric cancer, it is possible that MMP-7 is major sheddase of E-cadherin in these cancers.

MMP-7 over-expression is not unique to cancer, and can occur in response to injury. In a mouse lung injury model using bleomycin, MMP-7 is dramatically upregulated in injured lung epithelium (89, 131). McGuire *et al* also demonstrated that MMP-7 knockout mice did not generate sE-cad from wounded trachea explants, unlike their wild-type controls, implicating that the upregulation of MMP-7 in response to wounding is responsible for sE-cad generation in this model (131). MMP-7 upregulation occurs in pulmonary fibrosis patients (132), so MMP-7 generation of sE-cad may play a role in disease progression. Interestingly, in these studies only the lung cancer cells that were transfected with an auto-activating MMP-7 produced the active form of the enzyme; native full length cDNA for MMP-7 did not produce active enzyme (89), suggesting that there is a missing mediator required for MMP-7 activation in these epithelial lung cancer cells.

MMP-9 shedding of E-cadherin appears in ovarian, head and neck, and prostate cancer cell lines. MMP-9 expression is a negative predictor for survival in ovarian cancer, head and neck cancer, as well as prostate cancer (133-135). In ovarian cancer cell lines, aggregation of collagen binding integrins $alpha_2beta_1$ and $alpha_3beta_1$ induces MMP-9 expression which promotes E-cadherin shedding (90). Early studies of MMP-9 in head and neck cancer patients demonstrated that serum levels of MMP-9 were highest in patients with more advanced disease (135) and *in vitro*, stimulation of head and neck cell lines with

EGF demonstrated increased expression of MMP-9 and increased sE-cad (109). Finally, the re-expression of PKD1 in prostate cancer cells also resulted in increased MMP-9 expression, which correlates with increased sE-cad generation, and could be abrogated by the addition of MMP-9 inhibitors (82). Based on the high expression of MMP-9 in ovarian, head and neck, and prostate cancer patients, it is likely that MMP-9 contributes to sE-cad levels in these patients.

MT1-MMP (MMP-14) has been implicated in sE-cad generation in a model of kidney ischemia. Normal rat kidney cells under ischemic conditions generated sE-cad which, by inhibitor studies, was not mediated by MMP -1, -3, -8, or -9 (91). Covington *et al* did, however, observe an increase in MT1-MMP expression in response to ischemia, and determined that loss of MT1-MMP by shRNA decreased sE-cad accumulation, confirming that sE-cad can be generated by MT1-MMP under these conditions (91). In a mouse model of hind-limb ischemia, active MT1-MMP was up-regulated in the ischemic limb as compared to the control, sham operated limb (136), suggesting that MT1-MMP may be the sheddase of E-cadherin under ischemic conditions.

Plasmin

Plasmin is a serine protease with limited specificity, which can act on fibrin, fibrinogen, extracellular matrix components, and pro-forms of growth factors either directly or by activating metalloproteases (137). It is also a downstream component of the urokinase-type plasminogen activator (uPA)

system, which can be activated in ovarian cancer cells by Lysophosphatidic acid (LPA) (138). LPA is found in high concentration in ovarian cancer ascites and promotes growth in ovarian cancer cell lines *in vitro* and *in vivo* (139). In ovarian cancer cell lines, LPA activates the urokinase-type plasminogen activator (uPA) which activates plasmin, resulting in E-cadherin cleavage (92). Although the authors could not rule out metalloproteases downstream of plasmin, they did note that in their studies, LPA only increased pro-MMP-9 slightly, suggesting that plasmin may be directly acting upon E-cadherin (92). Other work in MDCK cells demonstrated that treating cells with plasmin can generate sE-cad and this process can be inhibited by the addition of aprotinin, a serine protease inhibitor (78). Since uPA system disregulation correlates with worse outcome in ovarian cancer patients (140), it is likely that an elevated level of plasmin in these patients generates sE-cad.

Unattributed sheddase activity

In addition to the studies which successfully define sE-cad sheddases, other studies demonstrate the existence of sE-cad as a consequence of stimuli, but do not identify the responsible protease. In these studies, the protease could be one of the aforementioned sheddases or it could be a novel sheddase. Ito *et al* demonstrated that calcium influx by serum withdrawal or ionomycin treatment allowed for sE-cad to accumulate in the conditioned media of cancer cells (141). Although they never identified a responsible sheddase, they did report only the membrane fractions and not cell supernatants were capable of cleaving E-

cadherin *in vitro*, suggesting a membrane bound metalloprotease was required and ruled out the classical MMPs in direct cleavage (141).

In the breast cancer MCF-7/AZ cell line, the phorbol ester PMA can induce the shedding of E-cadherin by a metalloprotease that is sensitive to tissue inhibitor of metalloprotease-2 (TIMP-2) inhibition (87). In the same study, immunopurified MMP-3 and MMP-7 are shown to cleave E-cadherin directly and from the cell surface of MDCK cells (87), but a direct sheddase from PMA induction was not demonstrated. Other studies of apoptotic MDCK cells also implicated a metalloprotease which was sensitive to TAPI, an ADAM17 inhibitor which can inhibit other metalloproteases (114).

Several studies have determined that the accumulation of sE-cad may be a biomarker for tissue damage and predict surgical outcome (142, 143). Goto *et al* applied this to a model of lung transplantation in rats and observed that rats with transplanted lungs had a higher level of sE-cad than the sham operated rats (144). Again, no direct evidence implicates a sheddase, but other studies have implicated MMP-7 in rodent lung damage studies (89, 131).

Proteolytic cascades

The study of sE-cad shedding is greatly complicated by the existence of proteolytic cascades, particularly those involving the MMPs and the uPA system. Synthesized as zymogens, MMPs require proteolytic processing to become active, and this process can be mediated by other MMP family members. As summarized in reviews by Egeblad and McCawley: MMP-2 can generate active

MMP-1, 2, 9, and 13; MMP-3 can generate active MMP 1, 3, 7, 8, 9, and 13; MMP-7 can generate active MMP-1, 2, 7 and 9; MMP-9 can generate active MMP-2; finally, MMP-14 can generate active MMP-2 and 13 (145, 146). Based on the ability of MMPs to activate other family members, studies examining upstream MMPs may have difficulty distinguishing effects due to catalytic activity on a substrate by the upstream MMP versus catalytic activation of a downstream MMP and its subsequent cleavage of the substrate. In the uPA system, the proteolytic cascade is more manageable. Here, uPA converts plasminogen to plasmin, which can then cleave proMMP-2 and 9 to active MMP-2 and 9 (147). Because plasmin is a serine protease which can activate zinc-dependent metalloprotease, these different enzyme classes allow for specific inhibitors and easier determination of the responsible sheddase. The existence of proteolytic cascades coupled with the redundancy observed in E-cadherin cleavage may explain why sE-cad is observed in multiple patient conditions.

Table 2-1: E-cadherin sheddases

Sheddase	Stimulus	System	Studies	Ref
ADAM10	IL-1-beta, TNF-alpha, IFN-gamma, TGF-beta, Lipopolysaccharide (LPS)	Normal keratinocytes	In, si	(104) [A]
	None (growing cultures)	Melanoma cell line	Exp.	
	Helicobacter pylori infection	Gastric carcinoma cell line	si, In	(85)
				(83)
	EGF	Benign prostatic hyperplasia cell line	In, sh	[B]
ADAM15	Serum withdrawal	Breast cancer cell line	OE, sh,	(44)
		Prostate cancer cell line	OE, sh, KO	[C]
		Bladder cancer cell line	OE, sh	[C]
BFT fragilysin	*B. fragilis* infection	Colorectal cancer cell line	PP	(106) [A]
Cathepsins (B, L, S)		Ms pancreatic cancer model	RP	(107)
Gingipains	*P. gingivalis* infection	Canine kidney cell line	PP	(105)
MMP-3 Stromelysin	?	Breast cancer cell line	RP	(87)
	? (Activated mutant)	Ms mammary cell line	aOE, In	(148)
MMP-7 Matrilysin	HGF	Gastric cancer cell line	Ind, sh	(108)
	HGF	Prostate cancer cell line	RP, si	(80)
	Lung injury (bleomycin)	Lung cancer cell line, mouse lung injury	aOE, In, KO	(89)
	?	Breast cancer cell line	RP	(87)
MMP-9	Collagen binding integrins ($alpha_2beta_1$, $alpha_3beta_1$) interaction	Ovarian carcinoma cell line	Ind, In, FBA	(90)
	EGF	Head and neck cancer cell line	Ind, si	(79)
	PKD1	Prostate cancer cell line	In	(82)
MT1-MMP	Ischemia (mineral oil	Normal rat kidney	In, FAB,	(91)

MMP-14	overlay)	cell line	sh	
Plasmin	Lysophosphatidic acid (LPA) None (growing cultures)	Ovarian carcinoma cell line Canine kidney cell line	In RP, In	(92)
?	Calcium influx, ionomycin	Lung tumor cell line	In	(141)
?	Ischemia (lung transplant)	Rat lung transplantation		(144)
TIMP-2 sensitive ? TAPI[E] sensitive	Phorbol ester (PMA) Serum withdrawal Apoptosis (staurosporine, camptothecin)	Breast cancer cell line Breast cancer cell line Canine kidney cell line	In In In	(87) (103)[D] (114)

[A]Read-out is the C-terminal fragment, not sE-cad. [B] Manuscript submitted. [C] Unpublished observations [D] Original report sE-cad [E]ADAM17 inhibitor which can block other metalloproteases. In: inhibitor. si: siRNA. sh: shRNA. Exp: expression. OE: Over-expression. RP: recombinant protein. PP: Purified protein. Ind: Induction of metalloprotease. aOE: auto-activating mutant metalloprotease. KO: knockout mouse. FBA: function blocking antibody

sE-cad is present in a variety of patient conditions

sE-cad was first observed in the conditioned media of MCF-7 cells by Wheelock *et al* (103), and since then, many studies have been conducted on patient fluids to determine whether sE-cad could serve as a biomarker for disease. The initial report by Katayama *et al* determined that levels of sE-cad do not vary significantly between men and women or different age groups (149). Although the initial focus on sE-cad was as a cancer biomarker for disease, progression, or recurrence, today there are several studies which describe the presence of sE-cad in other disease states, such as HIV infection and benign prostatic disease (150, 151). In order to be included, studies must have reported on the presence of sE-cad in more than one patient. For example, the initial

report of sE-cad in patient samples by Katayama *et al* included a report for one pancreatic and one ovarian cancer patient (149), which was not sufficient for inclusion in this review (Table 2-2).

Cancer

Bladder

Sera from newly diagnosed bladder cancer patients have significantly (P = 0.017) higher levels of sE-cad than normal controls (1,013 ng/ml v. 3,955 ng/ml) (152). Additionally, high levels of sE-cad correlate with higher grade, number of tumors, and recurrence but not tumor bulk (152). In the urine, healthy controls exhibited 582 ng/ml of sE-cad in the urine, while bladder cancer patients averaged 1,272 ng/ml across all stages and grades (P < 0.001) (153). The authors suggested, however, that using total protein in urine is equally effective at this determination (153). In a later study, Shi *et al* found that urine levels of sE-cad normalized to creatinine were significantly (P < .01) lower in normal (1.306 mg/mol) versus cancer samples (3.724 mg/mol), and that samples from recurrent patients (10.497 mg/mol) had significantly (P < 0.01) higher levels of sE-cad than primary tumors (154). Additionally, they found that sE-cad correlated well with tumor grade, but not with stage, size, and the number of tumors (154). Based on these data, both serum and urine concentrations of sE-cad can be used to stratify bladder cancer patients.

Colorectal

In colorectal cancer, the initial report determined that there was no statistically significant difference between sE-cad levels from healthy controls and colorectal cancer patients (155). Later, Willmanns *et al* found that sE-cad levels were statistically different between healthy controls versus benign disease ($P = 0.005$) versus cancer ($P = 0.009$) (3,476 ng/ml; 5,248 ng/ml; 5,495 ng/ml) and that the highest levels were found in metastatic patients (156). They also observed that in this cancer cohort, patients with renal or hepatic failure had high levels of sE-cad and that patients who had been treated with chemotherapy had lower sE-cad levels compared to untreated patients (156). From these data, it is apparent that while sE-cad serum levels may be useful in determining cancer spread in untreated patients, it would be important to rule out organ failure or dysfunction.

Esophageal squamous cell carcinoma

The recent study in squamous cell carcinoma compared the pre-operative levels of sE-cad for patients who had surgery alone to those patients who had chemoradiation therapy (CRT) before surgery. Patients in the surgery alone arm had significantly ($P = 0.032$) higher (5,108 ng/ml) levels of sE-cad than patients who had already received chemoradiation therapy (3,688 ng/ml) (157). This decrease of sE-cad levels after chemotherapy agrees with data from colorectal cancer patients (156), and suggests sE-cad could be used to monitor patient response to therapy. For the patients who received surgery, levels of sE-cad

higher than the median pre-surgery sE-cad concentration correlated with a decrease in survival; however, there was no prognostic significance for patients who had undergone neoadjuvant CRT (157). Therefore, sE-cad as prognostic marker for esophageal squamous cell carcinoma would be limited to patients who have yet to undergo any treatment (157).

Gastric

Initials reports of elevated sE-cad in gastric cancer came from Katayama *et al* (2,000 ng/ml vs. 3,515 ng/ml; $P < 0.0001$) (149), which were confirmed by Gofuku *et al* (158). Later studies by Chan *et al* demonstrated that not only was sE-cad elevated in gastric cancer patients (5,616 ng/ml vs. 9,344 ng/ml; $P = 0.001$) but also that this correlated with tumor size and poor outcome markers (159). When Chan *et al* determined the optimal sensitivity and specificity of sE-cad following tumor resection by ROC analysis, they determined 10,000 ng/ml as a point of elevated sE-cad. Once a patient's serum concentration of sE-cad exceeded 10,000 ng/ml, the tumor would eventually recur (160). On average, elevated sE-cad levels predated the recurrence by 13 months (160). Most importantly, the sensitivity of this test was similar in patients with more and less advanced disease (160). In another study, Chan *et al* determined that a pre-therapeutic 10,000 ng/ml sE-cad concentration was also a predictor of survival, where 90% of patients whose sE-cad levels were above the cutoff had a survival time of less than three years ($P = 0.009$) (161). Chan *et al* acknowledged the substantial differences between normal sE-cad levels in the Katayama study

(149) and theirs (159) by suggesting that the differences may be attributed to the different populations used in the study. Later studies by Pedrazzani *et al* determined that while sE-cad is indeed elevated in gastric cancer patients as previously reported, there was a linear increase with sE-cad levels in normal controls and gastric tumor patients over time (162), which is inconsistent with previous observations (149).

sE-cad levels in gastric cancer patients can be decreased by resection or therapy. Resection alone can significantly ($P < 0.0001$) reduce sE-cad levels (158). Later studies by Zhou *et al* demonstrated that if surgery was coupled with neoadjuvant Celecoxib therapy, patients showed a significant ($P < 0.01$) decrease in sE-cad levels during therapy and a significant ($P < 0.01$) decrease in sE-cad post-surgery (163). Based on the data, the use of sE-cad in gastric cancer would be quite informative for patient survival and recurrence, particularly since there is a significant amount of time between elevated sE-cad levels and actual recurrence, which would allow for appropriate therapeutic intervention (160). Additionally, future studies of sE-cad in gastric patient response could provide an early indication of failed therapy and appropriate therapeutic intervention.

Liver

Patients with liver cancer have an increased level of sE-cad ($P <0.0001$; $P < 0.05$) (149, 164). The levels reported, however, are quite disparate with normal controls being reported as 2000 ng/ml or 5,798 ng/ml and cancer levels at 5550

ng/ml versus 10,759 ng/ml (149, 164). Soyama *et al* also demonstrated that levels of sE-cad in the serum of patients did not correlate with levels of E-cadherin in hepatic lesions, tumor markers, size, number, vascular invasion, stage, gender, age, or viral status (164). However, patients with levels higher than 8,000ng/ml were more likely to recur and metastasize ($P < 0.05$) (164). It appears that sE-cad could be a useful biomarker for disease spread and recurrence in liver cancer.

Non-epithelial

sE-cad levels can also be found in patients with non-epithelial tumors such as leukemia, multiple myeloma, and leiomyosarcoma. Patients with leukemia (myelogenous, monocytic, lymphatic) have increased levels of sE-cad ($P < 0.01$), as do patients with leiomyosarcoma ($P < 0.05$) (144). Multiple myeloma patients have five times higher levels of serum sE-cad than control samples ($P < 0.0001$) (165). sE-cad is also a survival predictor, where patients with levels of sE-cad below 3,000 ng/ml lived longer ($P = 0.0015$), and an increase in sE-cad of 100ng/ml increased their risk of death from multiple myeloma by 6% ($P = 0.013$) (165). In a non-epithelial setting, the source of sE-cad cannot come from the tumor cells themselves; instead it is more likely due to the tumors invasion into epithelial tissue. For example, leiomyosarcomas can occur in the smooth muscles cells of the stomach and grow into the stomach proper, resulting in epithelial tissue damage and shed sE-cad. In new multiple myeloma patients, sE-

cad levels could be used as a prognostic marker because high levels correlate with poor disease outcome (165).

Non-small cell lung (NSCLC)

In NSCLC patients, sE-cad serum levels are much higher than in healthy volunteers (3,455 ng/ml vs. 1,015 ng/ml; $P < 0.001$) and the highest levels of sE-cad also correlate with metastasis ($P < 0.001$) (166). There was, however, no statistically significant difference between the levels of sE-cad and histological type of cancer (adenocarcinoma, squamous cell carcinoma, or large cell carcinoma), sex, or smoking habit (166). Later studies confirmed these observations in NSCLC, but also demonstrated elevated levels of sE-cad in small cell lung cancer (SCLC) and that increasing levels of sE-cad correlated with metastasis in SCLC (167). This suggests that while sE-cad might be useful in determining whether a patient has metastatic disease, it would not be useful in disease classification.

As in gastric cancer, sE-cad levels in NSCLC can decrease following therapy. Reckamp *et al* evaluated serum sE-cad levels in NSCLC patients before and after Celecoxib and Erlotinib treatment (168). Although there was no difference between sE-cad levels between patients with partial response, stable disease, and progressive disease initially, after 8 weeks of therapy, patients who achieved a partial response had significantly lower levels of sE-cad than those with stable or progressive disease ($P = 0.021$) (168), suggesting sE-cad may be a useful marker for therapeutic response.

Ovarian

In an early report of sE-cad levels in ovarian cancer, Darai *et al* determined that the levels of serum sE-cad between luteal cyst, dermoid tumor, cystadenoma and malignant tumors did not vary significantly (169). Conversely, when the cyst fluid was examined, the levels of sE-cad were significantly (P = 0.001) higher in patients with malignant versus benign disease (169). Other researchers examined the ascites of benign ovarian disease or ovarian cancer patients and determined that patients with ovarian cancer had very high levels of sE-cad ($P < 0.000005$) (90). Gil *et al* later confirmed the presence of sE-cad in malignant ascites of women with advanced ovarian cancer (92). Because serum sE-cad levels fail to distinguish between benign and malignant disease, the use of sE-cad as a biomarker in ovarian cancer would have to be limited to cyst fluid or ascites.

Prostate

The initial report of sE-cad in prostate cancer by Kuefer *et al* demonstrated the presence of sE-cad in prostate cancer tissues, with increased expression in metastatic deposits and significantly elevated serum levels in patients with metastatic disease ($P < 0.001$) (170). Later studies comparing BPH, localized and metastatic prostate cancer sE-cad concentrations to healthy controls demonstrated significant differences (normal v. BPH P = 0.023; BPH v. localized prostate cancer P =0.011; localized v. metastatic $P < 0.001$) (151). In this study, Kuefer *et al* also evaluated sE-cad as a biomarker to predict outcome.

Surprisingly, sE-cad at the time of diagnosis could predict biochemical failure, mainly that localized disease with high levels of sE-cad (above 7.9ug/l) would likely result in late biochemical failure ($P < 0.05$) (151). In prostate cancer, therefore, sE-cad may be useful in stratifying patients, but the greatest use might be in categorizing high-risk for recurrence patients.

Skin

Levels of sE-cad in different types of skin cancer vary according to type. In basal or squamous cell carcinoma, the levels of serum sE-cad did not vary significantly from the healthy controls (171). In Paget's disease, the levels of sE-cad were significantly elevated above control samples, but only once the disease became invasive (171). In melanoma, early reports suggested that levels of sE-cad were elevated once patients had metastatic disease (171). Later studies confirmed that levels of sE-cad in melanoma patients were higher than in normal controls (3,198 ng/ml v. 4,975 ug/ml; $P < 0.05$), and the expression of sE-cad correlated with rising S100 values, indicating melanoma progression ($P < 0.05$) (85). Interestingly, high sE-cad levels were observed in some patients with low levels of S100, which the authors suggest, may be an indication that generation of sE-cad may serve as an early marker of progression for a subgroup of patients (85).

Non-cancer

Although sE-cad has been extensively studied as a biomarker in cancer, it has also been observed and evaluated as a biomarker for non-cancer conditions such as BPH, dermatitis, psoriasis, acute pancreatitis, diabetes, and diabetic nephropathy. In BPH patients, the levels of sE-cad were significantly higher than in normal control patients ($P = 0.023$) , but not as high as those patients with prostate cancer (151). Similarly, patients suffering from acute psoriasis and dermatitis had elevated levels of sE-cad in their serum, but unlike skin cancers where sE-cad levels correlated with invasion (85, 171), in the non-cancer setting, sE-cad correlated with the severity of the disease (171).

Serum concentrations of sE-cad are also predictive of acute pancreatitis. As of 2009, when the study was conducted, the standard tests for acute pancreatitis were poor predictors of severity (172), so Sewpaul *et al* hypothesized that because patients with systemic inflammatory response shed sE-cad (142), sE-cad could be a used as a marker for acute pancreatitis. Indeed, sE-cad levels were elevated in patients with mild acute pancreatitis (7,358 ng/ml) versus acute severe pancreatitis (17,789 ng/ml) versus healthy controls (5,181 ng/ml) ($P = 0.0166$; $P = 0.0039$) (172). The levels of sE-cad in severe acute pancreatitis were also significantly higher ($P = 0.0073$) than other abdominal inflammatory pathologies (acute diverticulitis, perforated duodenal ulcer, cholangitis, acute appendicitis, and acute cholecystitis), suggesting that sE-cad levels could be a specific predictor for acute severe pancreatitis (172). Most importantly, this study demonstrated that sE-cad levels at 12 hours from onset of

pain could predict the severity of pancreatitis, allowing for appropriate intervention (172).

In diabetes, levels of sE-cad in the sera or urine of healthy controls versus diabetic patients do not show significant difference (149, 173). However, sE-cad levels in the urine may be useful in determining which diabetic patients are suffering from diabetic nephropathy (173). The urine levels of diabetic patients with normoalbuminuria, microalbuminuria, and macroalbuminuria vary significantly ($P < 0.001$) , suggesting that sE-cad might be a biomarker for diabetic nephropathy (173).

Infection

For HIV infection, the levels of sE-cad correlate with viral load in patients. Interest in sE-cad in HIV infection arose from the observation that the intestine is a site of increased permeability in infected patients, suggesting a disruption in E-cadherin function (150). Indeed, high HIV viral titers significantly ($P = 0.004$) correlate with high levels of serum sE-cad, suggesting that sE-cad is a marker for severity of infection (150). Conversely, acute hepatitis does not elevate the levels of sE-cad above controls (149).

Organ dysfunction

The levels of sE-cad are significantly (P 0.0019) higher in patients with sepsis and organ dysfunction as compared to normal controls, and tend to increase with the amount of organ dysfunction and sepsis in the patient (142). In

surgery, the levels of sE-cad can be used as a biomarker of tissue injury and inflammation. For example, a comparison of open to laparoscopic cholecystectomy demonstrated that the less invasive laparoscopic procedure resulted in less sE-cad generated (P = 0.04) (143). These studies suggest that sE-cad levels in patient serum can be used to determine the extent of tissue damage and systemic inflammatory response.

Table 2-2: sE-cad can be found in the fluids of patients with multiple conditions

Patient diagnosis	Type	sE-cad correlates with:	Source	sE-cad Levels (ng/mL)	Ref
Cancer	Bladder	Cancer, grade, number, recurrence	Serum	N: 1013 C: 3955	(152)
		Cancer	Urine	N: .516 mg/mol C: 1.536 mg/mol	(153)
		Cancer, grade Recurrence	Urine	N: 1.306 +/- 1.249 mg/mol C: 3.724 +/- 1.892 mg/mol R: 10.497 +/- 7.47.1 mg/mol	(154)
	Colorectal	Cancer, Progression	Serum	N[1]: 3467 B[1]: 5248 C[1]: 5495	(156)
		Not significant	Serum	N: 3.53 C: 3.17	(155)
	Esophageal squamous cell carcinoma	Survival (surgery only)	Serum	PreOp: 5108.96 PreCRT: 3688.932 PostCRT: 3981.029	(157)
	Gastric	Cancer	Serum	N: 2515 +/- 744 C: 4735 +/- 2310	(158)
		Cancer	Serum	N: 5616 C: 9344	(159)
		Recurrence	Serum	sE-cad above 10000	(160)
		Survival	Serum	sE-cad above 10000	(161)
		Cancer	Serum	N: 2000 C: 3510 +/- 1790	(149)
	Liver	Cancer	Serum	N: 2000 C: 5550 +/- 3110	(149)
		Cancer	Serum	N: 5798 C: 10759	(174)
		Recurrence (early)		sE-cad above 8000	(174)
	Non-small cell lung	Cancer	Serum	N: 1015 C: 3455	(166)
		Metastasis	Serum	L[2]: 2487.8 M[2]: 4422.2	(75)
	Non-epithelial				

	Leimyosarcoma	Cancer	Serum	N: 2000 C: 3280 +/- 720	(149)
		Cancer	Serum	C: 2520 +/- 1000	(149)
	Leukemia	Cancer	Serum	N: 622.9 C: 3291.4	(165)
	Multiple Myeloma	Survival	Serum	s-Ecad above 3000	(74)
	Ovarian	Not significant	Serum	Luteal cyst: 3677 Dermoid tumor: 2325 Cystadenoma: 2200	(169)
		Cancer	Cyst	C: 2250 Luteal cyst: 2035 Dermoid tumor: ND Cystadenoma: 2000	(169)
		Malignant ascites	Ascites	C: 14500 N: 2061 +/-1968 C: 12241 +/-5314	(90)
		Present in ascites	Ascites	C: 89.96 (ug/uL)/ug total protein	(92)
	Prostate	Cancer, metastasis	Serum	N: 6.270 ug/l L: 9.460 ug/l M: 27.490 ug/l	(151)
	Skin				
	Basal cell	Not significant	Serum	N: 808 +/- 272 C: 879 +/-485	(171)
	Melanoma	Cancer, rising S100	Serum	N: 3198 C: 4975	(85)
		Cancer, metastasis	Serum	N: 808 +/- 272 M: Values not reported	(171) (171)
	Paget's	Invasion	Serum	C: Not reported	(171)
	Squamous cell	Not significant	Serum	C: 838 +/- 374	
Non-cancer	Acute pancreatitis	Severe cases	Serum	N: 5181 +/- 1350 D: 17780 +/- 7853	(172)
	Benign prostatic hyperplasia (BPH)	BPH	Serum	N: 6.27 ug/l B: 7.26 ug/l	(151)
	Diabetes	Not significant	Serum	N: 2000 D: 2330 +/- 1580	(149)
		Not significant	Urine	N: 652.7 +/-87 Diabetic: 721.9 +/-93	(173)
	Diabetic nephropathy (DN)	Nephropathy	Urine	N: 652.7 +/-87 DN0: 721.9 +/-93 DN1: 2751.5 +/- 164 DN2: 5839.6 +/- 428	(173)

	Inflammatory skin diseases Psoriasis Dermatitis	 Severe cases Severe cases	 Serum Serum	 Values not reported Values not reported	(171)
Infection	HIV	Viral load	Plasma	Values not reported	(175)
	Hepatitis	Not significant	Serum	N: 2000 D: 2340 +/- 520	(149)
Organ dysfunction	Multi-organ	Sepsis, organ dysfunction	Serum	N: 3280 D: 6000	(142)
	Cholecystectomy	Inflammation	Serum	Lap: 1850 +/- 250 Open: 3110 +/- 330	(143)

N: normal, C: cancer, M: metastatic D: disease, R: recurrence, NR: No recurrence, PreOp: Preoperative . CRT: neoadjuvant chemoradiation therapy. L: localized, M: metastatic, Mult: Multiple, ND: not detected, DN0: diabetic, no nephropathy, DN1: diabetic nephropathy, microalbuminuria, DN2: diabetic nephropathy, macroalbuminuria, Lap: laparoscopic [1]Value conversion from log (sE-cad ng/mL) to sE-cad ng/mL by Grabowska and Day. [2]Observation reported by study's author, but numbers generated by Grabowska and Day.

Consequences of sE-cad presence

Disruption of cell-cell interactions

The initial report by Wheelock *et al* demonstrated that sE-cad purified from MCF-7 cells was capable of disrupting cell-cell adhesion between mouse mammary tumor cells which were already growing in clusters (103) (Table 2-3). Later work demonstrated that treatment of ovarian cancer cell lines with a recombinant human ectodomain of E-cadherin fused to Fc, resulted in disruption of established cell junctions (90). In re-aggregation assays, pancreatic cancer cells and MDCK cells treated with sE-cad immunodepleted media, were more efficient at re-aggregating than the cells which were re-aggregating in the presence of conditioned media with sE-cad present (78, 86). The presence of sE-

cad can, therefore, not only disrupt established adherens junctions, but can also interfere with establishing adherence junctions in cell re-aggregation assays.

sE-cad can also interfere with immune cell interactions by serving as a dummy ligand for KLRG1 and interfering with anti-viral functions. In HIV-infected peripheral blood mononuclear cells, the presence of a recombinant sE-cad interfered with the ability of T cells to secrete IFN-gamma in response to HIV-1 Gag stimulation (150). Because KLRG1 on the $CD8^+$ T cells bound sE-cad, the HIV infected $CD4^+$ T cells were not targeted, resulting in an increase in survival of infected cells (150). These data suggest that sE-cad is sufficient to disrupt cell-cell interactions which has implications for epithelial tissue stability and immune response.

Migration and invasion

The presence of sE-cad can also induce cells to invade. Ovarian cancer cells exposed to Fc-Ecadherin invade through a modified Boyden chamber (92). Similarly, pancreatic cancer and MDCK cells exposed to conditioned media containing sE-cad versus conditioned media immunodepleted of sE-cad, show much greater inclination toward migration in the presence of sE-cad (86, 176). In the case of lung cancer, the presence of sE-cad in the conditioned media or in the form of an activating HAV peptide based on EC1 of E-cadherin, can induce MMP-2, -9, -14 transcription and activity as evaluate by zymography and increased invasion (177). sE-cad, therefore, can promote migration and invasion,

which may be due to its ability to induce additional metalloprotease activity to aid in these processes.

Signaling, proliferation, and survival

There have been several studies that have examined the specific effects of sE-cad presence on cells. In breast cancer cells, endogenous sE-cad can be observed bound to HER2 and HER3 by immunoprecipitation (44). Stimulation with exogenous Fc-Ecadherin results in phosphorylation of HER2 and HER3, as well as downstream ERK signaling (44). Work by Najy *et al* also demonstrated that using a recombinant sE-cad resulted in a proliferative response in breast cancer cells, which was not mediated by full length E-cadherin since the line has a homozygous deletion for CDH1 (44). In our studies, sE-cad can also bind EGFR and signal downstream through ERK (unpublished observations).

Conversely, in MDCK cells under serum free conditions, the anti-apoptotic signals provided by a myc-tagged sE-cad required E-cadherin expression (178). Treatment of these MDCK cells with a myc-tagged sE-cad resulted in signaling through EGFR and ERK (178). These studies suggest that sE-cad signaling is mediated by EGFR family members and, depending on the cellular context, may or may not be dependent on full length E-cadherin. Moreover, these studies suggest that sE-cad can stimulate proliferation and survival in non-transformed and transformed cells.

Discussion

Although the accumulation of sE-cad was initially believed to be solely related to tumorigenesis, cell culture studies have revealed that the generation of sE-cad can be mediated by several mechanisms in a variety of pathological states. E-cadherin cleavage can be induced by pro-inflammatory cytokines, bacterial infection, serum withdrawal, apoptosis, and growth factors (44, 78, 80-83, 85-87, 89-92, 104-109). To date, ADAMs (10 and 15), bacterial proteases (gingipains and BFT), cathepsins (B, L, S), MMPs (2, 3, 7, 9, and 14), KLK7, and plasmin have all been implicated in the generation of sE-cad (44, 78, 80-83, 85-87, 89-92, 104-109), but the study of E-cadherin processing is complicated by redundancy and the presence of proteolytic cascades.

Proteolytic cascades, much like signal transduction cascades, allow for the amplification of a stimulus. Mainly, when protease A is activated, it can activate protease B or C. The problem lies in determining whether it is protease A which is acting on the substrate or protease B or C, particularly when both protease belong to the same family, for example MMP-2, 9, and 13. The only true way to determine if a protease of interest cleaves a substrate is to use recombinant or purified proteins in an *in vitro* cleavage assay. This method requires the protease to be able to act upon the substrate without activating another mediator. The downside to this approach, however, is that it removes the protease and substrate from physiologically relevant situations, such as activation of the protease, presence of protease inhibitors, cell membrane interactions, as well as proteins associated with the substrate. Therefore, while

an *in vitro* cleavage assay will demonstrate cleavage in a best case scenario, it does not prove that the protease can act on the substrate in the context of a cell or biological system. The most thoroughly researched proteases, therefore, have extensive studies into their *in vitro* cleavage capabilities as well as complementing studies utilizing knockout animals, protease targeting shRNAs, as well as inhibitor studies.

Assuming all reports of E-cadherin sheddases are accurate, there is an astounding amount of redundancy in the generation of sE-cad. Because cell culture evidence suggests that sE-cad can disrupt cell adhesion, immune response, as well as induce signaling and invasion (Table 3) and is associated with disease severity in patients (Table 2), sE-cad may be more than a symptom of protease disregulation and may actually be contributing to the progression or severity of disease. Inhibiting E-cadherin cleavage, particularly in cancer, could be beneficial to patients and accomplished either by specific targeting of proteases implicated in a patient's disease or using broad-spectrum inhibitors. Due to the poorly understood complex role of protease families such as the MMPs in early clinical trials, unintentional targeting of the entire zinc metalloprotease family (MMPs and ADAMs), showed little efficacy in cancer patients with advanced disease (124), and has prompted the development of more specific inhibitors for specific proteases and families, such as inhibitors for ADAM10 and 17 and the MMPs (31, 32, 124). Although these specific inhibitors have not been designed for inhibiting E-cadherin cleavage per se, preventing the

generation of sE-cad could provide an additional, albeit unintended, benefit to patients undergoing cancer therapy.

Regardless of the source of sE-cad, based on the published data, there are several observations that come to mind. First, sE-cad is present in a myriad of conditions from cancer to infection to organ failure, which suggests sE-cad will not be a singular biomarker for any specific disease or type. Instead, the use of sE-cad in a clinical setting would, most likely, be a prognostic marker and be used in conjunction with other biomarkers. Another issue with sE-cad as a biomarker is the ranges of sE-cad reported vary greatly for normal controls, and whether this has to do with race (159), healthy volunteers with unknown medical problems, or technical differences between laboratories executing the ELISA remains unclear. Should sE-cad be used as a biomarker for severity of disease, then the ELISA would have to be standardized on a national or international level, and part of that would have to entail analyzing different populations for serum sE-cad concentrations. Another approach would be to divide the sE-cad values by the normal control values, generating fold change values, but even this method produces considerable by overlap between various disease states (Figure 2-1).

There are, however, several appealing aspects to using sE-cad in a clinical setting. For one, the majority of conditions use serum or urine samples, which are easy collection procedures versus needle biopsies, etc. Additionally, since sE-cad can be used to screen for many health issues, the ELISA could be run often in a diagnostic laboratory and contribute insights into disease severity,

progression, recurrence, therapeutic response, and prognosis. In disease severity, sE-cad can predict cases of severe acute pancreatitis after 12 hours of pain (172) as well as the levels of kidney dysfunction in diabetes patients (173). sE-cad levels can also predict disease progression and recurrence. On average, elevated sE-cad predicts gastric cancer recurrence an average 13 months before the recurrence (160), and higher levels of sE-cad in localized prostate cancer predict early recurrence (151). In melanoma, elevated levels of sE-cad in patients with low S100 values may also indicate patients likely to progress rapidly (85). Bladder, gastric, and liver cancer patients with high sE-cad levels are also more likely recur than patients with lower levels of sE-cad (152, 154, 160, 164). In terms of therapeutic response, NSCLC patients who have a partial response to Celecoxib and Erlotinib treatment show a decrease in sE-cad levels at 8 weeks (168). sE-cad is also an indicator of patient survival: esophageal squamous cell carcinoma, gastric cancer, and multiple myeloma patients with higher levels of sE-cad have a much shorter survival time than lower sE-cad patients (157, 161, 165). These studies provide convincing evidence that sE-cad may provide additional information on disease severity, progression, recurrence, and therapeutic response which could aid in determining appropriate therapeutic intervention.

Table 2-3: Consequences of sE-cad presence

Result	System	sE-cad source	Mechanism (if known)	Ref.
Disruption of adherens junctions	Ovarian cancer cell line Mouse mammary tumor cells	Recombinant, Fc fusion Antibody affinity chromatography		(90) (103)
Disruption of anti-viral function	Peripheral blood mononuclear cells from HIV patients	Recombinant sE-cad	Abrogation of IFN-gamma response	(175)
Disruption of cell aggregation	Pancreatic cancer cell line Canine kidney cell line	Immunodepletion Immunodepletion		(86) (176)
Invasion	Ovarian cancer cell line Pancreatic cancer cell line Lung cancer cells Canine kidney cells	Recombinant, Fc fusion Immunodepletion Immunodepletion; HAV peptide Immunodepletion	 Induction of MMP-2, 9, 14	(92) (86) (177) (176)
Proliferation	Breast cancer cells	Recombinant, Fc fusion	HER2/HER3 phosphorylation	(44)
Signaling	Breast cancer cells Canine kidney cells Peripheral blood mononuclear cell from HIV patients	Endogenous; Recombinant, Fc fusion Recombinant, myc tag Recombinant sE-cad	Binding to HER2/HER3 ERK signaling pERK/pAKT via EGFR KLRG1 ligation	(44) (178) (175)
Survival	Canine kidney cells	Recombinant, myc tag	EGFR signaling	(178)

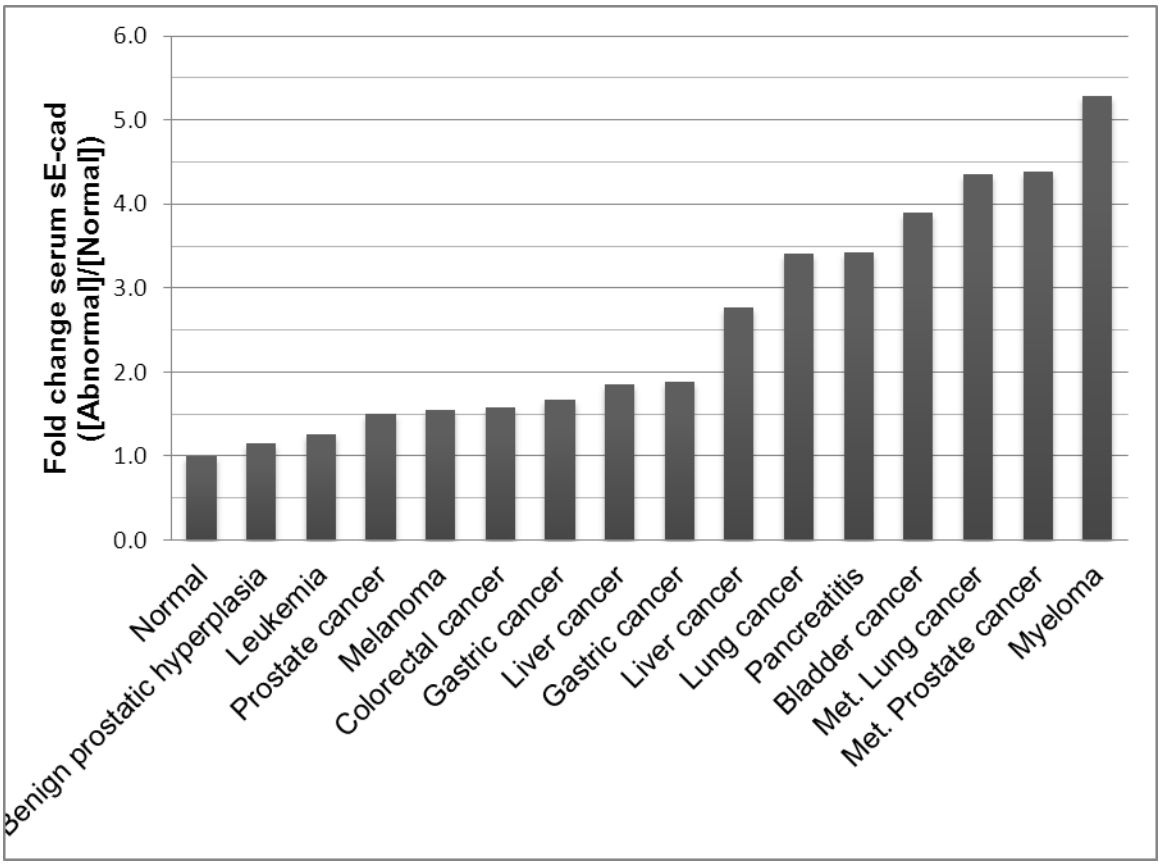

Figure 2-1: Comparison of serum sE-cad levels among various malignancies. Malignancy concentrations of sE-cad were divided by the average normal concentrations within each study to provide fold change values.

This work is an invited, peer-reviewed, and accepted review in *Frontiers in Bioscience* (citation unavailable at time of dissertation completion)

Chapter 3: EGF Promotes the Shedding of Soluble E-cadherin in an ADAM10-dependent Manner in Prostate Epithelial Cells

Abstract

During the progression of prostate cancer, the epithelial adhesion molecule (E)-cadherin can be lost from the cell surface by proteolytic processing, generating an extracellular 80kDa fragment referred to as soluble E-cadherin (sE-cad). Contrary to observations in cancer, the generation of sE-cad appears to correlate with ADAM10 activity in benign prostatic epithelium. The ADAM10-specific inhibitors INCB008765 and proA10 inhibit the generation of sE-cad, as well as downstream signaling and cell proliferation. Addition of EGF or amphiregulin to these untransformed cell lines increases the amount of sE-cad shed into the conditioned media and sE-cad bound to EGFR. EGF-associated shedding appears to be mediated by ADAM10 as shRNA knockdown of ADAM10 results in reduced shedding of sE-cad. To examine the physiologic consequence of sE-cad on benign prostatic epithelium, we treated BPH-1 and PrEC immortalized prostate epithelial cells with a sE-cad analog comprised of the human Fc domain of IgG_1, fused to the extracellular domains of E-cadherin (Fc-Ecad). The treatment of untransformed prostate epithelial cells with Fc-Ecad resulted in phosphorylation of EGFR and downstream signaling through ERK,

resulting in increased cell proliferation. Pre-treating BPH-1 and PrEC cells with cetuximab, a therapeutic monoclonal antibody against EGFR, decreased the ability of Fc-Ecad to induce EGFR phosphorylation, downstream signaling and proliferation. These data suggest that ADAM10-generated sE-cad may have a role in EGFR signaling independent of traditional EGFR ligands.

Introduction

The human prostate, which is the size of a walnut, is a secretory organ that sits at the base of the bladder and is comprised of epithelial cell acini, separated by fibromuscular stroma (1). Each acinus contains two compartments. The luminal compartment is comprised of AR positive, terminally differentiated, secretory luminal cells and terminally differentiating intermediate cells (2). The basal compartment contains proliferating, AR negative stem cells and transit amplifying cell, which can differentiate into terminally differentiating cells and finally luminal secretory cells (2).

Epithelial (E)-cadherin is a homophilic adhesion molecule, which is expressed at the baso-lateral membrane of epithelial tissues. At the adherens junction, adhesion requires E-cadherin dimerization with an adjacent homodimer and then further dimerization with a homodimer on an adjacent cell (65). Intracellular interactions of E-cadherin with beta-catenin, p120, and alpha catenin also support adhesion and stabilization of the adherens junction (72-75). E-cadherin can be lost from the cell surface by promoter hypermethylation, gene deletion and mutation or proteolytic cleavage (77, 94). Previously, we have

observed that E-cadherin can be shed into the serum of benign prostatic hyperplasia and prostate cancer patients (93). One of the sheddases implicated in E-cadherin cleavage is ADAM10 (83, 84, 179).

ADAM10 is a member of the A Disintegrin And Metalloprotease (ADAM) family of zinc-dependent metalloproteases which is composed of 40 members, of which 12 members (including ADAM10) are catalytically active (26). Family members are characterized by five extracellular domains: prodomain, metalloprotease, disintegrin, cysteine-rich, and EGF-like. The multiple domains of ADAMs allow for a myriad of functions including proteolysis, integrin binding, and signal transduction (26). ADAM10 disregulation in inflammation and disease has made the protein's catalytic domain a target for therapy (28, 31, 32). ADAM10 has been implicated in E-cadherin cleavage in keratinocytes and gastric cancer cell lines (83, 84). In the prostate, membranous ADAM10 expression is high in BPH patient samples (36), and E-cadherin and ADAM10 co-localizes at the adherens junction (29). Because ADAM10 is predominantly a sheddase, which is known to cleave epidermal growth factor (EGF)-like ligands from the cell-surface, thus promoting epidermal growth factor receptor (EGFR) family signaling (27), we hypothesized that ADAM10-generated sE-cad impacts EGFR signaling by binding EGFR.

The EGFR family (EGFR/HER1/ErbB1, HER2/Neu/ErbB2, HER3/ErbB3, and HER4/ErbB4) is a prominent group of receptor tyrosine kinases. Comprised of an extracellular ligand binding domain, a transmembrane region, and a cytoplasmic tail containing the tyrosine kinase domain, these receptors play

critical roles in development and cancer (7). In the normal adult prostate, EGFR is expressed in basal cells and is localized in the lateral membrane junctions between the basal and luminal epithelium, while in BPH patients, EGFR staining expands to include moderate staining in a portion of luminal epithelium (14). 36% of BPH samples over-express EGFR (15), and increased levels of EGFR expression correlate with BHP grade (16). Some studies have even reported that by immunohistochemistry, BPH samples express more EGFR than prostate cancer samples (14, 17). These results suggest that EGFR may be a component of a regulatory pathway involved in aberrant epithelial hyperproliferation and disease in the prostate gland (16, 18).

This is the first study demonstrating a functional interaction between sE-cad and EGFR using benign prostatic epithelial models. This study also describes a novel and potentially important signaling axis involving sE-cad shedding and EGFR binding. Characterization of this signaling mechanism in the prostate would establish the sE-cad/EGFR axis as a potentially important mechanism of benign prostatic epithelial proliferation and possibly tumorigenesis.

Materials and Methods

Cell culture

Benign prostatic hyperplasia -1 (BPH-1) cells were generated by immortalizing human BPH cells with SV40 Large T antigen by Hayward *et al* (180). BPH-1 cells express cytokeratins consistent with prostatic luminal epithelial cells (positive for keratins 7, 8 18, 19; negative for the basal marker

keratin 14), but do not express AR protein or mRNA (180). BPH-1 and prostate epithelial cells immortalized with large T antigen (PrEC) were cultured in RPMI 1640 (Lonza) with 8% fetal bovine serum (HyClone) and 2mmol/L L-glutamine (Invitrogen) and Pen/Strep Amphotericin B (Pen/Strep: 10,000U/mL, Ampho 25ug/mL; Bio Whittaker). Knockdown cells lines were additionally supplemented with 100ug/uL Zeocin. Cells were incubated at in cell culture dishes (BD Falcon) at 37°C and 5% CO_2 in Forma Series II incubators (Thermo) with water pans (80% relative humidity achieved from evaporation).

Cell treatments

Cells were pretreated with or treated in serum free (SF), phenol free RPMI (Gibco) and 2mmol/L L-glutamine (Invitrogen) and Pen/Strep Amphotericin B (Pen/Strep: 10,000U/mL, Ampho 25ug/mL; Bio Whittaker). Cells in Figure 3-4C,D were pre-treated with SF media for 1hr prior to abrogate autocrine EGFR signaling. Stock solutions of cell treatments: 10ng/uL EGF in PBS, 100ng/uL amphiregulin in PBS, 100ng/uL Fc-Ecadherin in PBS (R&D Systems), 100ng/uL Fc in PBS (R&D Systems); .05M 1,10 phenanthroline in methanol (Sigma); 10mM INCB008765 in DMSO (Incyte); prodomain of ADAM10 (proA10) in 10% glycerol/PBS (Biozyme); 2mg/mL cetuximab (ImClone).

Protein isolation, Western blotting and immunoprecipitation

Cells were harvested by scraping and lysed as previously reported (24). Lysates were pelleted at 12,000rpm for 8 minutes at 4°C. The supernatants were

collected and quantitated using a Bradford assay (BioRad) with each sample being run in triplicate. For western blotting, equal amounts of protein were loaded into precast Tris-glycine SDS gels (Invitrogen) and transferred to nitrocellulose membranes (Millipore). Blots were blocked with 10% milk in TBST buffer, probed with antibodies diluted in 2.5% milk in TBST, and developed using ECL (Pierce; high sensitivity Millipore). Antibodies: E-cadherin (HECD-1, Invitrogen); EGFR (Ab-15, Neomarkers); ADAM10, tubulin (Millipore); phosphoERK, ERK, phosphoEGFR Y992, phosphoEGFR Y1068 (Cell Signaling). Signaling Western blots were quantitated using ImageJ (NIH) software, dividing phosphorylated by total amounts of protein, and normalized to untreated control lanes.

For immunoprecipitation (IP), 500ug of protein were pre-cleared with 100ul of a 50/50 mix of Sepharose A beads (Invitrogen), 2.5% milk in TBST, and 1ug of control IgG for 30 minutes with end over end rotation. Lysates were then spun down for 3min at 8,000rpm and supernatants were transferred to new tubes containing 1ug of antibody and rotated end over end for 1hr at 4°C. Beads were then added and after another hour of rotation, IPs were spun down for 3min at 8,000rpm and supernatants aspirated. Beads were washed three times in PBS and spun down. After final wash, the supernatant was removed and 35ul of βmercaptoethanol-containing loading buffer (50 mM Tris-HCl, pH 6.8; 2% SDS; 10% Glycerol; 1% β-Mercaptoethanol;12.5 mM EDTA, 0.02 % Bromophenol Blue) was added to the beads. After 5min incubation at 100°C, IPs were again spun down and supernatants collected.

In vitro cleavage assay

The in vitro cleavage assay has been previously described (24). Briefly, immunopurified ADAM10 and E-cadherin were combined in Eppendorf tubes in PBS for 8hrs at 37°C. After incubation, 15ul of BME-containing loading buffer were added and samples were boiled for 5min, spun down, and supernatants collected.

Proliferation assays

5,000 BPH-1 or 10,000 PrEC cells were plated in each well of a 96 well dish and allowed to grow for 24hrs. Cells were then washed and placed in serum free media and allowed to recover for 1hr. After 1hr in serum free media, cells were supplemented with treatments for 24hr to 48hrs in quadruplicate, at which point, CellTiter-Blue (Promega) was added and incubated for 1-4hrs. CellTiter Blue is a metabolic assay which determines cell viability by measuring the amount of resazurin dye converted to fluorescent resorufin by live cells (Promega). Plates were read on a Gemini Microplate Reader and normalized to serum-free control values at each time point. With the exception of Figure 3-6, which is a representative experiment analyzed using the Kruskal-Wallis and Dunn's multiple comparison test, three independent experiments were combined, and statistical analysis was performed by Graphpad Prism utilizing the one-way ANOVA or paired t-test, as appropriate, and graphed as the mean with the standard error of the mean (SEM) for error bars. Values were considered significant if $P < 0.05$.

Generation of shA10 and shEGFP constructs

Knockdown cell lines for BPH-1 and PrEC were generated by lentiviral transduction of short hairpin constructs for ADAM10 (forward: CAC CGC AGG TTC TAT CTG TGA GAA ACT CGA GTT TCT CAC AGA TAG AAC CTG C; reverse: AAA AGC AGG TTC TAT CTG TGA GAA ACT CGA GTT TCT CAC AGA TAG AAC CTG C) and EGFP (forward: CAC CGC CAC AAC GTC TATA TCA TGG CGA ACC ATG ATA TAG ACG TTG TGG C, rev: AAA AGC CAC AAC GTC TAT ATC ATG GTT CGC CAT GAT ATA GAC GTT GTG GC) with Zeocin antibiotic resistance (Invitrogen). Lentivirus was generated by transfection (Tfx^{TM}-20, Promega) of HEK 293T cells with plasmids encoding lentiviral components (pFG12 containing shRNA, RCE, HCMV promoter, RSV Reverse transcriptase) and treating BPH-1 and PrEC cells with Millex-HV PVDF (.45um; Millipore)-filtered conditioned media from infected cells for 24hrs in the presence of polybrene (6ug/ml). After infection, culture media was supplemented with 100ug/mL Zeocin.

Results

Proteolytic activation of ADAM10 correlates with generation of sE-cad in immortalized prostate epithelial cells.

Previously, we demonstrated that ADAM15-mediated shedding of sE-cad supported signaling through HER2 in human breast cancer cells (24). To determine whether this mechanism plays a role in normal prostate biology, we evaluated sE-cad in prostate epithelial cells immortalized with large T antigen

(PrEC) and benign prostatic hyperplasia cells (BPH-1). Under serum free conditions, sE-cad is generated in normal (PrEC) and hyperplastic (BPH-1) cells and shed into the media (Figure 3-1A). Unlike our previous studies, active ADAM15 does not correlate with sE-cad; instead presence of active ADAM10 correlates with increased sE-cad, suggesting that ADAM10 plays a role in the cleavage event of E-cadherin in untransformed epithelial cells. Indeed, ADAM10 immunopurified from BPH-1 cells is capable of cleaving E-cadherin to sE-cad *in vitro*, which can be inhibited by the addition of the ADAM10-specific inhibitors INCB008765 (INC, Incyte) and the prodomain of ADAM10 (BIO, Biozyme). The broad-spectrum metalloprotease inhibitor 1,10-phenanthroline (OPT) can also inhibit the generation of soluble E-cadherin (Figure 3-1B).

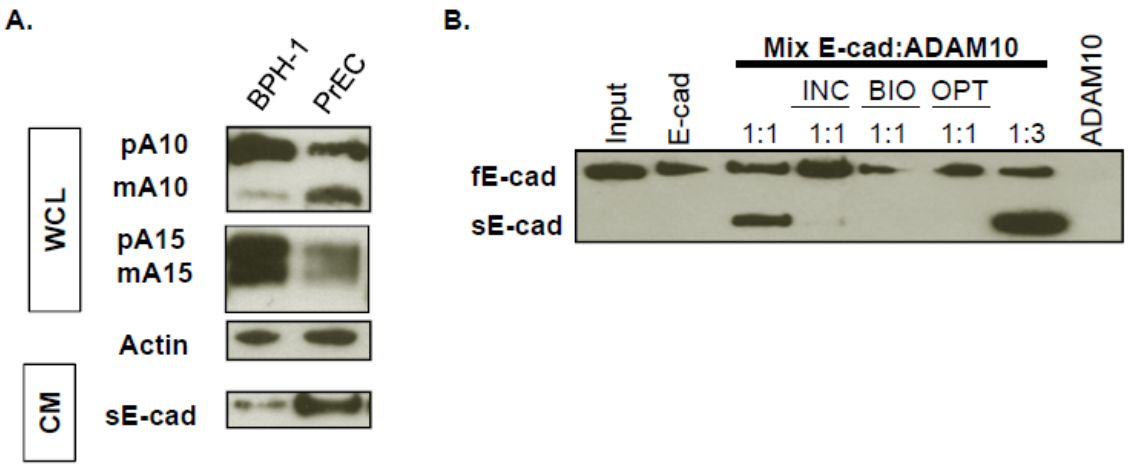

Figure 3-1: Generation of sE-cad is associated with active ADAM10 expression in untransformed prostate epithelial cells. A. ADAM10 and ADAM15 profiles of BPH-1 and PrEC cells treated with serum free medium for 24hrs. B. 8hr *in vitro* cleavage assay with ADAM10 and E-cadherin immunopurified from BPH-1 cells using ADAM10 specific inhibitors: Incyte inhibitor INCB008765 (INC), Biozyme ADAM10 prodomain (BIO), and broad spectrum metalloprotease inhibitor, 1,10-phenanthroline (OPT). CM: conditioned medium. WCL: whole cell lysate. sE-cad: soluble E-cadherin. fE-cad: Full length E-cadherin. pA10: pro form of ADAM10. mA10: mature form of ADAM10. pA15 pro form of ADAM15. mA15: mature form of ADAM15. E-cad: E-cadherin. 1:1: Reconstituted 1 aliquot E-cadherin with 1 unit ADAM10. 1:3: 1 unit E-cadherin with 3 units of ADAM10.

ADAM10 supports downstream signaling and proliferation in immortalized prostate epithelial cells.

Because ADAM10 is a major sheddase of pro-forms of growth factors, we hypothesized that ADAM10 supports cell signaling and proliferation in prostate epithelial cells. Unsurprisingly, inhibition of ADAM10 with the small molecule inhibitors (INC) or its prodomain (BIO) in BPH-1 cells reduces signaling through ERK (Figure 3-2A). OPT treatment of BPH-1 cells inhibits all metalloproteases and completely inhibits pERK signaling, suggesting there are metalloproteases beyond ADAM10 than contribute to ERK signaling. Inhibition of ADAM10 by INC also reduces proliferation in BPH-1 cells as compared to vehicle (DMSO) controls (Figure 2B). ADAM10 knockdown in PrECs results in a dramatic loss of phosphoERK signaling as compared to scrambled control cells, which cannot be rescued by the addition of EGF alone (Figure 3-2C). Loss of ADAM10 also results in a decrease in PrEC proliferation (Figure 3-2C, D).

sE-cad generation is promoted by EGF and mediated by ADAM10

In untransformed cells, the shedding of sE-cad into conditioned media is promoted by the addition of EGF or amphiregulin (AREG), and increasing concentrations of these EGFR ligands results in increasing levels of sE-cad as compared to serum free controls (Figure 3-3A). Interestingly, EGF promotes more sE-cad generation than AREG. We theorized that this EGFR ligand promoted generation of sE-cad was mediated by ADAM10 and we generated knockdown cell lines to test this hypothesis. As expected, ADAM10 knockdown in

BPH-1 and PrEC cells reduced sE-cad generation (Figure 3-3B,C), suggesting that ADAM10 is responsible for E-cadherin cleavage in normal prostate epithelium.

sE-cad binds EGFR in response to EGF and AREG

Based on our previous studies in breast cancer cells (24), we theorized that sE-cad could play a role in downstream signaling in normal prostate epithelium. In order to determine whether traditional ligands could compete with sE-cad for binding to EGFR, we treated BPH-1 and PrEC cells with the high-affinity ligand EGF or the low affinity (181) ligand AREG. In the presence of these ligands, there is more sE-cad bound to the receptor as compared to untreated controls (Figure 3-4A,B), suggesting that EGFR ligands promote the interaction between EGFR and sE-cad in BPH-1 and PrEC cells. As in the conditioned media experiment, EGF treatment resulted in more sE-cad bound to EGFR than AREG treatment.

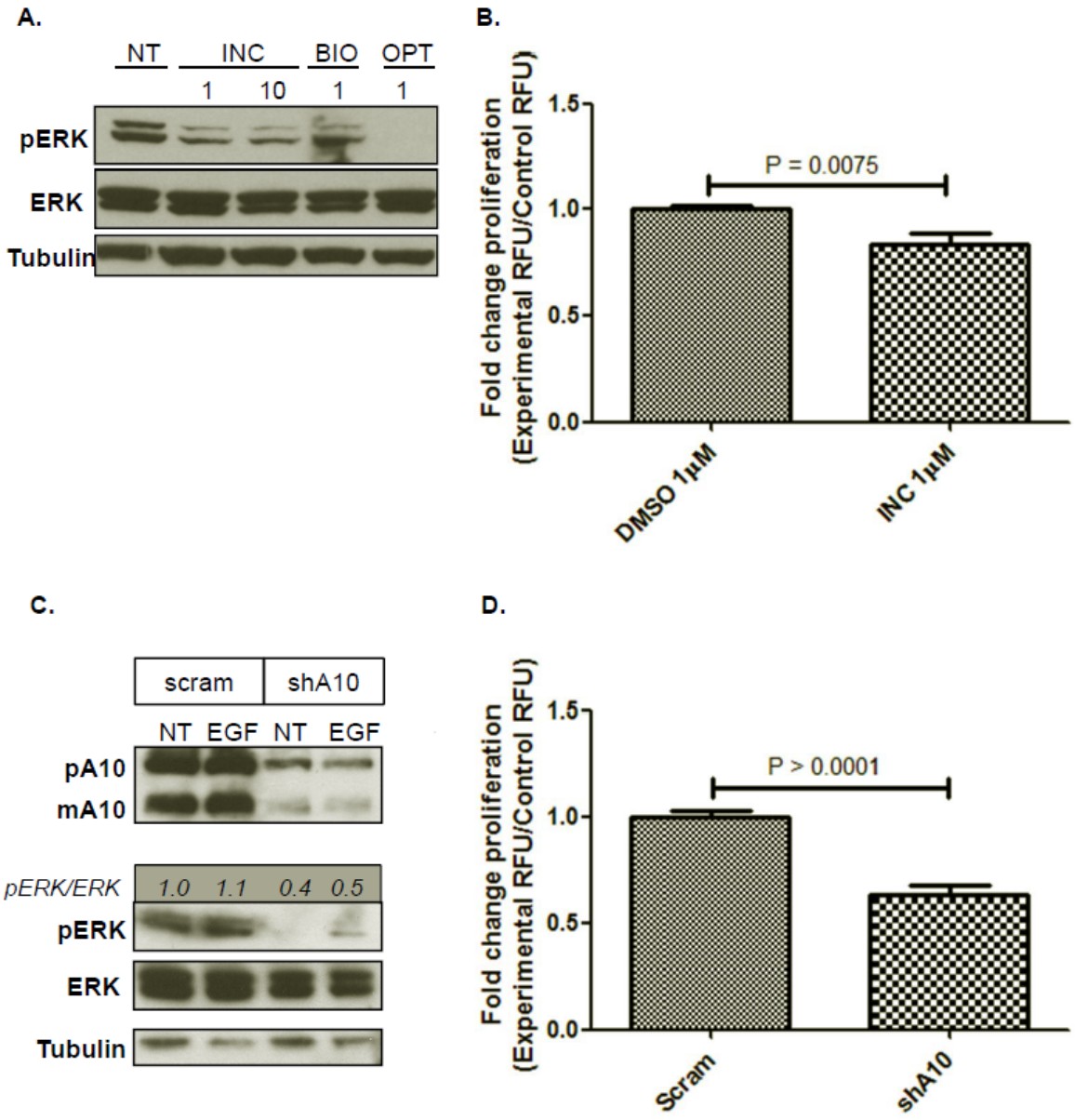

Figure 3-2: ADAM10 contributes to downstream signaling and proliferation in untransformed prostate epithelial cells. A. BPH-1 cells treated with ADAM10 specific inhibitors (1uM, 10uM INC;1uM BIO) for one hour show decreased pERK signaling, while the broad spectrum metalloprotease inhibitor OPT (1mM) abolishes all pERK signaling. B. BPH-1 cells treated with INC also show decreased proliferation at 24hrs compared to DMSO (vehicle). C. Knockdown of ADAM10 in PrEC correlates with a decrease in pERK signaling after 15min (without 1hr pre-treatment in serum-free medium), which could not be rescued by 5nM EGF treatment. D. ADAM10 knockdown also results in a decrease in proliferation at 24hrs. Western blots were quantitated using ImageJ and normalized to untreated cells. Changes in phosphorylated ERK (grey box) are represented as fold change over total ERK and normalized to the no treatment (NT) lanes. (D). Scram: non-specific shRNA control. shA10: shADAM10. pERK: phosphoERK. *pERK/ERK*: Fold change in ERK phosphorylation.

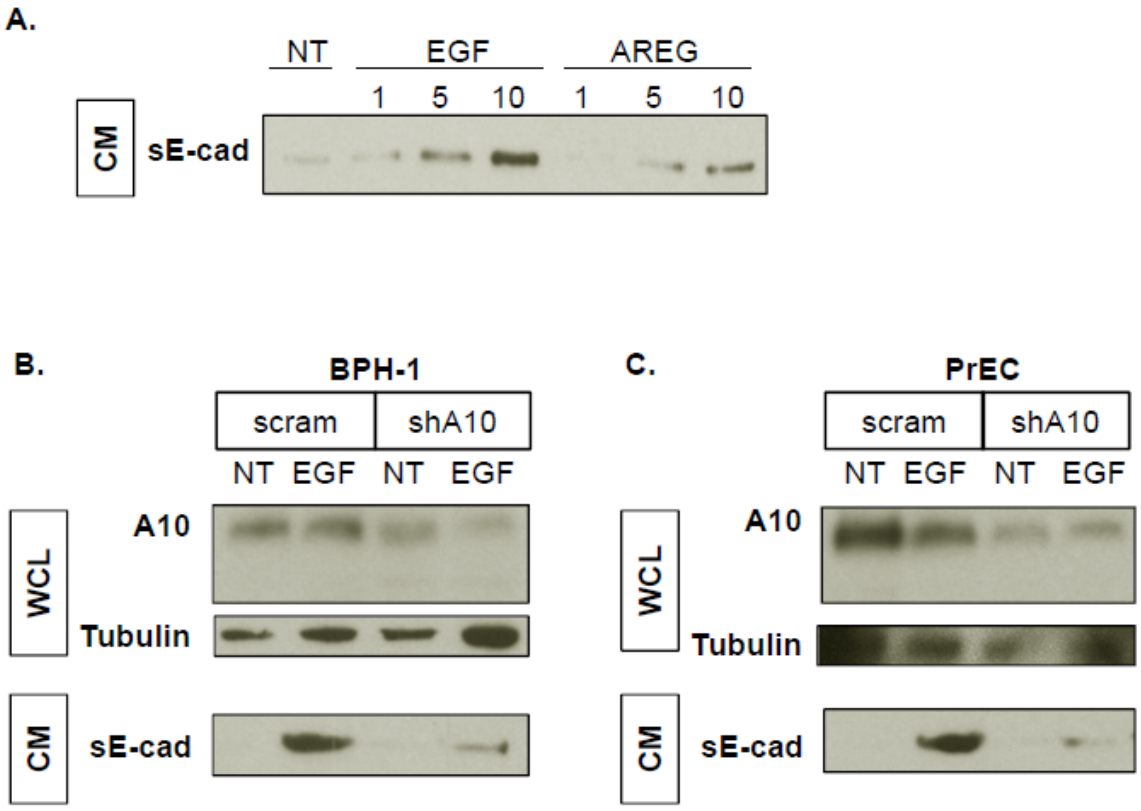

Figure 3-3: EGFR ligands promote the generation of sE-cadherin in an ADAM10-dependent manner. A. Treatment of BPH-1 cells with increasing concentrations of EGF and amphiregulin (AREG) results in increased sE-cad in the conditioned medium at 24 hours. The loss of ADAM10 by shRNA knockdown reduces the amount of sE-cad shed in response to 5nM EGF stimulation in BPH-1 (B) and PrEC (C) cells after 24hrs. CM: conditioned medium. WCL: whole cell lysate. NT: no treatment.

Fc-Ecadherin binds the extracellular domain of EGFR and induces receptor phosphorylation and downstream signaling.

In order to determine the effect of sE-cad on non-transformed epithelial cells, a commercially available sE-cad analog was used. Fc-Ecadherin (Fc-Ecad) is a chimeric protein of human IgG_1 and the five extracellular domains of E-cadherin, which is the same as sE-cad fused to human IgG_1. Treatment of BPH-1 and PrEC cells with 1nM Fc-Ecad results in the phosphorylation of EGFR at residues Y992 and Y1068, which correspond to activation of the ERK pathway (182, 183), and results in downstream ERK signaling as compared to treatment with Fc alone (Figure 3-4C, D). The addition of Fc-Ecad to the untransformed cell lines also supports an increase in proliferation as compared to the Fc domain alone (Figure 3-5A, B). The increased proliferation observed with Fc-Ecad can partially rescue the proliferation defect observed in the BPH-1 and PrEC shADAM10 cell lines, suggesting that sE-cad signaling may be a component of ADAM10-mediated proliferation and signaling (Figure 3-6A, B).

Because this proliferative effect is mediated by EGFR, we theorized that pre-treatment of BPH-1 and PrEC cells with cetuximab, a therapeutic monoclonal antibody against the extracellular domain of EGFR, would prevent Fc-Ecad induced signaling. Indeed, pre-treatment of BPH-1 and PrEC cells with cetuximab is enough to reduce the amount of ERK signaling induced by Fc-Ecad and EGF (Figure 3-7A, B). Cetuximab pre-treatment is also sufficient to reduce the proliferative effect of Fc-Ecad for BPH-1 and PrEC cells (Figure 3-7C, D).

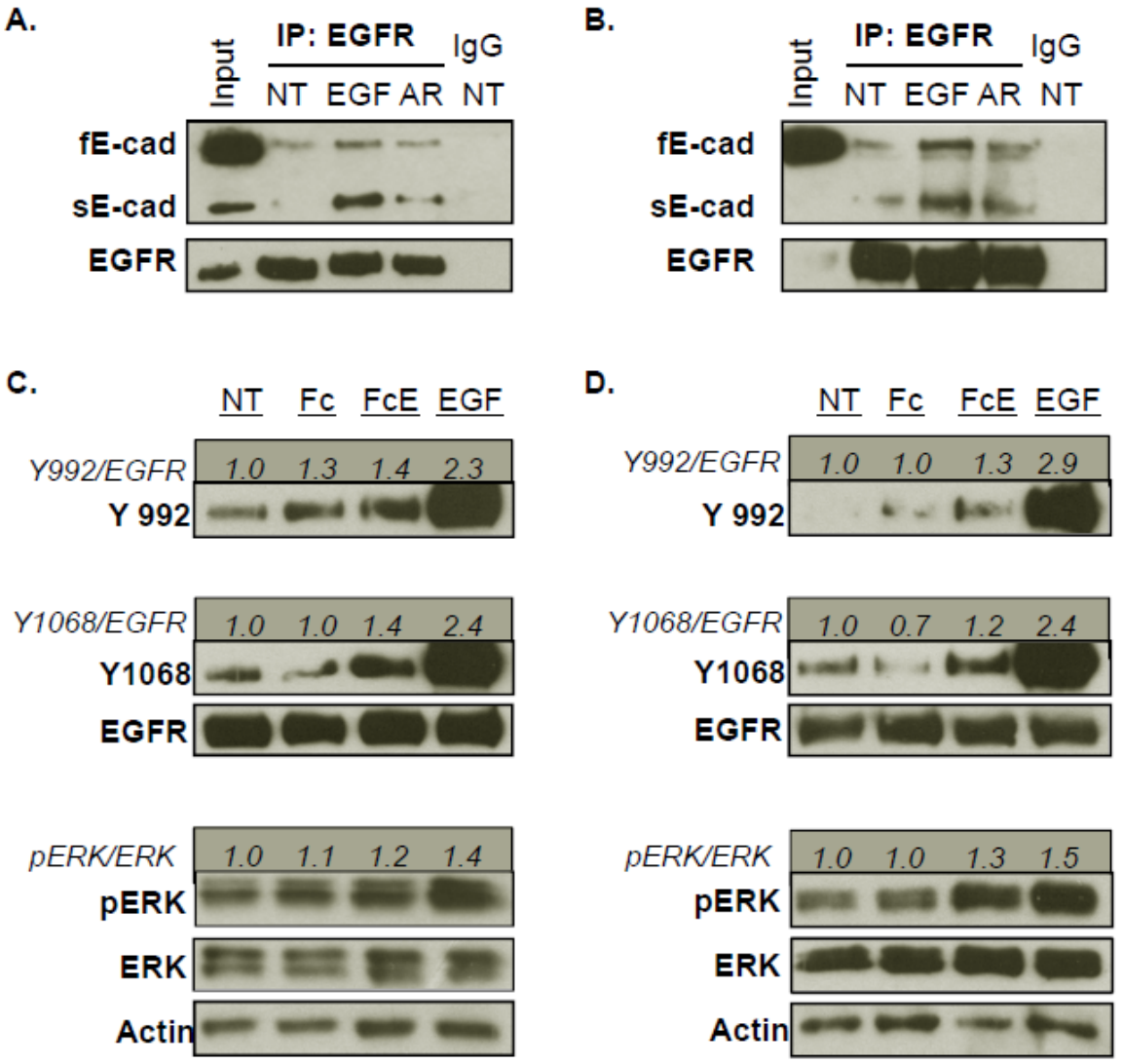

Figure 3-4: sE-cad can bind EGFR and result in downstream signaling. The addition of 5nM EGF and AREG (AR in figure due to space limitations) for 15 minutes also increases sE-cad association with EGFR in BPH-1 (A) and PrEC (B) cells. Treatment of BPH-1 cells (C) and PrEC (D) cells with 1nM Fc-Ecad for 15 minutes results in increased phosphorylation of EGFR at tyrosine residues 992 (Y992), 1068 (Y1068) and increased phosphorylation of ERK, as compared to untreated and 1nM Fc domain (Fc) treated cells. Western blots were quantitated using ImageJ and normalized to untreated cells. Changes in phosphorylated EGFR or phosphorylated ERK (grey boxes) are represented as fold change over total EGFR or ERK and normalized to the no treatment (NT) lanes. fE-cad: full length E-cadherin. sE-cad: soluble E-cadherin. *Y992/EGFR*: Fold change tyrosine residue 992 phosphorylation. *Y1068/EGFR*: Fold change tyrosine residue 1068 phosphorylation. *pERK/ERK*: Fold change in ERK phosphorylation.

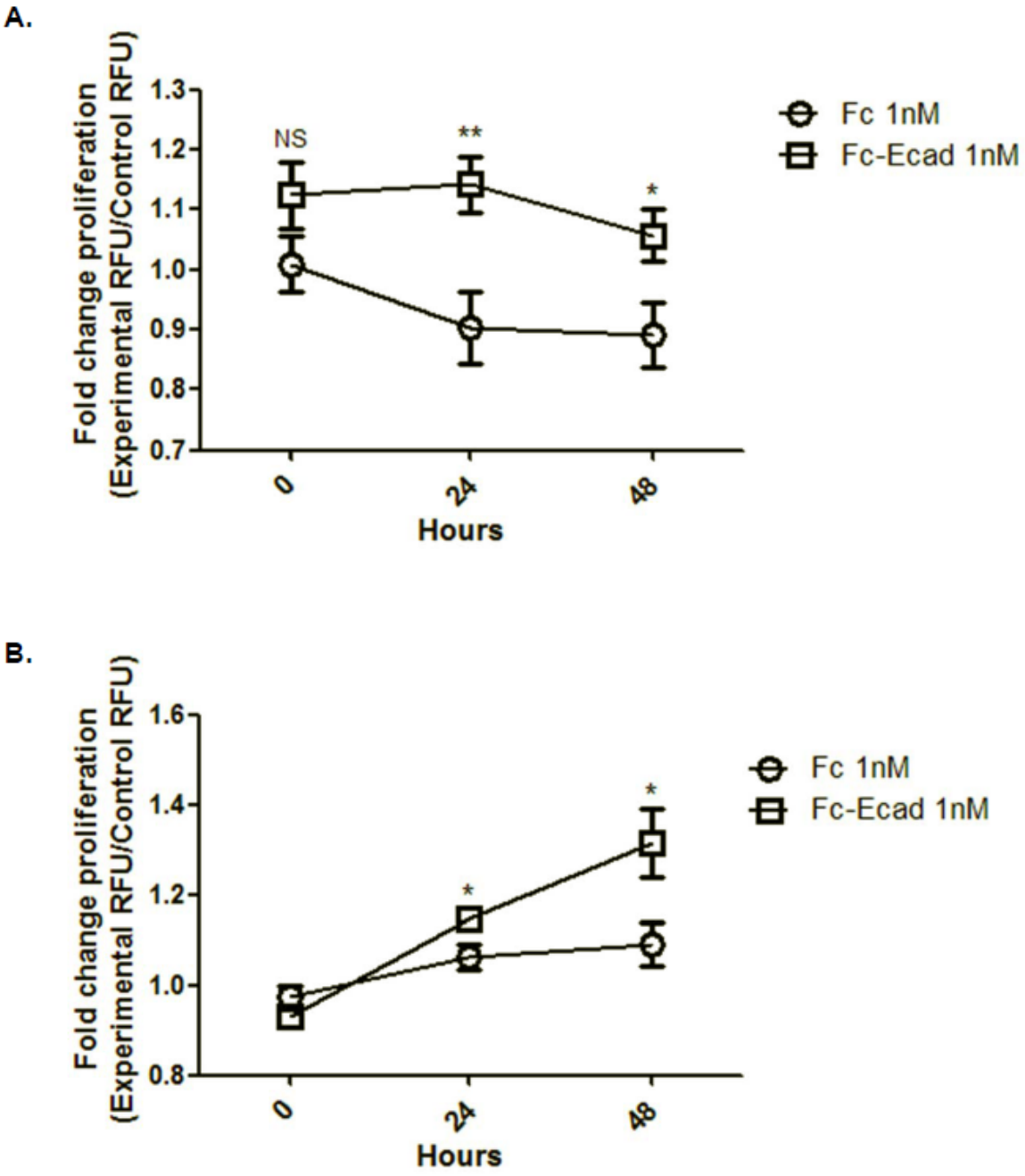

Figure 3-5: Fc-Ecad induces proliferation. BPH-1 cells (A) and PrEC (B) cells respond proliferatively to Fc-Ecad as compared to Fc domain alone. Values were considered significant if $p<0.05$. NS: not significant. *: $p< 0.05$. **: $p < 0.01$.

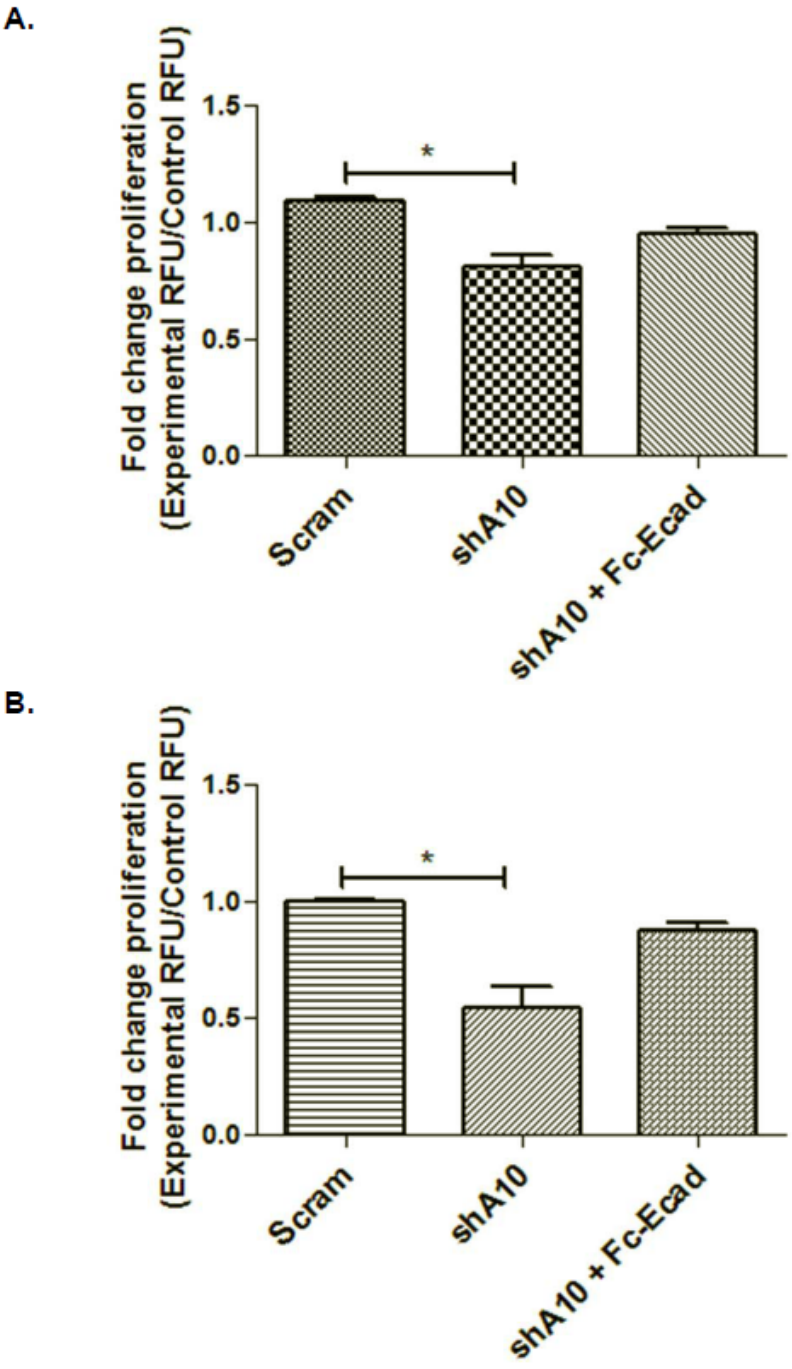

Figure 3-6: Fc-Ecad can partially rescue the proliferation defect in shADAM10 cells. Loss of ADAM10 in BPH-1 (A) or PrEC (B) cells results in decreased proliferation as compared to scramble control cells. 1nM Fc-Ecad stimulation of the BPH-1 shA10 (A) and PrEC shA10 (B) cells results in partial rescue of this proliferation defect. Values were considered significant if $p<0.05$. *: $p< 0.05$.

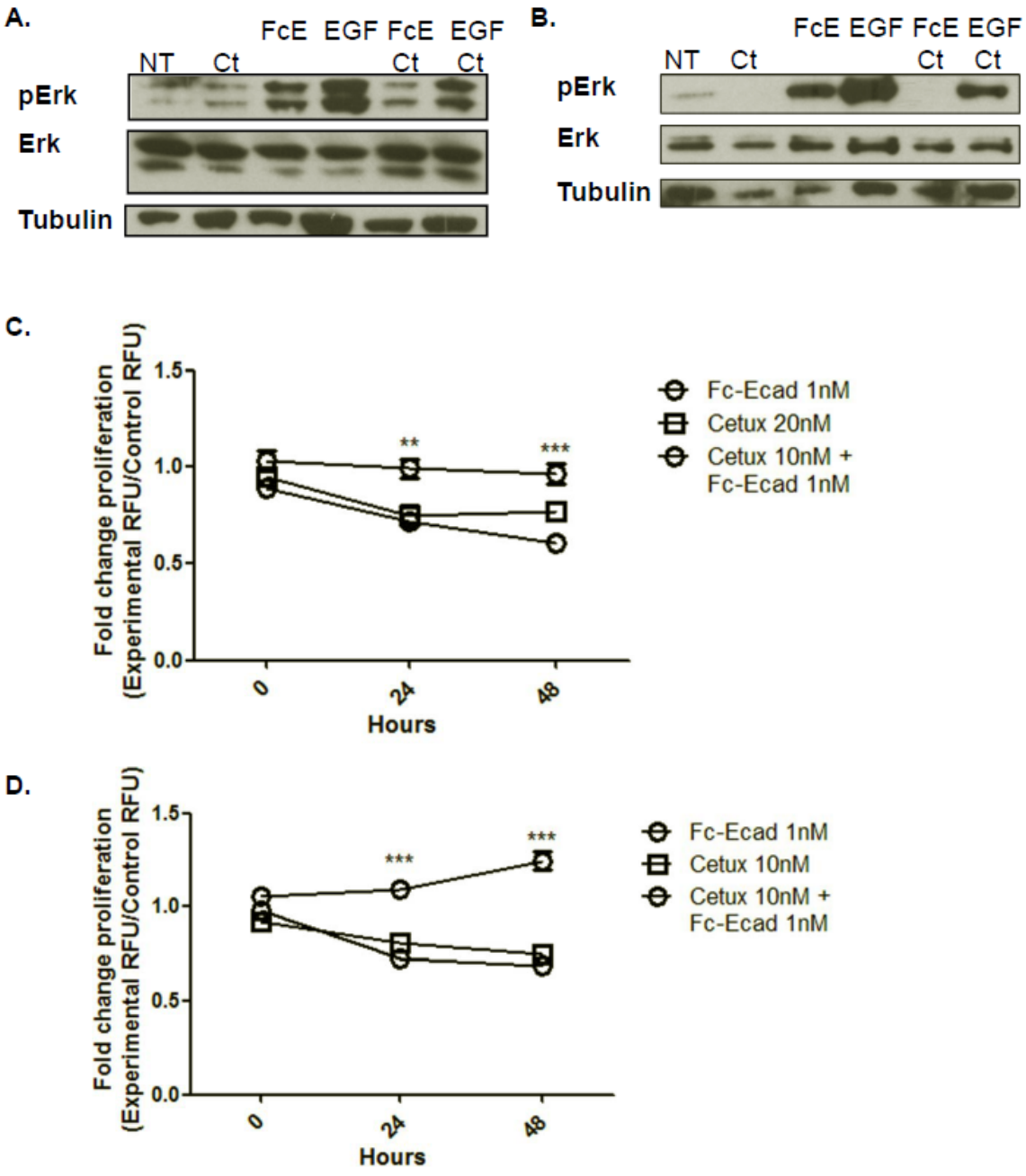

Figure 3-7: Cetuximab inhibits signaling and proliferation in response to Fc-Ecad. BPH-1 (A) and PrEC (B) cells pre-treated with 10nM cetuximab (Ct) for one hour show inhibition of phosphoERK signaling in response to 5nM EGF (E) and 5nM Fc-Ecad (FcE). BPH-1 (C) and PrEC (D) Fc-Ecad induced-cell proliferation is inhibited by cetuximab at 10nM and 20nM concentrations, respectively. Asterisks denote significant difference between Fc-Ecad and Fc-Ecad+Cetuximab treated cells NT: no treatment. *: $p< 0.05$. **: $p < 0.01$. *** $p < 0.001$.

Discussion

E-cadherin plays critical roles in epithelial cell maintenance, and its loss from the cell surface during tumor progression has been well documented. Previous work in the lab has focused on the accumulated 80kDa fragment known as sE-cad and the metalloprotease responsible during breast and prostate cancer progression (43, 93, 170). While ADAM15 appears to be the predominant metalloprotease responsible for sE-cad shedding in breast and prostate cancer, it may not play a significant role in normal prostate biology.

This work has demonstrated that ADAM10 plays a significant role in the proliferation of prostate epithelium, and that by blocking ADAM10 activity or reducing its expression results in decreased cell signaling and division, which is in accordance with earlier studies by Kasina *et al* (30). We also demonstrated that non-transformed prostate epithelial cells can be induced to generate sE-cad by the addition of EGF or AREG and that this process is dependent upon ADAM10. While the cleavage of E-cadherin by ADAM10 is not a novel finding (84, 179), this is first report of it in prostate epithelial cells.

Additionally, the promotion of sE-cad generation by EGF suggests that shedding of E-cadherin may contribute to epithelial to mesenchymal transition (EMT) in pathologies such as BPH and prostate cancer. The loss of differentiated epithelial phenotypes and the acquisition of motility and invasiveness which are the hallmarks of EMT, play critical roles in tumor progression (96, 184). In prostate cancer, EMT drives bone metastasis (97), and emerging evidence suggests EMT may play a role in BPH as well (99). In BPH, there is a substantial

increase in the amount of stroma surrounding the epithelium (2), and work by Alonso-Magdalena *et al* suggested that in human samples, the disease did not arise from stromal proliferation, but from mesenchymal cells derived from the epithelium, implicating the process of EMT (99). This process can be recapitulated *in vitro,* where BPH-1 cells can be induced to undergo EMT by TGF-β1 (185). Our observations of elevated levels of sE-cad in BPH patients (93), coupled with high expression of ADAM10 (36) and EGFR (14-16, 18), suggests that the cleavage of E-cadherin induced by an EMT activator such as EGF (186) may contribute to EMT progression. Furthermore, the emerging evidence for the role of inflammation in BPH (2), coupled with the ability of proinflammatory cytokines to induce ADAM10 activity (84), suggests other factors could induce sE-cad cleavage as well.

While previous publications from our group have demonstrated that sE-cad can bind to HER2 and HER3 (44), and other studies have reported the interaction of full length E-cadherin and EGFR extracellular domains (70), this is the first report of the sE-cad bound to EGFR in a prostate cell line model. Our studies have also demonstrated that Fc-Ecad can induce phosphorylation of EGFR, support downstream signaling and culminate in increased proliferation. These experiments suggest that sE-cad binding to EGFR may play a role in aberrant proliferation of prostate epithelial cells and EMT as described in BPH (Figure 3-8). Other studies have demonstrated that sE-cad can disrupt cell adhesion, anti-viral function, cell aggregation (77, 78, 86, 90, 175), and support invasion, migration, proliferation, and survival (44, 78, 86, 92, 175, 177, 178).

Taken together, these results suggest that EGF promoted-ADAM10 cleavage of E-cadherin may contribute to proliferative disorders by allowing sE-cad to bind EGFR and alter downstream signaling and proliferation in prostate epithelium.

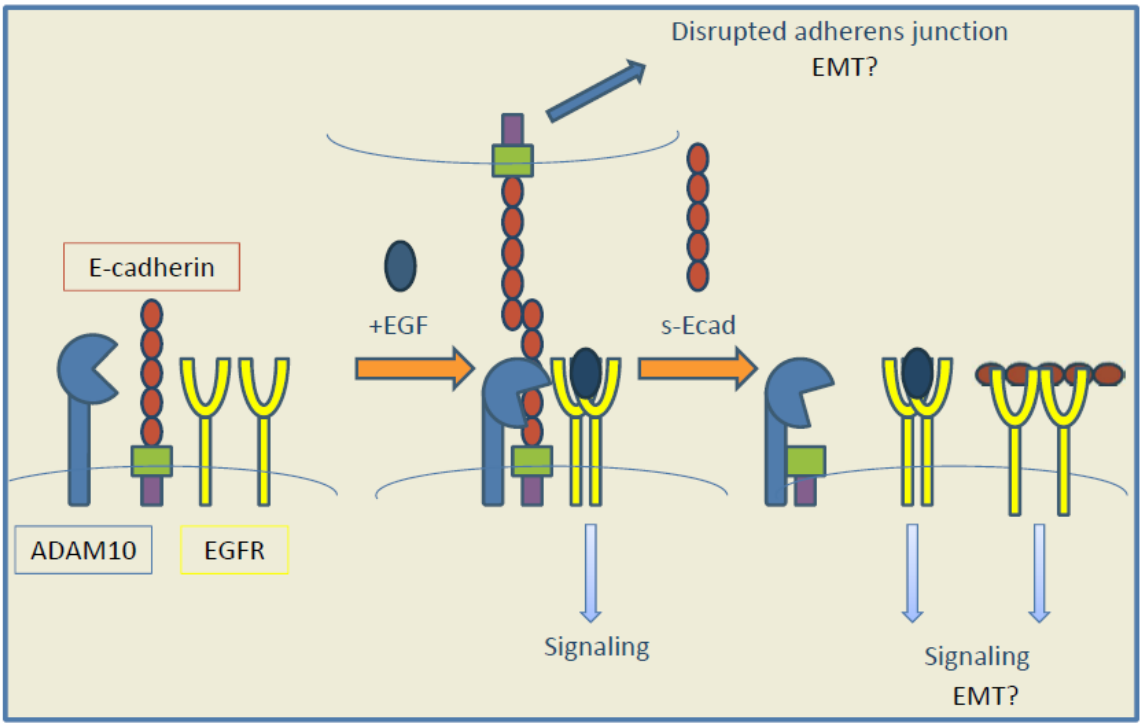

Figure 3-8: The sE-cad/EGFR signaling axis. EGF promotes the ADAM10-dependent cleavage of E-cadherin, disrupting the adherens junction and generating sE-cad, which may promote EMT. sE-cad can then bind EGFR, which can result in downstream signaling and may promote further promote EMT.

Acknowledgements

We would like to thank Dr. Stefan Stoll for providing the knockdown constructs, Dr. Marcia Moss (Biozyme) for providing the proA10, and Dr. Peggy Scherle (Incyte) for providing the INCB008765.

Chapter 4: Generation of a Prostate Specific ADAM10 Knockout Mouse

Abstract

ADAM10 and 15 disintegrins play important regulatory roles in prostate biology and disease. In order to better characterize the role of ADAM10 in normal prostate biology, we generated prostate specific knockout mice utilizing the probasin (Pb) driven Cre. *Adam10* $^{loxP/loxP}$ *Pb-Cre* mice are viable and reproduce normally, although early analysis indicates an epithelial hyperplasia into the luminal space, which warrants further investigation. The knockout cell lines are true knockouts as they express no ADAM10 and are currently being characterized in terms of E-cadherin shedding.

Introduction

The A Disintegrin and Metalloprotease (ADAM) family of zinc-dependent metalloproteases is composed of 40 members characterized by five extracellular domains: prodomain, metalloprotease, disintegrin, cysteine-rich, and EGF-like. The multiple domains of ADAMs allow for a myriad of functions including proteolysis, integrin binding, and signal transduction (26). Our interest in the disintegrin family arose from the observation that ADAM15 is over-expressed in prostate cancer and is critical in driving cancer progression (39, 43), while our studies in untransformed prostate biology indicated a role for ADAM10 in BPH.

In order to better characterize the roles of ADAM10 and 15 in normal prostate biology, we turned to mouse prostate knockout cell lines. *Adam15*$^{-/-}$ mice are viable (56) and prostate epithelial cells lines could be isolated from mature adult males. *ADAM10*$^{-/-}$ mice, however, are embryonic lethal at embryonic day 9.5, with defective central nervous system and heart developments, somite formation and vasculogenesis, which is a phenocopy of the *Notch*$^{-/-}$ mouse (55). Generation of prostate specific *Adam10* knockout mouse utilized an *Adam10* $^{loxP/loxP}$ mouse (60) crossed with a mouse carrying a Cre recombinase driven by the rat probasin (*Pb-Cre*) (187). The activation of *Pb-Cre* by androgens at sexual maturity of the male mice at six weeks results in recombination within the lobes by 8 weeks, with recombination efficiency varying by lobe (187). The generation of Cre recombinase results in the excision of *Adam10* exon 9, creating a frameshift mutation which interrupts translation (60) (Figure 4-1A).

Like the human prostate gland, the mouse prostate is comprised for AR positive luminal cells and AR negative basal cells which can differentiate into luminal cells (2). Due to the AR-dependence of the *Pb-Cre* promoter, recombination should only occur in the differentiated luminal cells. Studies of the *Adam10* $^{loxP/loxP}$ *Pb-Cre* mouse, therefore, focus on the role of ADAM10 in luminal cells.

We report that *Adam10* $^{loxP/loxP}$ *Pb-Cre* mice are viable and reproductively sound, although there does appear to be an unexpected hyperplasia associated with loss of ADAM10, the cause of which has not been determined. Additionally,

the prostate epithelial cell lines from *Adam10* $^{loxP/loxP}$ *Pb-Cre* mice are viable and do not express ADAM10 protein.

Materials and Methods

Generation of the tissue specific ADAM10 knockout mouse

Female *Adam10* $^{+/loxP}$ (provided by Dr. Peter Dempsey) mice on a congenic C57BL/6 background were crossed with male C57BL/6 *Pb-Cre* mice (available at Charles River, provided by June Wilke and Dr. Evan Keller). Resulting *Adam10* $^{+/loxP}$ *Pb-Cre* male mice were crossed with female *Adam10* $^{+/loxP}$ mice in order to generate breeding pairs with male *Adam10* $^{loxP/loxP}$ *Pb-Cre* males and female *Adam10* $^{loxP/loxP}$ mice.

Genotyping

Tail tips of four week old mice were frozen overnight upon removal. The following day, each tail was incubated at 55°C in a mix of 500ul of Nuclei Lysis Solution (Promega) and 100ul .5M EDTA with vortexing every hour. After three hours, 200ul of Protein Precipitation Solution (Promega) was added and tubes were incubated on ice for 10 minutes (min) prior to a 10 min spin at 4°C of 16,000 relative centrifuge units (rcf; Eppendorf centrifuge 5415 R). The supernatants were transferred to new tubes and the spin step was repeated. The supernatants were then transferred into new tubes containing 600ul isopropanol and mixed until threads of DNA appeared. Tubes were spun down for 2 min at 16,000rcf at 25°C, supernatants were removed, and pellets were washed with

70% ethanol, and spun as before. Finally, the ethanol was aspirated off and pellets were allowed to briefly air dry before reconstitution in DNase and RNase free water.

2ul of each DNA sample was then combined with 15ul of Platinum PCR mix (Invitrogen), and 2ul of primer mix (Invitrogen), and were then subjected to the following PCR protocols:

Cre: Step 1: 94°C x 2min. Step 2: 94°C x 1min. Step 3: 60°C x 1min. Step 4: 72°C x 1min. Step 5: Steps 2-4 x 35 times. Step 6: 72°C x 9min. Step 7: hold 4°C. Primers: Cre 3': ACC GTC AGT ACG TGA GAT ATC TT; Cre 5': ACC TGA AGA TGT TCG CGA TTA TCT

ADAM10: Step 1: 95°C x 5min. Step 2: 95°C x 20sec. Step 3: 55°C x 1min. Step 4: 72°C x 2min. Step 5: Steps 2-4 x 35 times. Step 6: 72°C x 10min. Step 7: hold 4°C. Primers: Exon 9: GTT GGA CAT AAC TTT GGA TCT CC. Intron 9: CGT ATC TCA AAA CTA CCC TCC C. Neo reverse: CAA GTT CTA ATT CCA TCA GAA GC. Intron 8: CAG TGT AAA TGT GAA CTC ACC C.

PCR samples were then run out on a 1.5% agarose gel for 1hr at 90V. The band sizes and corresponding genotypes are as follows: Exon 9/ Neo reverse: 327bp for loxP allele. Exon 9/Intron 9: 414bp Neo, 235 wild-type. Intron 8/Intron 9: 217bp Cre recombined, 955bp Neo unrecombined, 715bp wild type.

Processing of animal tissues

Experimental (*Adam10* $^{loxP/loxP}$ *Pb-Cre*) and control (*Adam10* $^{loxP/loxP}$) male mice were euthanized by approved UCCUCA protocols. Anterior, ventral, and

dorsolateral prostate lobes were removed from mice ages 12-24 weeks and processed as follows. For protein analysis: prostatic tissue was removed and flash frozen in liquid nitrogen then homogenized with a mortar and pestle and lysed in RIPA buffer and inhibitors as previously described (3). For DNA: samples were flash frozen in liquid nitrogen and DNA extraction followed the above genotyping protocol.

For frozen sections: Lobes were removed and stained with tissue marking dyes (Cancer Diagnostics, Inc) then fixed in 4% paraformaldehyde in .1M PBS on ice for 3hrs. Tissues were then washed 4-6 times in PBS over 4hrs at 4°C, and then placed in 30% sucrose overnight. In the morning, tissues were transferred to cassettes sitting on dry ice and covered with OCT (Tissue Tek). Once the mounting media firmed, cassettes were transferred to the -20°C freezer until sectioning.

For paraffin embedded sections: Prostate lobes were extracted and placed on PBS-dampened tissue paper and then dyed (red: anterior, blue: ventral, green: dorsolateral; Cancer Diagnostics, Inc). Tissue paper was folded around the tissues, and closed within a cassette. Cassettes were fixed overnight in 10% buffered formalin at 4°C, and then transferred to 70% ethanol for one hour before processing by the histology lab. Paraffin embedding, frozen and paraffin-embedded sectioning, hematoxylin and eosin (H&E) and immunohistochemistry was performed by the University of Michigan Cancer Center Research Histology & Immunoperoxidase Laboratory. Antibody: mouse ADAM10 (Millipore) diluted 1:100, incubated 1hr at room temperature.

Generation of mouse prostate epithelial cell lines

Prostates were extracted from male mice of 18 weeks. Prostate explants were diced in Primaria surface modified polystyrene plates (Falcon) and a drop of primary mouse cell media was added. Primary mouse culture media: 1:1 RPMI1640/Ham's F12 (Lonza, Gibco) with: 2mmol/L L-glutamine (Invitrogen); Pen/Strep Amphotericin B (Pen/Strep: 10,000U/mL, Ampho 25ug/mL; Bio Whittaker); 10mg/L Bovine Pituitary Extract (Sigma); .5mg/mL Cholera Toxin (Sigma); 5uM Dexamethasone (Sigma); Insulin, Transferin, Selenious Acid (ITS) Premix (Collaborative Res 5ug/mL Insulin, 5ug/mL Transferrin and 5ng/mL Selenious Acid); 10ng/mL EGF (Collaborative Res.); 5ug/L Insulin-like growth factor-1 (IGF-1) (Collaborative Res.). Cells were allowed to grow out from explants and passed in mouse media for 5 passages, at which point the spontaneously immortalized mouse prostate cells were transferred to normal plates and RPMI 1640 (Lonza) with 8% fetal bovine serum (HyClone) and 2mmol/L L-glutamine (Invitrogen) and Pen/Strep Amphotericin B (Pen/Strep: 10,000U/mL, Ampho 25ug/mL; Bio Whittaker).

Protein isolation, Western blotting and immunoprecipitation

Cells were harvested by scraping and lysed as previously reported (3). Lysates were pelleted at 12,000rpm for 8 minutes at 4°C. The supernatants were collected and quantitated using a Bradford assay (BioRad) with each sample being run in triplicate. For western blotting, equal amounts of protein were loaded into precast Tris-glycine SDS gels (Invitrogen) and transferred to nitrocellulose

membranes (Millipore). Blots were blocked with 10% milk in TBST buffer, probed with antibodies diluted in 2.5% milk in TBST with overnight incubation and developed using ECL (Pierce; high sensitivity Millipore). Antibodies: ADAM10 (1:1000, Millipore), actin (1:2000, Sigma).

Results:

Prostate-specific ADAM10 knockout mouse phenotype

Adam10 $^{loxP/loxP}$ *Pb-Cre* mice are viable, reproduce normally, and develop prostates. We observed tissue specific recombination in all three lobes of the prostate (Figure 4-1B). Preliminary analysis of anterior prostate morphology of *Adam10* $^{loxP/loxP}$ *Pb-Cre* mice at 28 weeks indicated some hyperplasia of the luminal compartment and changes in gross anatomical structure (Figure 4-2). In order to address whether this change was due to loss of ADAM10, we stained tissues with an anti-mouse ADAM10 antibody (Figure 4-3). Preliminary staining showed that the littermate control males had uniform expression of ADAM10 in luminal cells at the cell membrane. Surprisingly, *ADAM10*$^{loxP/loxP}$ *Pb-Cre* mice had areas of intense membranous staining and areas of diffuse cytoplasmic staining.

The unexpected presence of ADAM10 in these 28 week old mice, when we had observed recombination at 18 weeks, suggested that expression of ADAM10 on the luminal cell membrane may be critical for gland organization and loss of ADAM10 may result in luminal cell death. We postulated that these areas of increased proliferation into the luminal space and persistent ADAM10 staining could be differentiating basal cells which had not yet begun to express AR.

Conversely, these areas could represent a loss of guidance for differentiating basal cells, which could require ADAM10-mediated signaling for proper location and differentiation. Recent studies in dermatology have demonstrated a thickening of the epidermis in response to cytokeratin-5 driven ADAM10 ablation, which was due to basal cell hyperproliferation and disturbed differentiation (58), so it is possible we are observing a similar phenotype.

In an attempt to better characterize this phenotype, we generated a cohort of two experimental and two control animals aged 12-24 weeks at two week increments for future studies. The samples collection is complete; all tissues are embedded and awaiting further analysis. Future studies will examine the loss of ADAM10 expression over time, as well as examine rates of apoptosis and differentiation markers.

ADAM10 knockout prostate epithelial cell lines

Establishment of prostate epithelial cell cultures took approximately one year. We generated a cell line from the anterior prostate of a littermate control (A10 Ant +/+) and two cell lines from the anterior (A10 Ant-/-) and ventral (Vent A10 -/-) prostates of an *Adam10* $^{loxP/loxP}$ *Pb-Cre* mouse. Knockout cells are true knockouts with no ADAM10 expression (Figure 4-4). Future studies of these cell lines will include characterization of differentiation markers, E-cadherin shedding, and proliferation rates.

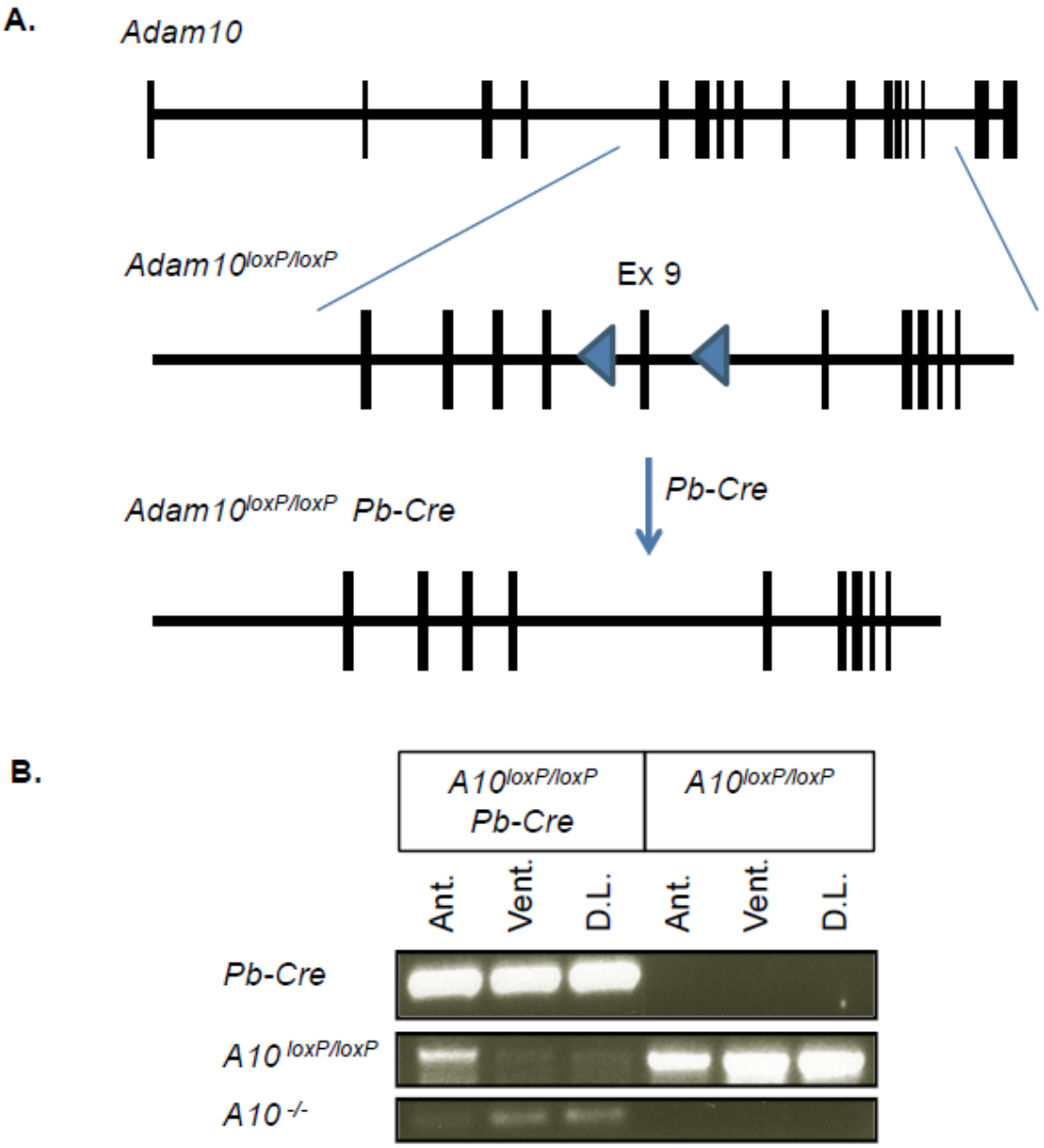

Figure 4-1: Generation of *ADAM10* $^{loxP/loxP}$ *Pb-Cre* mice. A. Exon 9 of the *ADAM10* $^{loxP/loxP}$ mouse is targeted for excision by Cre, which results in a frameshift mutation and loss of protein expression (6). Figure adapted from Gibb *et al (*6). B. Genotyping of 18 week old mouse prostates. *ADAM10* $^{loxP/loxP}$ *Pb-Cre* mice have Cre expression and recombine the *ADAM10* $^{loxP/loxP}$ to the knockout allele. Wild-type controls do not express Cre and retain the *ADAM10* $^{loxP/loxP}$ allele.

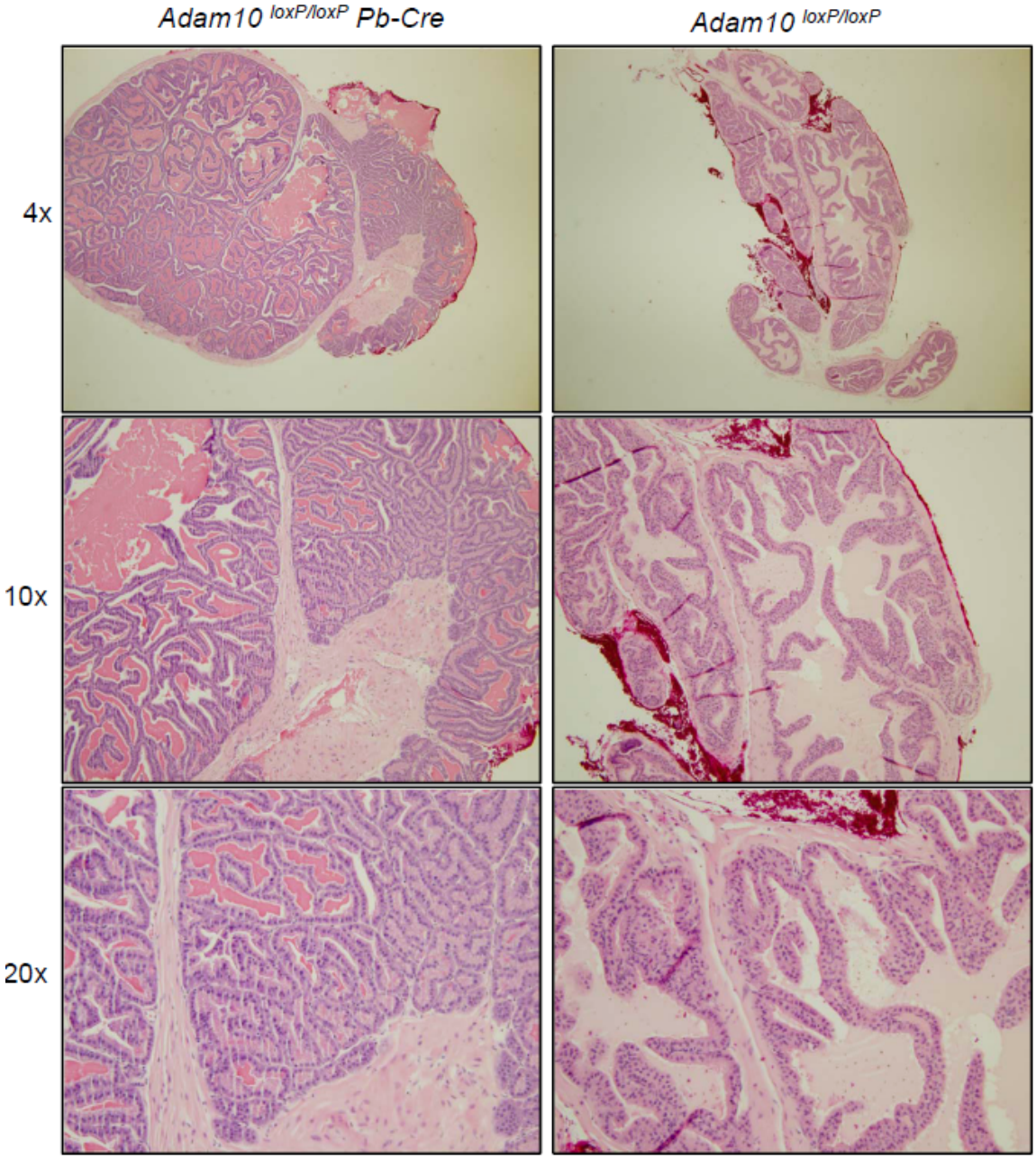

Figure 4-2: Morphology of 28 week old mouse prostates. The anterior prostate of experimental and control animals, aged 28 weeks, was stained with H&E. Red staining on sections is tissue dye for lobe identification purposes.

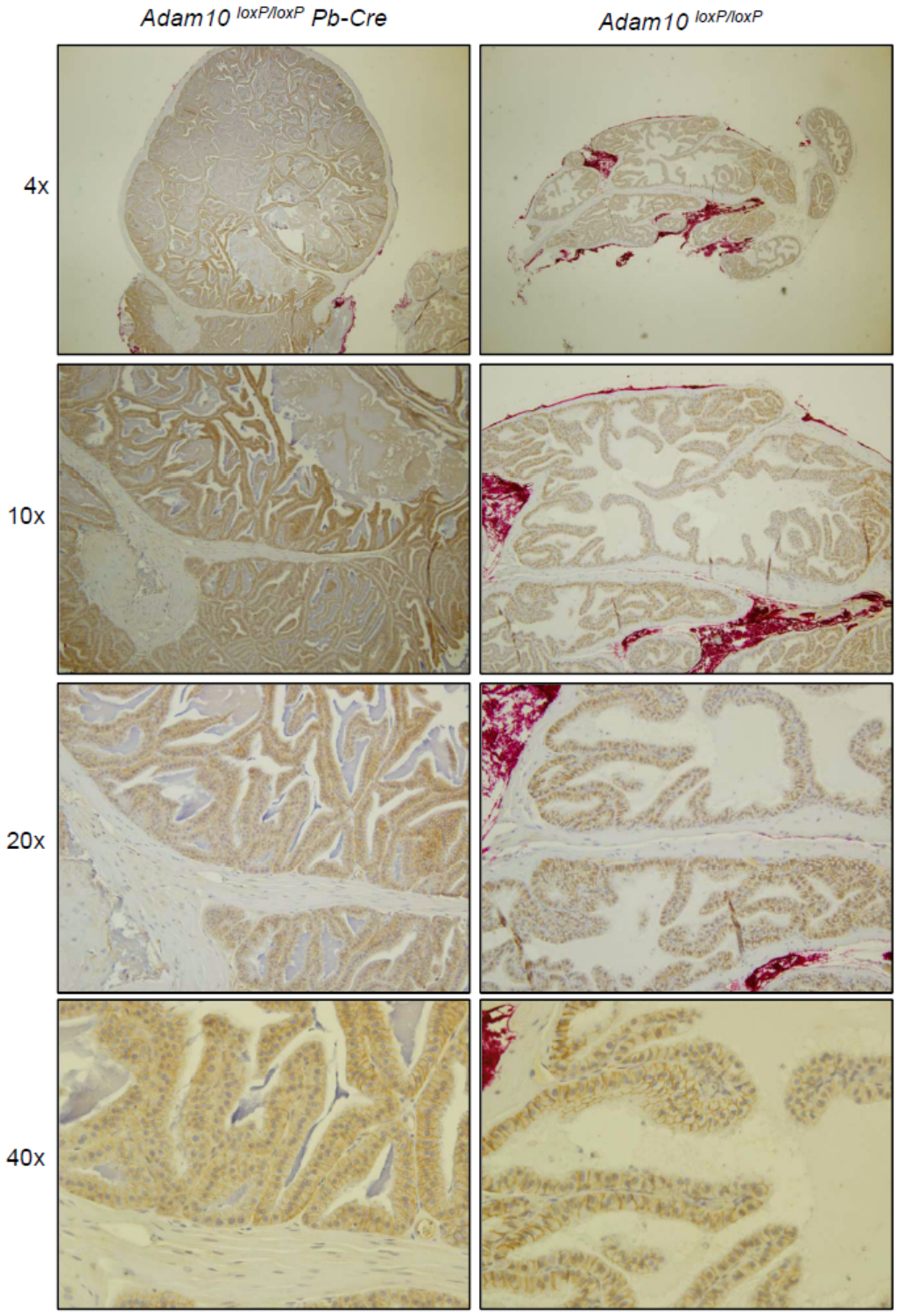

Figure 4-3: ADAM10 staining of 28 week old mouse prostates. Serial sections from Figure 2 with immunohistochemistry for ADAM10 performed. Red stain is tissue dye for lobe identification purposes.

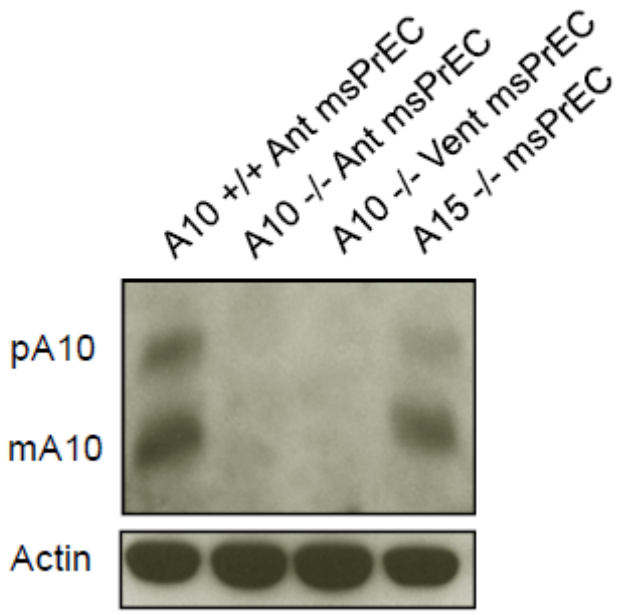

Figure 4-4: Mouse prostate epithelial cells derived from 18 week old mice. Comparison of prostate epithelial cells derived from *ADAM10* $^{loxP/loxP}$ anterior prostate, anterior and ventral *ADAM10* $^{loxP/loxP}$ *Pb-Cre* prostates, and prostate tissue from an ADAM15$^{-/-}$mouse. msPrEC: mouse prostate epithelial cells. pA10: ADAM10 pro form. mA10: mature ADAM10.

Discussion:

We have generated a prostate-specific *Adam10*$^{-/-}$ mouse (*ADAM10* $^{loxP/loxP}$ *Pb-Cre*), which has lost *Adam10* expression in all lobes of the prostate and allowed for the establishment of knockout prostate epithelial cells. Our preliminary data indicates a role for ADAM10 in prostate tissue homeostasis. Loss of ADAM10 appears to initiate a hyperproliferative response, which results in cell proliferation into the luminal space. This process appears to be coupled with basal cell differentiation since areas of strong ADAM10 expression persist in experimental prostates. In order to better characterize this phenotype, we have

also generated a cohort of control and experimental prostatic tissue samples of mouse ages 12-24 weeks and embedded them in paraffin blocks. These samples will serve in determining the timeline for ADAM10 loss in luminal cells and expression by differentiating cells. It will also allow for examination of inflammatory mediators and lineage markers which could determine whether the hyperproliferation is due to wound healing or misguided differentiation.

Based on our early observations, coupled with our data in ADAM10 function in BPH and data of others in cancer, we believe it would be interesting to breed our prostate-knockouts to models of BPH and cancer. Unfortunately, studies of BPH in the laboratory setting are complicated by a lack of good models. Rodents do not develop spontaneous BPH, but treatments with androgens and estrogens, as well as LXR knockout and over-expression of prolactin or murine IL-8, can induce prostate hyperproliferation with stromal involvement (1). We could quite easily treat our mice with androgen and estrogen or breed them onto one of these backgrounds and examine the consequences on BPH. Conversely, other groups have focused on xenografting cell lines either orthotopically or in the sub-renal capsule with mouse urogenital sinus as a model of BPH (188), which we could pursue with our *ADAM10-/-* cell lines as well.

In terms of cancer, there are many well-established models of prostate cancer in mice and it would be interesting to examine the effect of ADAM10 loss on tumor progression in the TRAMP mouse which relies on probasin-driven over-expression of the SV40 oncogene. Because castration of TRAMP mice with established tumors results in androgen independent disease (189), it would be

interesting to examine if ADAM10 plays a role in tumor development in this model. Other studies could also examine ADAM10 involvement in the tumor progression of Pten, Akt-1, and HER2 transgenic prostate cancer models (189).

Beyond further characterization of the *Adam10* $^{loxP/loxP}$ *Pb-Cre* mice and examining the role of ADAM10 in mouse models of BPH and cancer, the established cell lines will also be further analyzed. The prostate epithelial cell lines established from an *Adam10* $^{loxP/loxP}$ *Pb-Cre* mouse are viable and do not express ADAM10. Studies are currently underway to better characterize these cells in terms of E-cadherin cleavage. Also, in conjunction with previously generated *Adam15*$^{-/-}$ prostate epithelial cell lines, the *ADAM10*$^{-/-}$ prostate cell lines will be tremendously useful in determining what roles ADAM10 and ADAM15 play in normal biology. Because ADAM10 and ADAM15 share some substrates, knockout cell lines will aid in determining the specificity of our future therapeutics. For example, highly specific ADAM15 inhibitors should have no effect on the shedding profile of *ADAM15*$^{-/-}$ cells. Additionally, the knockout cells will provide additional information on the requirements for ADAM10 and ADAM15 interaction and inhibition (covered in Chapter 5).

Chapter 5: Characterizing the Interactions Between ADAM10 and ADAM15

Abstract

The disintegrins ADAM10 and ADAM15 have both been implicated in prostate cancer progression and E-cadherin cleavage. Because of our interest in targeting ADAM15 in prostate cancer, we set out to characterize ADAM domains in terms of E-cadherin cleavage, investigate ADAM10 inhibitors for ADAM15 inhibition, and to better characterize the interaction between ADAM10 and ADAM15. Our preliminary studies suggest that over-expression of ADAM15 in BPH-1 cells increases sE-cad generation but this process is EGF-independent. For ADAM15, the EGF-like domain appears to be critical for substrate specificity, and expression of an EGF-like mutant reduces sE-cad generation. We have also observed the ADAM10 inhibitor INCB08765 can inhibit ADAM15 activity during the *in vitro* and CD23 peptide cleavage assay and that ADAM15 and ADAM10 co-immunoprecipitate as a catalytically active unit. These preliminary studies further confirm our observation that EGF-promoted generation of sE-cad is an ADAM10-driven process, demonstrate a novel role for the EGF-like domain, and present an interesting observation of ADAM10 and 15 functional interactions.

Introduction

The human A Disintegrin and Metalloprotease (ADAM) family of disintegrins is comprised of zinc-dependent metalloproteases which contains 25 members, of which only 13 members (including ADAM10 and 15) are catalytically active (26). Family members are characterized by five extracellular domains: prodomain, metalloprotease, disintegrin, cysteine-rich, and EGF-like. The multiple domains of ADAMs allow for a myriad of functions including proteolysis, integrin binding, and signal transduction which have been implicated in development and disease (26).

Previously, Kuefer *et al* reported that ADAM15 is significantly over-expressed in breast, prostate, ovarian, gastric, and lung cancer (39). Further studies have implicated ADAM15 in prostate cancer progression and breast cancer proliferation (39, 43, 44), and ADAM15 catalytic and disintegrin activity has also been reported to mediate inflammation (52, 53) and platelet aggregation (54). The multidomain structure of ADAM15 allows its unique RGD sequence in the disintegrin domain to interact with $\alpha_v\beta_3$, $\alpha_5\beta_1$, and $\alpha_9\beta_1$ (45-47) to support adhesion, while its metalloprotease domain can cleave substrates such as CD23, pro-amphiregulin, pro-HB-EGF, E-cadherin, N-cadherin, and ADAM10 (38, 40-44).

ADAM10 is predominantly a sheddase, which is known to shed epidermal growth factor (EGF)-like ligands from the cell-surface and promote epidermal growth factor receptor (EGFR) family member signaling (27) and plays a critical role in the regulated intramembrane proteolysis (RIP) of Notch, CD44, and Fas

ligand, whereby sequential processing of the pro-form by ADAM10 and gamma-secretase allows the intramembrane fragment to enter the nucleus and induce transcription (28). ADAM10 itself can undergo RIPping mediated by ADAM15 (38), and this process may play a role in prostate cancer where ADAM10 staining expands to the nucleus in patient samples and, *in vitro,* is promoted by DHT (36). Interestingly, the soluble ADAM10 retains its catalytic activity to some degree (38), suggesting it may continue to act on substrates even after processing. Cleavage of ADAM10 by ADAM15 is particularly interesting because ADAM10 is the other disintegrin implicated in epithelial (E)-cadherin cleavage (84).

E-cadherin is a homophilic, calcium-dependent, adhesion protein, which is expressed at adherens junctions between epithelial cells and contains an extracellular region comprised of 5 domain repeats, each domain containing a set of seven beta-sheets arranged in an immunoglobulin fold (64). Adhesion depends on dimerization between E-cadherin molecules on the same cell, which interacts with an E-cadherin homodimer on a neighboring cell via cadherin repeat 1 (EC1) (65). E-cadherin can also interact with receptor tyrosine kinases, such as EGFR, and this depends upon the extracellular domain of E-cadherin (70). Cleavage of E-cadherin to soluble E-cadherin (sE-cad) not only disrupts adherens junctions (77), but it also allows sE-cad to bind members of the EGFR family and result in downstream signaling (44) (Chapter 3).

The EGFR family is comprised of four transmembrane tyrosine kinase members: EGFR (ErbB1, HER1), HER2 (ErbB2, Neu), HER3 (ErbB3), and HER4 (ErbB4) (7). EGF-like ligand binding to a single receptor allows for dimerization

with an adjacent ligand bound receptor and transautophosphorylation of the kinase domain, which allows for the docking of Src homology (SH2) domain or phosphotyrosine binding (PTB) containing proteins, which mediate further downstream signaling events (8, 9). In prostate cancer, EGFR staining is strongly associated with castration resistant prostate cancer (CRPC) and EGFR family member signaling may contribute to androgen independence (19). HER2 expression in prostate cancer has been associated with androgen-independent AR signaling, poor survival in CRPC, and promotes prostate cancer cell growth in bone (22-24).

Because ADAM10 and ADAM15 are both over-expressed in prostate cancer and support EGFR family member signaling, we and others have determined that they are good candidates for targeted therapy. Frequent disregulation of ADAM10 in inflammation and disease has made the protein's catalytic domain a target for therapy and specific ADAM10 inhibitors are available today (31-34). On the other hand, ADAM15 targeting is still nascent, but work on generating ADAM15-specific inhibitors is underway. The purpose of these studies, therefore, was to determine the domain requirements for E-cadherin cleavage by ADAM15, investigate cross-reactivity of available therapeutics for ADAM10 on ADAM15, and to better characterize the interaction between ADAM10 and 15.

Methods and Materials

Cell culture

Benign prostatic hyperplasia -1 (BPH-1), LNCaP, and PC-3 cells were cultured in RPMI 1640 (Lonza) with 8% fetal bovine serum (HyClone) and 2mmol/L L-glutamine (Invitrogen) and Pen/Strep Amphotericin B (Pen/Strep: 10,000U/mL, Ampho 25ug/mL; Bio Whittaker). ADAM15 over-expressing cell lines generated by Dr. Abdo Najy (LNCaP, PC-3) (43, 44) and Dr. Neali Lucas (BPH-1) were additionally supplemented with 800mg/mL G418. LNCaP ADAM15 knockdown cells were generated with previously reported constructs (43). Cells were incubated at 37°C.

Cell treatments

Cells were pretreated with or treated in serum free, phenol free RPMI (Gibco). Stock solutions of cell treatments: 10ng/uL EGF in PBS (R&D Systems); 10mM INCB008765 in DMSO, 10mM INCB012881in DMSO (Incyte); prodomain of ADAM10 in 10% glycerol/PBS (Biozyme).

Protein isolation, Western blotting and immunoprecipitation

Cells were harvested by scraping and lysed as previously reported (43). Lysates were pelleted at 12,000rpm for 8 minutes at 4°C. The supernatants were collected and quantitated using a Bradford assay with each sample being run in triplicate. For western blotting, equal amounts of protein were loaded into precast Tris-glycine SDS gels (Invitrogen) and transferred to nitrocellulose membranes

(Millipore). Blots were blocked with 10% milk in TBST buffer, probed with antibodies diluted in 2.5% milk in TBST overnight at 4ºC, and developed using ECL (Pierce; high sensitivity Millipore). Antibodies: E-cadherin (HECD-1, 1:2000, Invitrogen); EGFR (Ab-15, 1:2000, Neomarkers); ADAM10 (1:1000), ADAM15 (1:1000) , tubulin (1:2000, Millipore).

For immunoprecipitation (IP), 500ug of protein were pre-cleared with 100ul of a 50/50 mix of Sepharose A beads (Invitrogen) and 2.5% milk in TBST containing control IgG (mouse or rabbit IgG) for 30 minutes with end over end rotation. Lysates were then spun down for 3min at 8,000rpm and supernatants were transferred to new tubes containing 1ug of antibody and rotated end over end for 1hr at 4°C. Beads were then added and after another hour of rotation, and IPs were spun down for 3min at 8,000rpm and supernatants aspirated. Beads were washed three times and spun down. After final wash, supernatant was aspirated off and 35ul of beta-mercaptoethanol-containing loading buffer was added. After 5min at 100°C, IPs were again spun down and supernatants collected.

In vitro cleavage assay

The in vitro cleavage assay has been previously described (43). Briefly, immunopurified ADAM10 or ADAM15 and E-cadherin were combined in Eppendorf tubes in PBS for 8hrs at 37°C. After incubation, 15ul of BME-containing loading buffer were added and samples were boiled for 5min, spun down, and supernatants collected.

CD23 cleavage assay

Immunopurification of ADAM10 and 15 proceeded as described above. If appropriate, during the pre-clear step, lysates were pre-cleared with ADAM10 or ADAM15 in order to remove the reciprocal ADAM from the complex (Figure 5-1). Sepharose A beads containing immunopurified ADAM10 or ADAM15 were loaded into wells of a 96 well dish and topped with 100uM of CD23 peptide (PEPDAB013) provided by Dr. Marcia Moss (Biozyme). Plates were read after 2-4 hours of incubation with a fluorescence Gemini Microplate Reader with an excitation wavelength of 485nm and emission 530nm. Statistical analysis was performed by Graphpad Prism utilizing the Kruskal-Wallis test and Dunn's multiple comparison test.

Protein structure modeling

ADAM10 and 15 extracellular domains were modeled by Dr. Ron Rubin using PyMol (DeLano Scientific).

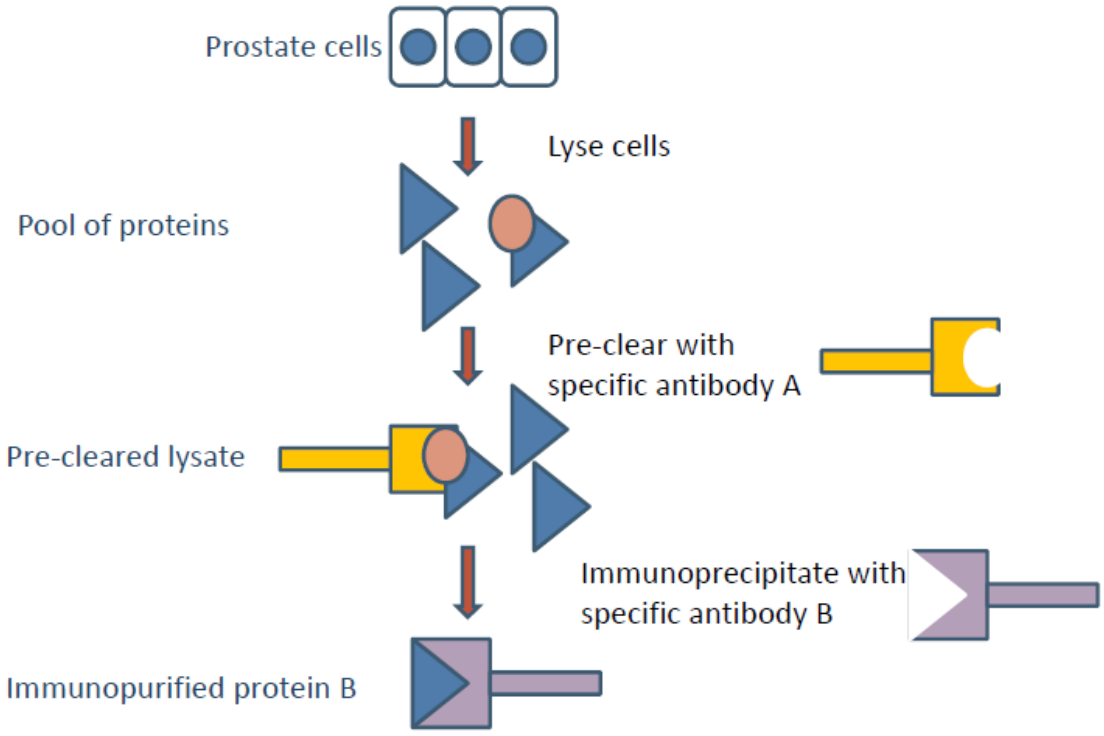

Figure 5-1: Modified immunoprecipitation protocol for CD23 peptide cleavage assay.

Results

ADAM15 over-expression in BPH-1 cells increases E-cadherin cleavage

Although the involvement of ADAM15 in E-cadherin cleavage in BPH-1 cells appears limited (Chapter 3), over-expressing ADAM15 does result in increased sE-cad bound to EGFR (Figure 5-2). Unlike ADAM10, however, the addition of EGF does not aid in sE-cad generation, suggesting that EGF-mediated E-cadherin cleavage is unique to ADAM10.

In ADAM15 cleavage of E-cadherin, we observed that cells containing a mutated EGF-like domain had less sE-cad in their conditioned media than non-mutant ADAM15 over-expressing cell lines (Figure 5-3A). By comparing each cell

line's ratio of untreated sE-cad to EGF treated sE-cad generation, we discovered that the parental and vector control cells treated with EGF had 1.2 and 1.4 fold more sE-cad than untreated counterparts. Over-expression of ADAM15 resulted in a 1:1 ratio of untreated to EGF treated sE-cad. Interestingly, the ADAM15 EGF-like mutant had 1.3 fold more sE-cad in response to EGF and had regained its sensitivity to EGF, suggesting that ADAM15 activity had been abolished in these cells. Similarly, the amount of sE-cad bound to EGFR is also greatly reduced in response to the EGF-like domain mutant (Figure 5-3B). Since the EGF-like mutant still bound E-cadherin, we hypothesized that the EGF-like domain might aid in substrate recognition or alignment in ADAM15 cleavage. An *in vitro* cleavage assay revealed that in fact, the EGF like domain ADAM15 mutant cannot cleave full length E-cadherin into sE-cad (Figure 5-3C). Previous work in our laboratory has demonstrated that ADAM15 cleavage of E-cadherin requires a functional metalloprotease domain (44), but this is the first observation of the EGF-like domain being required for proteolysis.

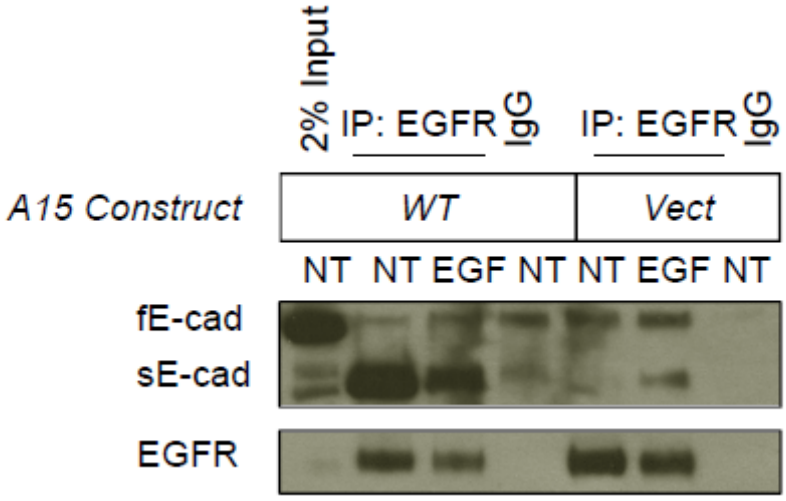

Figure 5-2: ADAM15 over-expression increases sE-cad bound to EGFR. BPH-1 cells transfected with an ADAM15 construct (WT) generate more sE-cad bound to EGFR than vector transfected cells at 15min of treatment. In the ADAM15 over-expressing cells, 5nM EGF does not induce additional sE-cad generation. NT: no treatment. fE-cad: full length E-cadherin. sE-cad: soluble E-cadherin

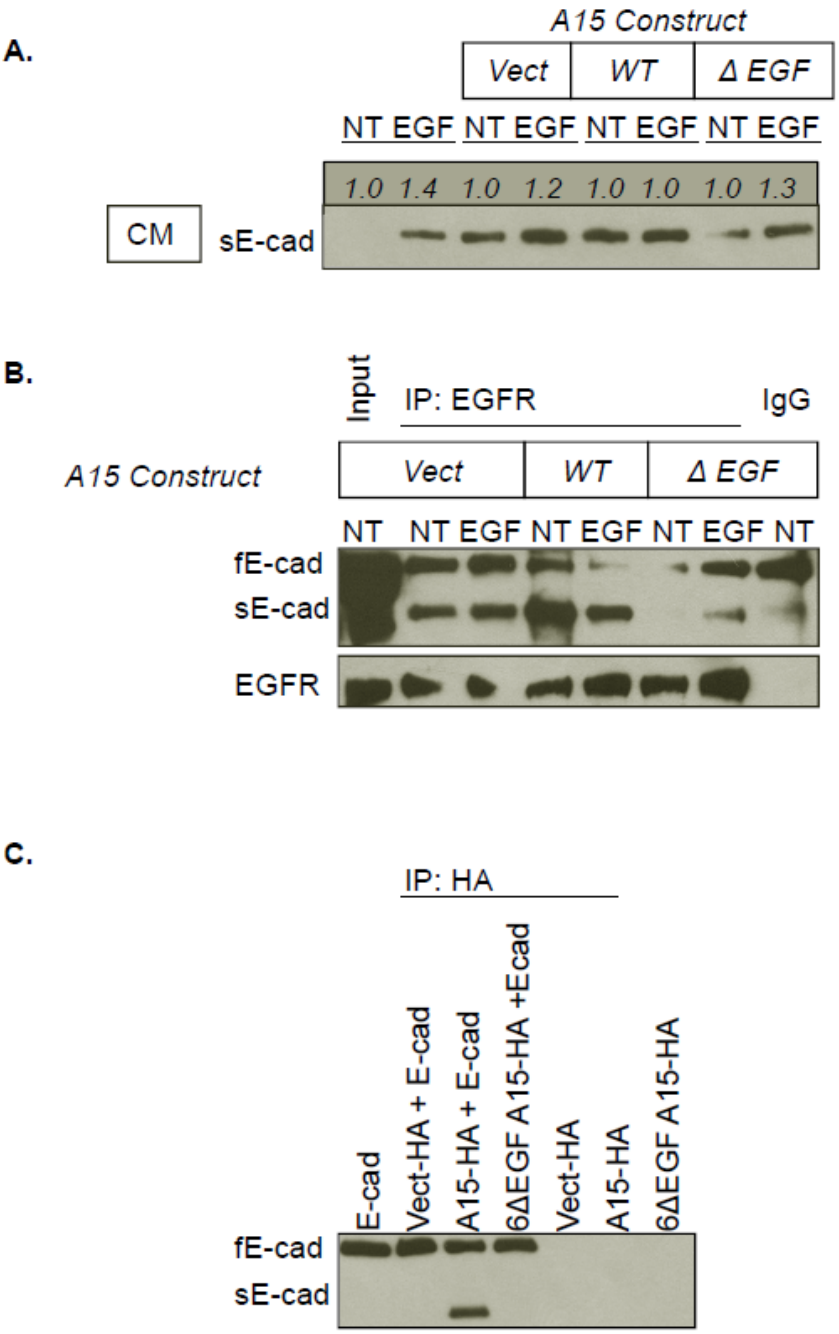

Figure 5-3: E-cadherin cleavage is mediate by ADAM15's EGF-like domain. A. Conditioned medium (CM) analysis of BPH-1 parental, vector, ADAM15 wild-type (WT), and ADAM15 ΔEGF mutant (ΔEGF) cell lines' generation of sE-cad in response to no treatment (NT) or 5nM EGF for 24hrs. Western blot was quantitated using Image J and NT vs. EGF were compared within each cell line to determine the relative ratio of sE-cad shed into conditioned medium. B. Analysis of sE-cad bound to EGFR in response to 5nM EGF treatment for 15min of BPH-1 vector, ADAM15 (WT), and ADAM15 ΔEGF (ΔEGF). C. 8hr *in vitro* cleavage assay of ADAM15 immunopurified by HA tag and reconstituted with E-cadherin.

ADAM10 and ADAM15 exist in complex

One of the observations during our studies was that the ADAM10 inhibitor INC (Incyte, 008765) could also inhibit ADAM15 activity in an *in vitro* cleavage assay (Figure 5-4A). Interestingly, an ADAM17 inhibitor does not inhibit ADAM15 in the *in vitro* cleavage assay (Figure 5-4A), suggesting that maybe only ADAM10 specific drugs will target ADAM15. The ADAM10 inhibitor can also inhibit ADAM15 in the CD23 peptide cleavage assay (Figure 5-4B). These observations suggest two explanations: either the inhibitor was targeting both metalloproteases or ADAM10 and 15 exist in a complex and the activity of purified ADAM15 depends on bound ADAM10. Immunoprecipitation of ADAM15 revealed bound ADAM10, suggesting that ADAM10 and ADAM15 do exist in a complex (Figure 5-5A), which was later reported by another group (38). Although cross-reactivity between ADAM antibodies and epitopes has yet to be ruled out, future studies could evaluate whether the ADAM10 antibody recognizes recombinant ADAM15 (and vice versa) in an ELISA.

In order to determine which of the complex components was catalytically active, the CD23 peptide cleavage assay was modified to include ADAM10 and ADAM15 samples which had been pre-cleared with antibody against the opposite ADAM. For both ADAM10 and ADAM15, pre-clearing with the other ADAM reduced cleavage activity dramatically (Figure 5-5B). However, there was no difference between the levels of ADAM10 and ADAM15 pre-cleared with ADAM15 and ADAM10, respectively, suggesting that both metalloproteases act on the peptide. Similarly, ADAM10 and 15 immunopurified from AR positive

LNCaP and AR negative PC-3 cells exhibit an association between ADAM10 and 15 (Figure 5-6A, B), suggesting the association occurs in BPH and cancer and is independent of AR status. There is evidence of ADAM10 processing seen in prostate cancer patient samples (36) and others have published data implicating ADAM15 in this process (38). It is possible, therefore, that our cleavage data is recapitulating an increased association between ADAM10 and ADAM15 seen in patients.

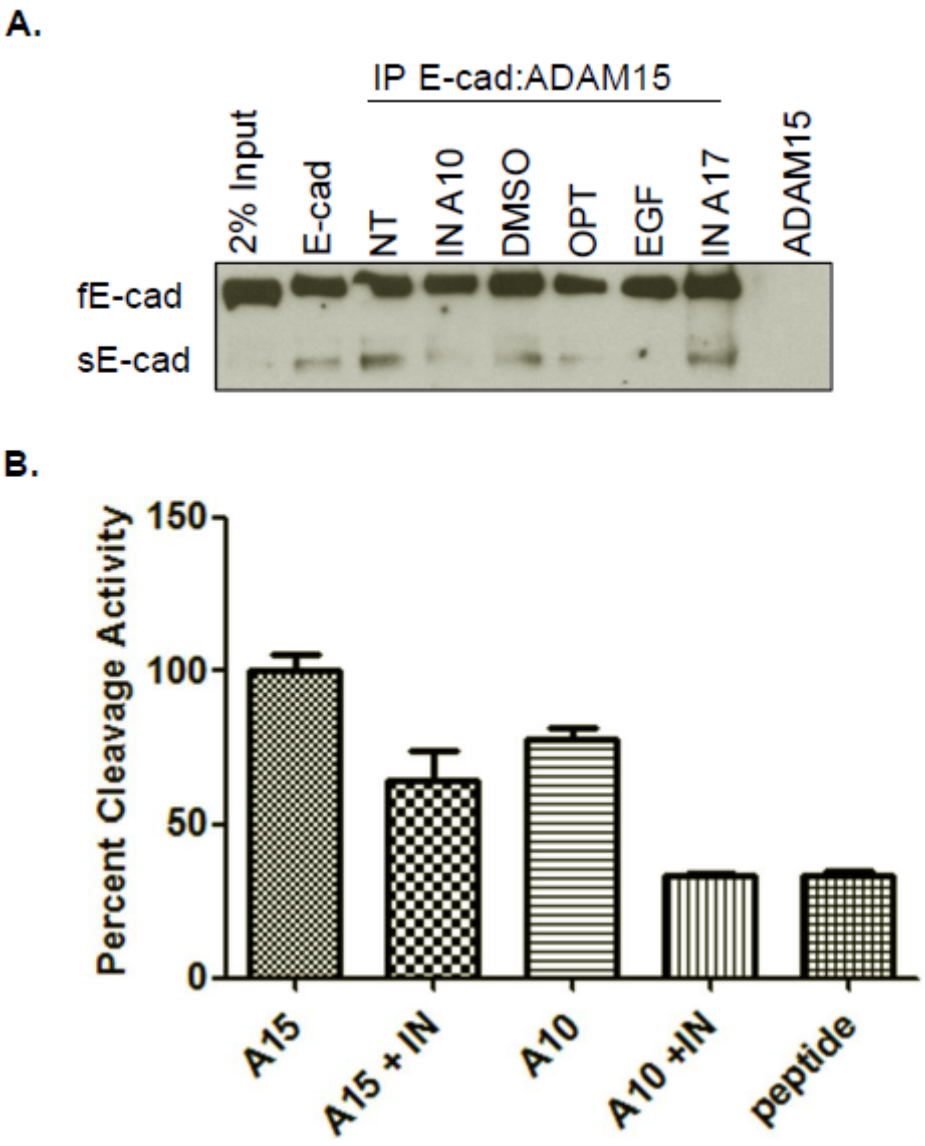

Figure 5-4: ADAM10-specific inhibitors are effective against ADAM15. A. 8hr *in vitro* cleavage assay with immunopurified ADAM15 and E-cadherin from BPH-1 cells. ADAM15 cleavage reactions treated with no treatment (NT) or vehicle (DMSO) show higher levels of sE-cad generation than ADAM10 inhibitor (IN A10) treated reactions. B. CD23 cleavage assay. Immunopurified ADAM15 (A15) or ADAM10 (A10) was combined with CD23 peptide and ADAM10 inhibitor (IN, INCB08765). NT: no treatment. IN A10: ADAM10 inhibitor, INCB08765. IN A17: ADAM17 inhibitor INCB012881. IN: INCB08765. Peptide: CD23 peptide.

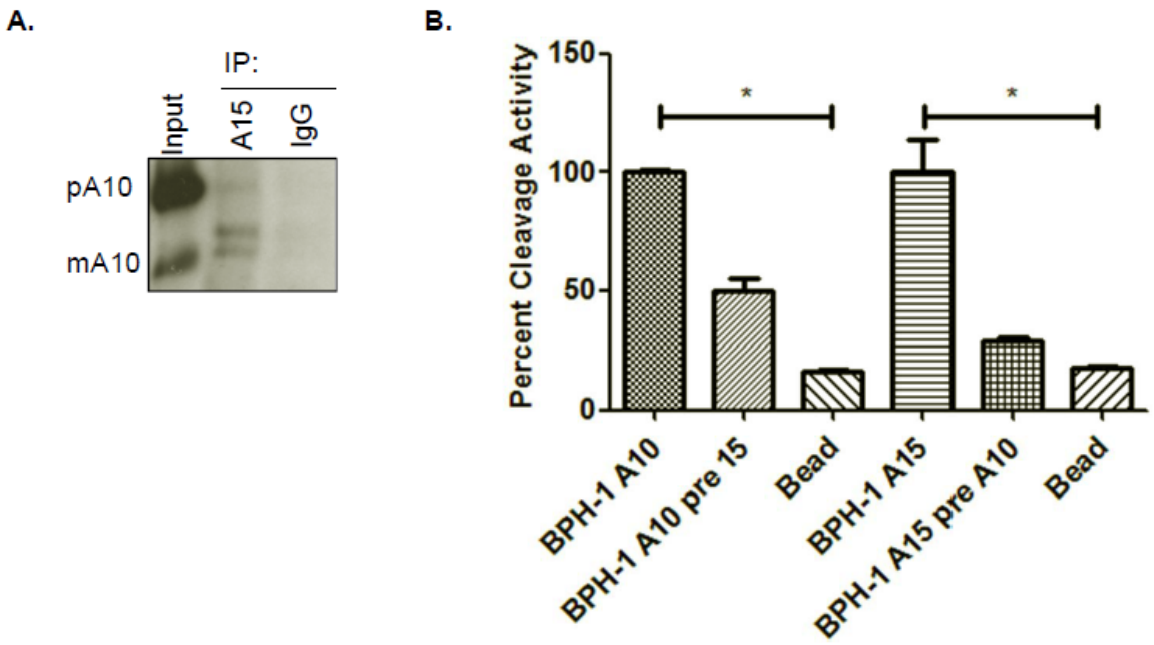

Figure 5-5: ADAM10 and ADAM15 exist in a functional complex in BPH-1 cells. A. Immunoprecipitation of ADAM15 reveals that ADAM10 is bound to ADAM15. B. CD23 peptide cleavage assay. ADAM10 immunopurified from BPH-1 cells loses some catalytic activity when pre-cleared with an antibody against ADAM15 (pre A15). The converse is also true. *: $p > 0.05$

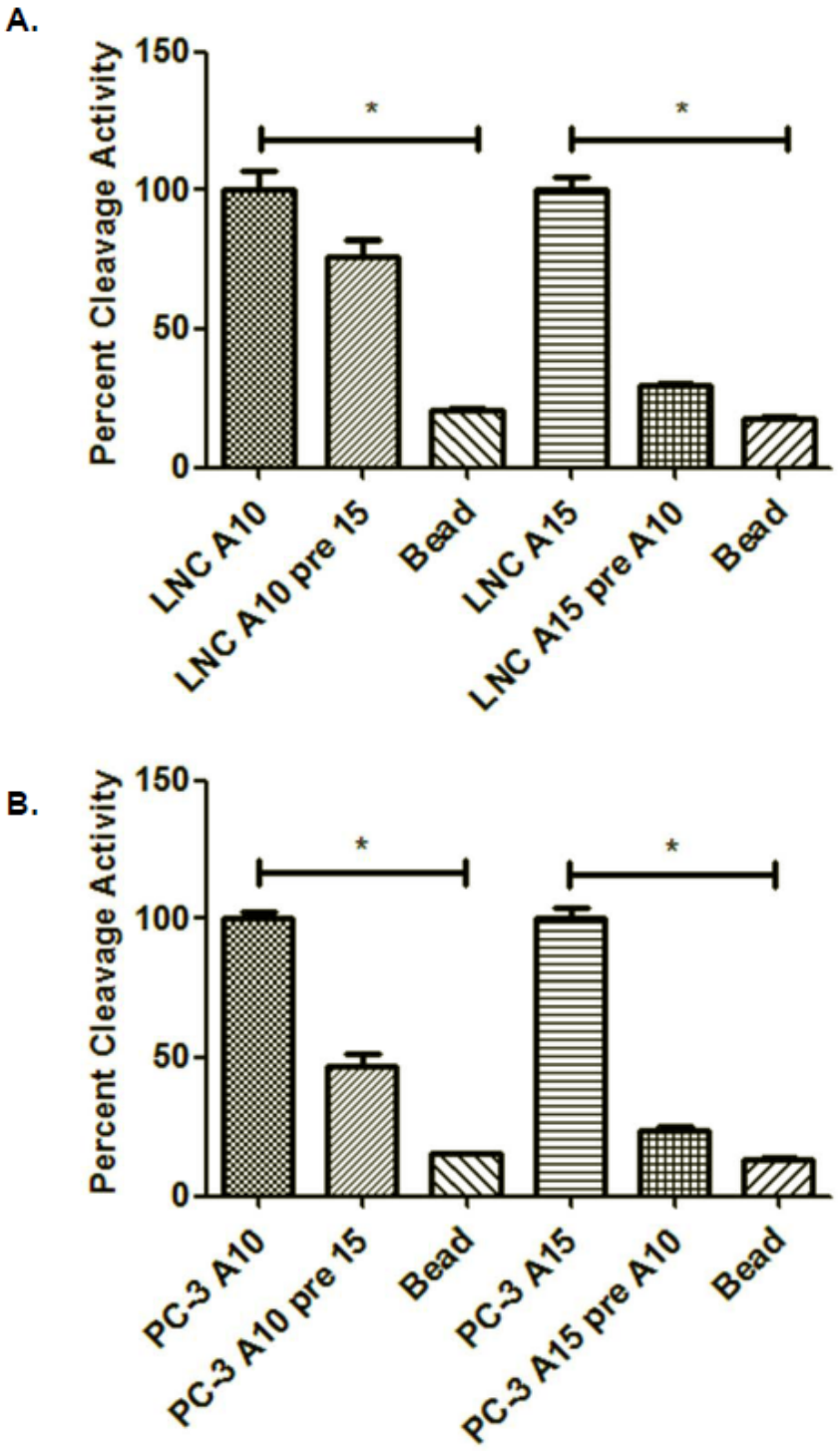

Figure 5-6: ADAM10 and ADAM15 exist in a functional complex in cancer cell lines. CD23 cleavage assay with ADAM10 and 15 immunopurified from (A) LNCaP and (B) PC-3 cells. LNCaP and PC-3 cells also have significant association between ADAM10 and 15. *: $p > 0.05$

Discussion

The focus of these preliminary studies has been to better characterize the roles of ADAM10 and ADAM15 in the prostate. The mutational analysis of ADAM15 in BPH-1 cells has been quite informative. First, we have made the observation that while ADAM15 over-expression can increase the amount of sE-cad generated by BPH-1 cells, this process is not EGF dependent as observed under normal conditions (Chapter 3). Moreover, the process of E-cadherin cleavage by ADAM15 appears to be mediated by the EGF-like domain of ADAM15, which has not been previously reported. Disruption of this domain results in loss of sE-cad generation but not association with the full length E-cadherin, suggesting that the EGF-like domain is responsible for substrate specificity.

Interestingly, while the EGF-like domain appears critical for E-cadherin processing by ADAM15, ADAM10 does not contain an EGF-like domain (26) but processes E-cadherin successfully. This suggests a fundamental difference between ADAM10 and ADAM15 processing of substrates, which might be useful in drug design (Figure 5-7). Because the *Adam15* $^{-/-}$ knockout mouse is viable (56), while the *Adam10* $^{-/-}$ mouse is embryonic lethal (55), our goal would be to target ADAM15 specifically to avoid systemic effects in patients. In these studies, the ADAM10-specific inhibitor INCB008765 showed activity against ADAM15, indicating that ADAM-specific drug design may be challenging.

Our studies have also suggested that ADAM10 and ADAM15 exist in a complex, which has been reported previously (38). Based on our CD23 peptide

cleavage data, it appears that both members of the complex are catalytically active, and that association occurs in BPH and cancer cells, independent of AR status. The specific consequences of this association for patients remain to be determined, although there is evidence suggesting that processing of ADAM10 from the cell surface of cancer patient samples correlates with high grade prostate cancer (36) and our own studies have demonstrated high ADAM15 expression in advanced disease (39). These preliminary studies have revealed a complex interaction between ADAM10 and ADAM15, which warrants further investigation.

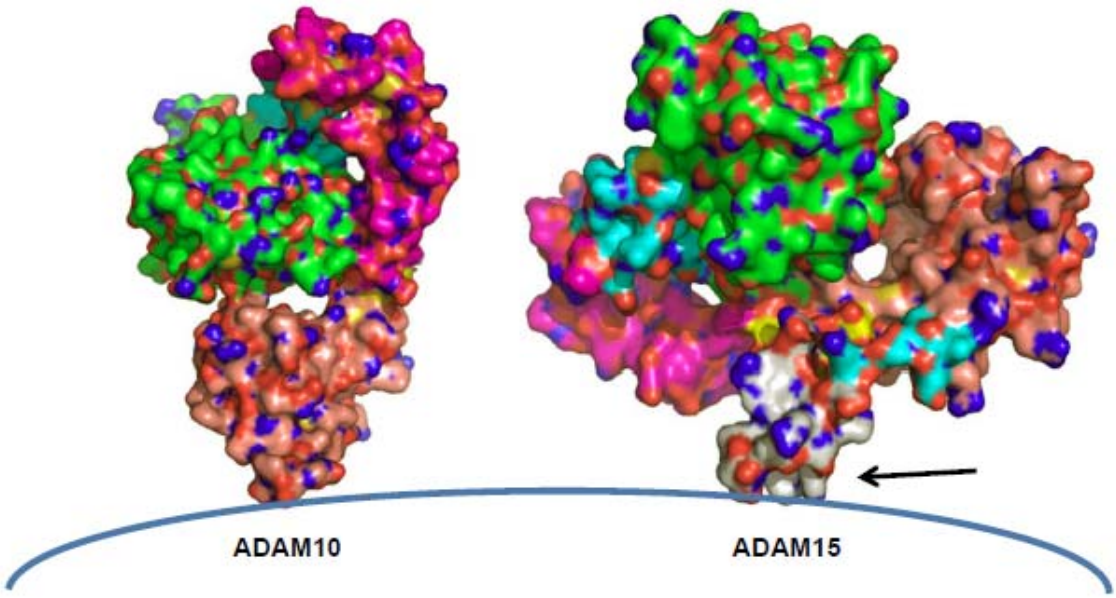

Figure 5-7: The extracellular domains of ADAM10 and 15. Although ADAM10 and 15 share substrates, ADAM15 contains an EGF-like domain (arrow) which it requires for E-cadherin cleavage while ADAM10 does not. Modeling by Dr. Ron Rubin.

Chapter 6: Discussion

Our interest in the disintegrin family was initiated by the observation that E-cadherin, which plays critical roles in epithelial cell maintenance, can be processed to sE-cad by ADAM15 during breast and prostate cancer progression (44, 170). Although ADAM15 is critical for E-cadherin processing in breast and prostate cancer, our preliminary studies suggested it does not play a significant role in normal prostate biology. The aims of this thesis project, therefore, were to identify and characterize the E-cadherin sheddase in untransformed prostate cell lines, generate prostate specific knockouts of said sheddase, and examine any interactions ADAM15 might have with this sheddase.

Our initial studies of E-cadherin shedding in untransformed prostate epithelial cells (BPH-1 and PrEC) illustrated that expression of active ADAM15 did not correlate with sE-cad levels. A related disintegrin, ADAM10, had been previously implicated in E-cadherin processing in keratinocytes (84), and expression of active ADAM10 correlated well with sE-cad generation. After pilot experiments with ADAM10 inhibitors, we determined that ADAM10 could indeed cleave E-cadherin to the 80kDa sE-cad fragment, and we set out to determine the role of ADAM10 and sE-cad in normal prostate biology and disease.

By blocking ADAM10 activity or reducing ADAM10 expression, we established that ADAM10 plays a role in signaling and proliferation of prostate cells. We also demonstrated that non-transformed prostate epithelial cells can be induced to generate sE-cad by adding EGF or amphiregulin and that this process is dependent upon ADAM10. Interestingly, if ADAM15 is over-expressed in these cells, generation of sE-cad increases, but it is no longer EGF-dependent. This suggests that while ADAM10 and ADAM15 may both play a role in E-cadherin cleavage and prostate pathologies, their stimulus varies.

However it is generated, sE-cad can stimulate a variety of pro-survival effects (Chapter 2). While previous publications from our group have demonstrated that sE-cad can bind to HER2 and HER3 (44), this is the first report of the sE-cad bound to EGFR in a non-transformed prostate cell model. Our studies have also demonstrated that Fc-Ecad can induce phosphorylation of the receptor which results in downstream signaling. Moreover, these experiments have demonstrated that sE-cad may play a role in aberrant proliferation of prostate epithelial cells such as in BPH. This work and the literature supporting it suggests that the generation of sE-cad may contribute to the benign proliferative disorders by binding to EGFR and inducing downstream signaling. Additionally, the loss of E-cadherin at the cell membrane can also mediate epithelial to mesenchymal transition (EMT).

EMT is characterized by the loss of differentiated epithelial phenotypes and the acquisition of motility and invasiveness and plays a critical role in tumor progression (96, 184). In prostate cancer, EMT has been implicated in models of

bone metastasis (97), and emerging evidence suggests EMT also may play a role in BPH (99). In BPH patient sections, areas of BPH stain strongly for EMT transcription factors Snail and Slug, suggesting that it is the accumulation of mesenchymal cells derived from epithelium which is driving the disease (99). These data suggest that the cleavage of E-cadherin induced by a potent EMT activator, such as EGF, may contribute to BPH progression via EMT, and presents ADAM10 as a possible therapeutic avenue for BPH intervention.

In order to evaluate whether ADAM10 plays a role in normal prostate biology, we generated a prostate specific ADAM10 knockout mouse (*ADAM10* $^{loxP/loxP}$ *Pb-Cre*). Preliminary evidence has been confounding. On the one hand, there is a very dramatic phenotype in the anterior prostate of 28 week old *ADAM10* $^{loxP/loxP}$ *Pb-Cre* mice. However, ADAM10 immunohistochemistry staining revealed continued expression of ADAM10 in the luminal cells, particularly intense in areas of hyperproliferation. We believe that this preliminary data indicates a role for ADAM10 in prostate tissue homeostasis because loss of ADAM10 appears to initiate a hyperproliferative response, which results in cell proliferation into the luminal space. This process appears to be coupled with basal cell differentiation since areas of strong ADAM10 expression persist in experimental prostates. Although these studies are preliminary, they do suggest a role for ADAM10 in mouse prostate biology. Based on the strong response to ADAM10 loss, further analysis with mouse models of BPH should be considered in order to validate or exclude ADAM10 as a target for BPH therapy. Additionally, further studies of adult ADAM10 knockout mice utilizing a tetracycline-induced

Cre could be highly informative for determining the role of ADAM10 in adult tissues.

Beyond further characterization of the *Adam10* $^{loxP/loxP}$ *Pb-Cre* mice, the established cell lines will also be further analyzed. The prostate epithelial cell lines established from an *Adam10* $^{loxP/loxP}$ *Pb-Cre* mouse are viable and do not express ADAM10, and studies are currently underway to better characterize these cells in terms of epithelial (E)-cadherin cleavage. It would be interesting to determine whether our knockout cells are capable of regenerating prostatic tissue in a tissue recombination model. Based on the hyperproliferation observed in our animals in our preliminary studies, we hypothesize these cells would most likely not give rise to normal prostate.

Whether or not the tissue recombination studies are undertaken, the *ADAM10*$^{-/-}$ prostate cell lines, along with previously generated *Adam15*$^{-/-}$ prostate epithelial cell lines will be tremendously useful in determining what roles ADAM10 and ADAM15 play in normal biology as well as in drug design. For example, highly specific ADAM15 inhibitors should have no effect on the shedding profile of *ADAM15*$^{-/-}$ cells. Additionally, the knockout cells will provide null backgrounds for ADAM10 and 15, which is particularly critical since these two disintegrins share substrates and interact with each other.

Our studies have revealed that ADAM10 and ADAM15 exist in a complex, where it appears both members are catalytically active. ADAM15 has also been reported to aid in processing ADAM10 (38), and this could explain the observation that prostate cancer samples lose ADAM10 membranous expression

with increasing grade (36). Based on our CD23 peptide cleavage data, it would be interesting to repeat our observations in the context of DHT treatment. Because the processing of ADAM10 appears to be DHT dependent (36), we would hypothesize that treatment of AR positive LNCaP cells would result in increased association between ADAM10 and 15. For now, our observations hint at a regulated interaction between ADAM10 and ADAM15, which can become deregulated in prostate cancer.

In order to explore the disregulation of ADAM15 in prostate cancer, we over-expressed ADAM15 in BPH-1 cells, which resulted in increased amounts of sE-cad, but this process became EGF independent. During these studies, we also observed that E-cadherin cleavage by ADAM15 appears to be mediated by the EGF-like domain of ADAM15, which has not been previously reported. Disruption of this domain results in loss of sE-cad generation but not association with the full length E-cadherin, suggesting that the EGF-like domain is responsible for substrate specificity. It is important to note that ADAM10 does not contain an EGF-like domain (26) but processes E-cadherin successfully, suggesting this might be a way to add specificity to ADAM15 targeting drugs. Currently there are no targeted therapies against ADAM15, but the ADAM10-specific inhibitor INCB008765 shows activity against ADAM15, indicating that ADAM-specific drug design may be challenging.

The studies included in this thesis have provided novel insight into the role of ADAM10 in human prostate epithelium. We have also included work that suggests important interactions between ADAM10 and ADAM15, which may play

a role in prostate cancer progression. The CD23 peptide cleavage assay and the *Adam10* $^{-/-}$ cell lines will also be useful to future investigators in the laboratory for candidate drug screening. We believe the findings herein are novel, clinically relevant, and will provide a foundation for future studies of ADAM10 in the prostate gland.

Bibliography

1. K.-E. Andersson, M.C. Michel, J.P. Hieble: Animal Models for Benign Prostatic Hyperplasia. In: *Urinary Tract*. Springer Berlin Heidelberg (2011)

2. J.T. Isaacs: Prostate stem cells and benign prostatic hyperplasia. *Prostate* 68, 1025-1034 (2008)

3. G.R. Cunha: Mesenchymal-epithelial interactions: past, present, and future. *Differentiation* 76, 578-586 (2008)

4. Group Prostate Cancer Trialists' Collaborative: Maximum androgen blockade in advanced prostate cancer: an overview of 22 randomised trials with 3283 deaths in 5710 patients. *The Lancet* 346, 265-269 (1995)

5. A.N. Vis, F.H. Schröder: Key targets of hormonal treatment of prostate cancer. Part 1: the androgen receptor and steroidogenic pathways. *BJU Int* 104, 438-448 (2009)

6. C. Cai, S. Balk: Intratumoral androgen biosynthesis in prostate cancer pathogenesis and response to therapy. *Endocr Relat Cancer* (2011)

7. M.A. Olayioye, R.M. Neve, H.A. Lane, et al.: The ErbB signaling network: receptor heterodimerization in development and cancer. *EMBO J* 19, 3159-3167 (2000)

8. M.A. Lemmon, Z. Bu, J.E. Ladbury, et al.: Two EGF molecules contribute additively to stabilization of the EGFR dimer. *EMBO J* 16, 281-294 (1997)

9. N. Prenzel, O.M. Fischer, S. Streit, et al.: The epidermal growth factor receptor family as a central element for cellular signal transduction and diversification. *Endocr Relat Cancer* 8, 11-31 (2001)

10. J.T. Jones, R.W. Akita, M.X. Sliwkowski: Binding specificities and affinities of egf domains for ErbB receptors. *FEBS Lett* 447, 227-231 (1999)

11. T.P.J. Garrett, N.M. McKern, M. Lou, et al.: The Crystal Structure of a Truncated ErbB2 Ectodomain Reveals an Active Conformation, Poised to Interact with Other ErbB Receptors. *Mol Cell* 11, 495-505 (2003)

12. A. Citri, K.B. Skaria, Y. Yarden: The deaf and the dumb: the biology of ErbB-2 and ErbB-3. *Exp Cell Res* 284, 54-65 (2003)

13. K.L. Carraway, M.X. Sliwkowski, R. Akita, et al.: The erbB3 gene product is a receptor for heregulin. *J Biol Chem* 269, 14303-14306 (1994)

14. I. Leav, J.E. McNeal, J. Ziar, et al.: The localization of transforming growth factor alpha and epidermal growth factor receptor in stromal and epithelial compartments of developing human prostate and hyperplastic, dysplastic, and carcinomatous lesions. *Hum Pathol* 29, 668-75 (1998)

15. S. Schwartz, C. Caceres, I. De Torres, et al.: Androgen-independent basal cell re-epithelialization, c-erbB-2 mRNA expression and androgen-dependent EGFr mRNA expression in benign prostatic hyperplasia explant cultures treated with finasteride. *Int J Cancer* 76, 519-522 (1998)

16. V.L. Kumar, P.K. Majumder, V. Kumar: Observations on EGFR gene amplification and polymorphism in prostatic diseases. *Int Urol Nephrol* 32, 73-75 (2000)

17. G. Ibrahim, B. Kerns, J. MacDonald, et al.: Differential immunoreactivity of epidermal growth factor receptor in benign, dysplastic and malignant prostatic tissues. *J Urol* 149, 170-3 (1993)

18. V.L. Kumar, P.K. Majumder, S. Gujral, et al.: Comparative analysis of epidermal growth factor receptor mRNA levels in normal, benign hyperplastic and carcinomatous prostate. *Cancer Lett* 134, 177-180 (1998)

19. R.B. Shah, D. Ghosh, J.T. Elder: Epidermal growth factor receptor (ErbB1) expression in prostate cancer progression: Correlation with androgen independence. *Prostate* 66, 1437-1444 (2006)

20. C. Cai, D.C. Portnoy, H. Wang, et al.: Androgen Receptor Expression in Prostate Cancer Cells Is Suppressed by Activation of Epidermal Growth Factor Receptor and ErbB2. *Cancer Res* 69, 5202-5209 (2009)

21. A.M. Traish, A. Morgentaler: Epidermal growth factor receptor expression escapes androgen regulation in prostate cancer: a potential molecular switch for tumour growth. *Br J Cancer* 101, 1949-1956 (2009)

22. C.W. Gregory, Y.E. Whang, W. McCall, et al.: Heregulin-Induced Activation of HER2 and HER3 Increases Androgen Receptor Transactivation and CWR-R1 Human Recurrent Prostate Cancer Cell Growth. *Clin Cancer Res* 11, 1704-1712 (2005)

23. J. Edwards, P. Traynor, A.F. Munro, et al.: The Role of HER1-HER4 and EGFRvIII in Hormone-Refractory Prostate Cancer. *Clin Cancer Res* 12, 123-130 (2006)

24. S.R. Chinni, H. Yamamoto, Z. Dong, et al.: CXCL12/CXCR4 Transactivates HER2 in Lipid Rafts of Prostate Cancer Cells and Promotes Growth of Metastatic Deposits in Bone. *Mol Cancer Res* 6, 446-457 (2008)

25. M.K. Jathal, L. Chen, M. Mudryj, et al.: Targeting ErbB3: the New RTK(id) on the Prostate Cancer Block. *Immunol Endocr Metab Agents Med Chem* 11, 131-149 (2011)

26. D.R. Edwards, M.M. Handsley, C.J. Pennington: The ADAM metalloproteinases. *Mol Aspects Med* 29, 258-289 (2008)

27. C.P. Blobel: ADAMs: key components in EGFR signalling and development. *Nat Rev Mol Cell Biol* 6, 32-43 (2005)

28. H.C. Crawford, P.J. Dempsey, G. Brown, et al.: ADAM10 as a Therapeutic Target for Cancer and Inflammation. *Curr Pharm Des* 15, 2288-2299 (2009)

29. C. Wild-Bode, K. Fellerer, J. Kugler, et al.: A Basolateral Sorting Signal Directs ADAM10 to Adherens Junctions and Is Required for Its Function in Cell Migration. *J Biol Chem* 281, 23824-23829 (2006)

30. S. Kasina, P.A. Scherle, C.L. Hall, et al.: ADAM-mediated amphiregulin shedding and EGFR transactivation. *Cell Prolif* 42, 799-812 (2009)

31. M.L. Moss, M. Bomar, Q. Liu, et al.: The ADAM10 Prodomain Is a Specific Inhibitor of ADAM10 Proteolytic Activity and Inhibits Cellular Shedding Events. *J Biol Chem* 282, 35712-35721 (2007)

32. X. Liu, J.S. Fridman, Q. Wang, et al.: Selective inhibition of ADAM metalloproteases blocks HER-2 extracellular domain (ECD) cleavage and potentiates the anti-tumor effects of trastuzumab. *Cancer Biol Ther* 5, 648-656 (2006)

33. L. Witters, P. Scherle, S. Friedman, et al.: Synergistic Inhibition with a Dual Epidermal Growth Factor Receptor/HER-2/neu Tyrosine Kinase Inhibitor and a Disintegrin and Metalloprotease Inhibitor. *Cancer Res* 68, 7083-7089 (2008)

34. J.S. Fridman, E. Caulder, M. Hansbury, et al.: Selective Inhibition of ADAM Metalloproteases as a Novel Approach for Modulating ErbB Pathways in Cancer. *Clin Cancer Res* 13, 1892-1902 (2007)

35. B.-B.S. Zhou, M. Peyton, B. He, et al.: Targeting ADAM-mediated ligand cleavage to inhibit HER3 and EGFR pathways in non-small cell lung cancer. *Cancer Cell* 10, 39-50 (2006)

36. T. Arima, H. Enokida, H. Kubo, et al.: Nuclear translocation of ADAM-10 contributes to the pathogenesis and progression of human prostate cancer. *Cancer Sci* 98, 1720-1726 (2007)

37. D.R. McCulloch, M. Harvey, A.C. Herington: The expression of the ADAMs proteases in prostate cancer cell lines and their regulation by dihydrotestosterone. *Mol Cell Endocrinol* 167, 11-21 (2000)

38. T. Tousseyn, A. Thathiah, E. Jorissen, et al.: ADAM10, the Rate-limiting Protease of Regulated Intramembrane Proteolysis of Notch and Other Proteins, Is Processed by ADAMS-9, ADAMS-15, and the gamma-Secretase. *J Biol Chem* 284, 11738-11747 (2009)

39. R. Kuefer, K.C. Day, C.G. Kleer, et al.: The ADAM15 disintegrin is associated with aggressive prostate and breast cancer disease. *Neoplasia* 8, 319-29 (2006)

40. S. Hart, O.M. Fischer, N. Prenzel, et al.: GPCR-induced migration of breast carcinoma cells depends on both EGFR signal transactivation and EGFR-independent pathways. *Biol Chem* 386, 845-855 (2005)

41. A.M. Fourie, F. Coles, V. Moreno, et al.: Catalytic Activity of ADAM8, ADAM15, and MDC-L (ADAM28) on Synthetic Peptide Substrates and in Ectodomain Cleavage of CD23. *J Biol Chem* 278, 30469-30477 (2003)

42. B. Schafer, B. Marg, A. Gschwind, et al.: Distinct ADAM Metalloproteinases Regulate G Protein-coupled Receptor-induced Cell Proliferation and Survival. *J Biol Chem* 279, 47929-47938 (2004)

43. A.J. Najy, K.C. Day, M.L. Day: ADAM15 Supports Prostate Cancer Metastasis by Modulating Tumor Cell-Endothelial Cell Interaction. *Cancer Res* 68, 1092-1099 (2008)

44. A.J. Najy, K.C. Day, M.L. Day: The Ectodomain Shedding of E-cadherin by ADAM15 Supports ErbB Receptor Activation. *J Biol Chem* 283, 18393-18401 (2008)

45. X.-P. Zhang, T. Kamata, K. Yokoyama, et al.: Specific Interaction of the Recombinant Disintegrin-like Domain of MDC-15 (Metargidin, ADAM-15) with Integrin alphavbeta3. *J Biol Chem* 273, 7345-7350 (1998)

46. D. Nath, P.M. Slocombe, P.E. Stephens, et al.: Interaction of metargidin (ADAM-15) with alphavbeta3 and alpha5beta1 integrins on different haemopoietic cells. *J Cell Sci* 112, 579-587 (1999)

47. K. Eto, W. Puzon-McLaughlin, D. Sheppard, et al.: RGD-independent Binding of Integrin alpha9beta1 to the ADAM-12 and -15 Disintegrin Domains Mediates Cell-Cell Interaction. *J Biol Chem* 275, 34922-34930 (2000)

48. Z. Poghosyan, S.M. Robbins, M.D. Houslay, et al.: Phosphorylation-dependent Interactions between ADAM15 Cytoplasmic Domain and Src Family Protein-tyrosine Kinases. *J Biol Chem* 277, 4999-5007 (2002)

49. A. Yasuia, K. Matsuuraa, E. Shimizua, et al.: Expression of Splice Variants of the Human ADAM15 Gene and Strong Interaction between the Cytoplasmic Domain of One Variant and Src Family Proteins Lck and Hck. *Pathobiology* 71, (2004)

50. J.L. Zhong, Z. Poghosyan, C.J. Pennington, et al.: Distinct Functions of Natural ADAM-15 Cytoplasmic Domain Variants in Human Mammary Carcinoma. *Mol Cancer Res* 6, 383-394 (2008)

51. T. Maretzky, S.M. Le Gall, S. Worpenberg-Pietruk, et al.: Src Stimulates Fibroblast Growth Factor Receptor-2 Shedding by an ADAM15 Splice Variant Linked to Breast Cancer. *Cancer Res* 69, 4573-4576 (2009)

52. L. Charrier-Hisamuddin, C.L. Laboisse, D. Merlin: ADAM-15: a metalloprotease that mediates inflammation. *The FASEB Journal* 22, 641-653 (2008)

53. L. Charrier, Y. Yan, H.T.T. Nguyen, et al.: ADAM-15/Metargidin Mediates Homotypic Aggregation of Human T Lymphocytes and Heterotypic Interactions of T Lymphocytes with Intestinal Epithelial Cells. *J Biol Chem* 282, 16948-16958 (2007)

54. O.-H. Jeon, D. Kim, Y.-J. Choi, et al.: Novel function of human ADAM15 disintegrin-like domain and its derivatives in platelet aggregation. *Thromb Res* 119, 609-619 (2007)

55. D. Hartmann, B. de Strooper, L. Serneels, et al.: The disintegrin/metalloprotease ADAM 10 is essential for Notch signalling but not for alpha-secretase activity in fibroblasts. *Hum Mol Genet* 11, 2615-2624 (2002)

56. K. Horiuchi, G. Weskamp, L. Lum, et al.: Potential Role for ADAM15 in Pathological Neovascularization in Mice. *Mol Cell Biol* 23, 5614-5624 (2003)

57. E. Jorissen, J. Prox, C. Bernreuther, et al.: The Disintegrin/Metalloproteinase ADAM10 Is Essential for the Establishment of the Brain Cortex. *J Neurosci* 30, 4833-4844 (2010)

58. S. Weber, M.T. Niessen, J. Prox, et al.: The disintegrin/metalloproteinase Adam10 is essential for epidermal integrity and Notch-mediated signaling. *Development* 138, 495-505 (2011)

59. L. Tian, X. Wu, C. Chi, et al.: ADAM10 is essential for proteolytic activation of Notch during thymocyte development. *Int Immunol* 20, 1181-1187 (2008)

60. D.R. Gibb, M.E. Shikh, D.-J. Kang, et al.: ADAM10 is essential for Notch2-dependent marginal zone B cell development and CD23 cleavage in vivo. *J Exp Med* 207, 623-635 (2010)

61. C. Zhang, L. Tian, C. Chi, et al.: Adam10 is essential for early embryonic cardiovascular development. *Dev Dyn* 239, 2594-2602 (2010)

62. B.B. Böhm, T. Aigner, B. Roy, et al.: Homeostatic effects of the metalloproteinase disintegrin ADAM15 in degenerative cartilage remodeling. *Arthritis Rheum* 52, 1100-1109 (2005)

63. M. Marzia, V. Guaiquil, W.C. Horne, et al.: Lack of ADAM15 in mice is associated with increased osteoblast function and bone mass. *Biol Chem* 392, 877-85 (2011)

64. M. Overduin, T.S. Harvey, S. Bagby, et al.: Solution structure of the epithelial cadherin domain responsible for selective cell adhesion. *Science* 267, 386-389 (1995)

65. T.J. Boggon, J. Murray, S. Chappuis-Flament, et al.: C-Cadherin Ectodomain Structure and Implications for Cell Adhesion Mechanisms. *Science* 296, 1308-1313 (2002)

66. P.J. Kilshaw: Alpha E beta 7. *Mol Pathol* 52, 203-207 (1999)

67. C. Grundemann, M. Bauer, O. Schweier, et al.: Cutting Edge: Identification of E-Cadherin as a Ligand for the Murine Killer Cell Lectin-Like Receptor G1. *J Immunol* 176, 1311-1315 (2006)

68. M. Ito, T. Maruyama, N. Saito, et al.: Killer cell lectin-like receptor G1 binds three members of the classical cadherin family to inhibit NK cell cytotoxicity. *J Exp Med* 203, 289-295 (2006)

69. S. Nakamura, K. Kuroki, I. Ohki, et al.: Molecular Basis for E-cadherin Recognition by Killer Cell Lectin-like Receptor G1 (KLRG1). *J Biol Chem* 284, 27327-27335 (2009)

70. X. Qian, T. Karpova, A.M. Sheppard, et al.: E-cadherin-mediated adhesion inhibits ligand-dependent activation of diverse receptor tyrosine kinases. *EMBO J* 23, 1739–1784 (2004)

71. A. Bremm, A. Walch, M. Fuchs, et al.: Enhanced Activation of Epidermal Growth Factor Receptor Caused by Tumor-Derived E-Cadherin Mutations. *Cancer Res* 68, 707-714 (2008)

72. Y.-T. Chen, D.B. Stewart, W.J. Nelson: Coupling Assembly of the E-Cadherin/Beta-Catenin Complex to Efficient Endoplasmic Reticulum Exit and Basal-lateral Membrane Targeting of E-Cadherin in Polarized MDCK Cells. *J Cell Biol* 144, 687-699 (1999)

73. V. Vasioukhin, C. Bauer, M. Yin, et al.: Directed Actin Polymerization Is the Driving Force for Epithelial Cell Cell Adhesion. *Cell* 100, 209-219 (2000)

74. F. Drees, S. Pokutta, S. Yamada, et al.: Alpha-Catenin Is a Molecular Switch that Binds E-Cadherin-beta-Catenin and Regulates Actin-Filament Assembly. *Cell* 123, 903-915 (2005)

75. R.C. Ireton, M.A. Davis, J. van Hengel, et al.: A novel role for p120 catenin in E-cadherin function. *J Cell Biol* 159, 465-476 (2002)

76. B.M. Gumbiner: Regulation of Cadherin Adhesive Activity. *J Cell Biol* 148, 399-404 (2000)

77. M. Wheelock, C. Buck, K. Bechtol, et al.: Soluble 80-kd fragment of cell-CAM 120/80 disrupts cell-cell adhesion. *J Cell Biochem* 34, 187-202 (1987)

78. F. Ryniers, C. Stove, M. Goethals, et al.: Plasmin Produces an E-Cadherin Fragment That Stimulates Cancer Cell Invasion. *Biol Chem* 383, 159-165 (2002)

79. J.-H. Zuo, W. Zhu, M.-Y. Li, et al.: Activation of EGFR promotes squamous carcinoma SCC10A cell migration and invasion via inducing EMT-like phenotype change and MMP-9-mediated degradation of E-cadherin. *J Cell Biochem* n/a-n/a (2011)

80. G. Davies, W.G. Jiang, M.D. Mason: Matrilysin Mediates Extracellular Cleavage of E-Cadherin from Prostate Cancer Cells. *Clin Cancer Res* 7, 3289-3297 (2001)

81. A. Lochter, S. Galosy, J. Muschler, et al.: Matrix Metalloproteinase Stromelysin-1 Triggers a Cascade of Molecular Alterations That Leads to Stable Epithelial-to-Mesenchymal Conversion and a Premalignant Phenotype in Mammary Epithelial Cells. *J Cell Biol* 139, 1861-1872 (1997)

82. M.H.U. Biswas, C. Du, C. Zhang, et al.: Protein Kinase D1 Inhibits Cell Proliferation through Matrix Metalloproteinase-2 and Matrix Metalloproteinase-9 Secretion in Prostate Cancer. *Cancer Res* 70, 2095-2104 (2010)

83. W. Schirrmeister, T. Gnad, T. Wex, et al.: Ectodomain shedding of E-cadherin and c-Met is induced by Helicobacter pylori infection. *Exp Cell Res* 315, 3500-3508 (2009)

84. T. Maretzky, F. Scholz, B. Koten, et al.: ADAM10-Mediated E-Cadherin Release Is Regulated by Proinflammatory Cytokines and Modulates Keratinocyte Cohesion in Eczematous Dermatitis. *J Invest Dermatol* 128, 1737-1746 (2008)

85. K. Billion, H. Ibrahim, C. Mauch, et al.: Increased Soluble E-Cadherin in Melanoma Patients. *Skin Pharmacology and Physiology* 19, 65-70 (2006)

86. S.K. Johnson, V.C. Ramani, L. Hennings, et al.: Kallikrein 7 enhances pancreatic cancer cell invasion by shedding E-cadherin. *Cancer* 109, 1811-1820 (2007)

87. V. Noe, B. Fingleton, K. Jacobs, et al.: Release of an invasion promoter E-cadherin fragment by matrilysin and stromelysin-1. *J Cell Sci* 114, 111-118 (2001)

88. K. Lee, E. Choi, M. Hyun, et al.: Association of Extracellular Cleavage of E-Cadherin Mediated by MMP-7 with HGF-Induced in vitro Invasion in Human Stomach Cancer Cells. *Eur Surg Res* 39, 208-215 (2007)

89. J.K. McGuire, Q. Li, W.C. Parks: Matrilysin (Matrix Metalloproteinase-7) Mediates E-Cadherin Ectodomain Shedding in Injured Lung Epithelium. *American Journal of Pathology* 162, 1831-1843 (2003)

90. J. Symowicz, B.P. Adley, K.J. Gleason, et al.: Engagement of Collagen-Binding Integrins Promotes Matrix Metalloproteinase-9-Dependent E-Cadherin Ectodomain Shedding in Ovarian Carcinoma Cells. *Cancer Res* 67, 2030-2039 (2007)

91. M.D. Covington, R.C. Burghardt, A.R. Parrish: Ischemia-induced cleavage of cadherins in NRK cells requires MT1-MMP (MMP-14). *American Journal of Physiology - Renal Physiology* 290, F43-F51 (2006)

92. O.D. Gil, C. Lee, E.V. Ariztia, et al.: Lysophosphatidic acid (LPA) promotes E-cadherin ectodomain shedding and OVCA429 cell invasion in an uPA-dependent manner. *Gynecol Oncol* 108, 361-369 (2008)

93. R. Kuefer, M.D. Hofer, C.S.M. Zorn, et al.: Assessment of a fragment of e-cadherin as a serum biomarker with predictive value for prostate cancer. *Br J Cancer* 92, 2018-2023 (2005)

94. S. Hirohashi: Inactivation of the E-Cadherin-Mediated Cell Adhesion System in Human Cancers. *Am J Pathol* 153, 333-339 (1998)

95. E. Vincan, N. Barker: The upstream components of the Wnt signalling pathway in the dynamic EMT and MET associated with colorectal cancer progression. *Clin Exp Metastasis* 25, 657-663 (2008)

96. K. Polyak, R.A. Weinberg: Transitions between epithelial and mesenchymal states: acquisition of malignant and stem cell traits. *Nat Rev Cancer* 9, 265-273 (2009)

97. H. Zhau, V. Odero-Marah, H.-W. Lue, et al.: Epithelial to mesenchymal transition (EMT) in human prostate cancer: lessons learned from ARCaP model. *Clin Exp Metastasis* 25, 601-610 (2008)

98. Bryden, Freemont, Clarke, et al.: Paradoxical expression of E-cadherin in prostatic bone metastases. *BJU Int* 84, 1032-1034 (1999)

99. P. Alonso-Magdalena, C. Brössner, A. Reiner, et al.: A role for epithelial-mesenchymal transition in the etiology of benign prostatic hyperplasia. *Proc Natl Acad Sci USA* 106, 2859–2863 (2009)

100. C. Grundemann, M. Bauer, O. Schweier, et al.: Cutting Edge: Identification of E-Cadherin as a Ligand for the Murine Killer Cell Lectin-Like Receptor G1. *J Immunol* 176, 1311-1315 (2006)

101. Y.-T. Chen, D.B. Stewart, W.J. Nelson: Coupling Assembly of the E-Cadherin/Beta-Catenin Complex to Efficient Endoplasmic Reticulum Exit and Basal-lateral Membrane Targeting of E-Cadherin in Polarized MDCK Cells. *The Journal of Cell Biology* 144, 687-699 (1999)

102. V. Vasioukhin, C. Bauer, M. Yin, et al.: Directed Actin Polymerization Is the Driving Force for Epithelial Cell-Cell Adhesion. *Cell* 100, 209-219 (2000)

103. M.J. Wheelock, C.A. Buck, K.B. Bechtol, et al.: Soluble 80-kd fragment of cell-CAM 120/80 disrupts cell-cell adhesion. *J Cell Biochem* 34, 187-202 (1987)

104. T. Maretzky, F. Scholz, B. Koten, et al.: ADAM10-Mediated E-Cadherin Release Is Regulated by Proinflammatory Cytokines and Modulates Keratinocyte Cohesion in Eczematous Dermatitis. *J Invest Dermatol* 128, 1737-1746 (2008)

105. J. Katz, Q.-B. Yang, P. Zhang, et al.: Hydrolysis of Epithelial Junctional Proteins by Porphyromonas gingivalis Gingipains. *Infect Immun* 70, 2512-2518 (2002)

106. S. Wu, K.-c. Lim, J. Huan, et al.: *Bacteroides fragilis* enterotoxin cleaves the zonula adherens protein, E-cadherin. *Proc Natl Acad Sci U S A* 95, 14979-14984 (1998)

107. V. Gocheva, W. Zeng, D. Ke, et al.: Distinct roles for cysteine cathepsin genes in multistage tumorigenesis. *Genes Dev* 20, 543-556 (2006)

108. K.H. Lee, E.Y. Choi, M.S. Hyun, et al.: Association of Extracellular Cleavage of E-Cadherin Mediated by MMP-7 with HGF-Induced in vitro Invasion in Human Stomach Cancer Cells. *Eur Surg Res* 39, 208-215 (2007)

109. J.-H. Zuo, W. Zhu, M.-Y. Li, et al.: Activation of EGFR promotes squamous carcinoma SCC10A cell migration and invasion via inducing EMT-like phenotype change and MMP-9-mediated degradation of E-cadherin. *J Cell Biochem* 112, 2508-17 (2011)

110. P. Marambaud, J. Shioi, G. Serban, et al.: A presenilin-1/[gamma]-secretase cleavage releases the E-cadherin intracellular domain and regulates disassembly of adherens junctions. *EMBO J* 21, 1948-1956 (2002)

111. A. Kiss, R.B. Troyanovsky, S.M. Troyanovsky: p120-Catenin Is a Key Component of the Cadherin-{gamma}-Secretase Supercomplex. *Mol Biol Cell* 19, 4042-4050 (2008)

112. E.C. Ferber, M. Kajita, A. Wadlow, et al.: A Role for the Cleaved Cytoplasmic Domain of E-cadherin in the Nucleus. *J Biol Chem* 283, 12691-12700 (2008)

113. J. Rios-Doria, M.L. Day: Truncated E-cadherin potentiates cell death in prostate epithelial cells. *The Prostate* 63, 259-268 (2005)

114. U. Steinhusen, J. Weiske, V. Badock, et al.: Cleavage and Shedding of E-cadherin after Induction of Apoptosis. *J Biol Chem* 276, 4972-4980 (2001)

115. S.B. Lee, A. Schramme, K. Doberstein, et al.: ADAM10 Is Upregulated in Melanoma Metastasis Compared with Primary Melanoma. *J Invest Dermatol* 130, 763-773 (2009)

116. T. Yoshimura, T. Tomita, M.F. Dixon, et al.: ADAMs (A Disintegrin and Metalloproteinase) Messenger RNA Expression in *Helicobacter pylori*- Infected, Normal, and Neoplastic Gastric Mucosa. *J Infect Dis* 185, 332-340 (2002)

117. R.J. Lamont, H.F. Jenkinson: Life Below the Gum Line: Pathogenic Mechanisms of Porphyromonas gingivalis. *Microbiol Mol Biol Rev* 62, 1244-1263 (1998)

118. J. Katz, V. Sambandam, J.H. Wu, et al.: Characterization of Porphyromonas gingivalis-Induced Degradation of Epithelial Cell Junctional Complexes. *Infect Immun* 68, 1441-1449 (2000)

119. B. Turk, V. Turk: Lysosomes as "Suicide Bags" in Cell Death: Myth or Reality? *J Biol Chem* 284, 21783-21787 (2009)

120. A. Vreemann, H. Qu, K. Mayer, et al.: Cathepsin B release from rodent intestine mucosa due to mechanical injury results in extracellular matrix damage in early post-traumatic phases. *Biol Chem* 390, 481-492 (2009)

121. J. Mai, R.L. Finley, D.M. Waisman, et al.: Human Procathepsin B Interacts with the Annexin II Tetramer on the Surface of Tumor Cells. *J Biol Chem* 275, 12806-12812 (2000)

122. M. Niedergethmann, B. Wostbrock, J.W. Sturm, et al.: Prognostic Impact of Cysteine Proteases Cathepsin B and Cathepsin L in Pancreatic Adenocarcinoma. *Pancreas* 29, 204-211 (2004)

123. G.M. Yousef, A. Scorilas, A. Magklara, et al.: The KLK7 (PRSS6) gene, encoding for the stratum corneum chymotryptic enzyme is a new member of the human kallikrein gene family -- genomic characterization, mapping, tissue expression and hormonal regulation. *Gene* 254, 119-128 (2000)

124. C.M. Overall, C. Lopez-Otin: Strategies for MMP inhibition in cancer: innovations for the post-trial era. *Nat Rev Cancer* 2, 657-672 (2002)

125. D. Trudel, Y. Fradet, F. Meyer, et al.: Significance of MMP-2 Expression in Prostate Cancer. *Cancer Res* 63, 8511-8515 (2003)

126. E.A. Garbett, M.W.R. Reed, N.J. Brown: Proteolysis in human breast and colorectal cancer. *Br J Cancer* 81, 287-293 (1999)

127. T. Shiomi, Y. Okada: MT1-MMP and MMP-7 in invasion and metastasis of human cancers. *Cancer Metastasis Rev* 22, 145-152 (2003)

128. K. Hashimoto, Y. Kihira, Y. Matuo, et al.: Expression of matrix metalloproteinase-7 and tissue inhibitor of metalloproteinase-1 in human prostate. *J Urol* 160, 1872-1876 (1998)

129. K.H. Lee, S.J. Shin, K.O. Kim, et al.: Relationship between E-cadherin, matrix metalloproteinase-7 gene expression and clinicopathological features in gastric carcinoma. *Oncol Rep* 16, 823-830 (2006)

130. W.G. Jiang, G. Davies, T.A. Martin, et al.: Targeting Matrilysin and Its Impact on Tumor Growth In vivo: The Potential Implications in Breast Cancer Therapy. *Clin Cancer Res* 11, 6012-6019 (2005)

131. A.M. Manicone, I. Huizar, J.K. McGuire: Matrilysin (Matrix Metalloproteinase-7) Regulates Anti-Inflammatory and Antifibrotic Pulmonary Dendritic Cells That Express CD103 (AlphaEBeta7-Integrin). *Am J Pathol* 175, 2319-2331 (2009)

132. S.E. Dunsmore, U.K. Saarialho-Kere, J.D. Roby, et al.: Matrilysin expression and function in airway epithelium. *The Journal of Clinical Investigation* 102, 1321-1331 (1998)

133. L. Zhang, J. Shi, J. Feng, et al.: Type IV collagenase (matrix metalloproteinase-2 and -9) in prostate cancer. *Prostate Cancer Prostatic Dis* 7, 327-332 (2004)

134. H.A. Alshenawy: Immunohistochemical expression of epidermal growth factor receptor, E-cadherin, and matrix metalloproteinase-9 in ovarian epithelial cancer and relation to patient deaths. *Ann Diagn Pathol* 14, 387-395 (2010)

135. F. Riedel, K. Gotte, J. Schwalb, et al.: Serum levels of matrix metalloproteinase-2 and -9 in patients with head and neck squamous cell carcinoma. *Anticancer Res* 20, 3045-3049 (2000)

136. B.E. Muhs, G. Plitas, Y. Delgado, et al.: Temporal expression and activation of matrix metalloproteinases-2, -9, and membrane type 1—matrix metalloproteinase following acute hindlimb ischemia. *J Surg Res* 111, 8-15 (2003)

137. B. McMahon, H.C. Kwaan: The Plasminogen Activator System and Cancer. *Pathophysiology of Haemostasis and Thrombosis* 36, 184-194 (2007)

138. T.B. Pustilnik, V. Estrella, J.R. Wiener, et al.: Lysophosphatidic Acid Induces Urokinase Secretion by Ovarian Cancer Cells. *Clin Cancer Res* 5, 3704-3710 (1999)

139. Y. Xu, D.C. Gaudette, J.D. Boynton, et al.: Characterization of an ovarian cancer activating factor in ascites from ovarian cancer patients. *Clin Cancer Res* 1, 1223-1232 (1995)

140. W. Kuhn, B. Schmalfeldt, U. Reuning, et al.: Prognostic significance of urokinase (uPA) and its inhibitor PAI-1 for survival in advanced ovarian carcinoma stage FIGO IIIc. *Br J Cancer* 79, 1746-1751 (1999)

141. K. Ito, I. Okamoto, N. Araki, et al.: Calcium influx triggers the sequential proteolysis of extracellular and cytoplasmic domains of E-cadherin, leading to loss of beta-catenin from cell-cell contacts. *Oncogene* 18, 7080-7090 (1999)

142. A.J. Pittard, R.E. Banks, H.F. Galley, et al.: Soluble E-cadherin concentrations in patients with systemic inflammatory response syndrome and multiorgan dysfunction syndrome. *British Journal of Anaesthesia* 76, 629-631 (1996)

143. A.J. Karayiannakis, K.N. Syrigos, A. Savva, et al.: Serum E-cadherin concentrations and their response during laparoscopic and open cholecystectomy. *Surg Endosc* 16, 1551-1554 (2002)

144. T. Goto, A. Ishizaka, M. Katayama, et al.: Involvement of E-cadherin cleavage in reperfusion injury. *Eur J Cardiothorac Surg* 37, 426-431 (2010)

145. L.J. McCawley, L.M. Matrisian: Matrix metalloproteinases: they're not just for matrix anymore! *Curr Opin Cell Biol* 13, 534-540 (2001)

146. M. Egeblad, Z. Werb: New functions for the matrix metalloproteinases in cancer progression. *Nat Rev Cancer* 2, 161-174 (2002)

147. R. Mazzieri, L. Masiero, L. Zanetta, et al.: Control of type IV collagenase activity by components of the urokinase-plasmin system: a regulatory mechanism with cell-bound reactants. *EMBO J* 16, 2319-2332 (1997)

148. A. Lochter, S. Galosy, J. Muschler, et al.: Matrix Metalloproteinase Stromelysin-1 Triggers a Cascade of Molecular Alterations That Leads to Stable Epithelial-to-Mesenchymal Conversion and a Premalignant Phenotype in Mammary Epithelial Cells. *The Journal of Cell Biology* 139, 1861-1872 (1997)

149. M. Katayama, S. Hirai, K. Kamihagi, et al.: Soluble E-cadherin fragments increased in circulation of cancer patients. . *Br J Cancer* 69, 580-585 (1994)

150. H. Streeck, D.S. Kwon, A. Pyo, et al.: Epithelial adhesion molecules can inhibit HIV-1-specific CD8+ T-cell functions. *Blood* 117, 5112-5122 (2011)

151. R. Kuefer, M.D. Hofer, C.S.M. Zorn, et al.: Assessment of a fragment of e-cadherin as a serum biomarker with predictive value for prostate cancer. *Br J Cancer* 92, 2018-2023 (2005)

152. T.R. Griffiths, I. Brotherick, R.I. Bishop, et al.: Cell adhesion molecules in bladder cancer: soluble serum E-cadherin correlates with predictors of recurrence. *Br J Cancer* 74, 579-584 (1996)

153. A.S. Protheroe, R.E. Banks, M. Mzimba, et al.: Urinary concentrations of the soluble adhesion molecule E-cadherin and total protein in patients with bladder cance. *Br J Cancer* 80, 273-278 (1999)

154. B. Shi, V. Laudon, S. Yu, et al.: E-cadherin tissue expression and urinary soluble forms of E-cadherin in patients with bladder transitional cell carcinoma. *Urol Int* 81, 320-4 (2008)

155. G. Velikova, R.E. Banks, A. Gearing, et al.: Serum concentrations of soluble adhesion molecules in patients with colorectal cancer. *Br J Cancer* 77, 1857-1863 (1996)

156. C. Wilmanns, J. Grossmann, S. Steinhauer, et al.: Soluble serum E-cadherin as a marker of tumour progression in colorectal cancer patients. *Clinical and Experimental Metastasis* 21, 75-78 (2004)

157. Y. Chung, S. Law, D.L.W. Kwong, et al.: Serum soluble E-cadherin is a potential prognostic marker in esophageal squamous cell carcinoma. *Dis Esophagus* 24, 49-55 (2011)

158. J. Gofuku, H. Shiozaki, Y. Doki, et al.: Characterization of soluble E-cadherin as a disease marker in gastric cancer patients. *Br J Cancer* 78, 1095-1101 (1998)

159. A. Chan, S. Lam, K. Chu, et al.: Soluble E-cadherin is a valid prognostic marker in gastric carcinoma. *Gut* 48, 808-811 (2001)

160. A.O.O. Chan, K.-M. Chu, S.K. Lam, et al.: Early prediction of tumor recurrence after curative resection of gastric carcinoma by measuring soluble E-cadherin. *Cancer* 104, 740-746 (2005)

161. A.O.-O. Chan, K.-M. Chu, S.-K. Lam, et al.: Soluble E-cadherin is an independent pretherapeutic factor for long-term survival in gastric cancer. *J Clin Oncol* 15, 2288-93 (2003)

162. C. Pedrazzani, S. Caruso, G. Corso, et al.: Influence of age on soluble E-cadherin serum levels prevents its utility as a disease marker in gastric cancer patients. *Scand J Gastroenterol* 43, 765-766 (2008)

163. Y. Zhou, J. Ran, C. Tang, et al.: Effect of celecoxib on E-cadherin, VEGF, microvessel density and apoptosis in gastric cancer. *Cancer Biology & Therapy* 6, 269-275 (2007)

164. A. Soyama, S. Eguchi, M. Takatsuki, et al.: Significance of the serum level of soluble E-cadherin in patients with HCC. *Hepatogastroenterology* 55, 1390-1393 (2008)

165. K.N. Syrigos, K.J. Harrington, A.J. Karayiannakis, et al.: Circulating Soluble E-Cadherin Levels are of Prognostic Significance in Patients with Multiple Myeloma. *Anticancer Res* 24, 2027-2031 (2004)

166. K. Charalabopoulos, A. Gogali, Y. Dalavaga, et al.: The clinical significance of soluble E-cadherin in nonsmall cell lung cancer. *Experimental Oncology* 28, 83-85 (2006)

167. A. Gogali, K. Charalabopoulos, I. Zampira, et al.: Soluble Adhesion Molecules E-Cadherin, Intercellular Adhesion Molecule-1, and E-Selectin as Lung Cancer Biomarkers. *Chest* 138, 1173-1179 (2010)

168. K.L. Reckamp, B.K. Gardner, R.A. Figlin, et al.: Tumor Response to Combination Celecoxib and Erlotinib Therapy in Non-small Cell Lung Cancer Is Associated with a Low Baseline Matrix Metalloproteinase-9 and a Decline in Serum-Soluble E-Cadherin. *J Thorac Oncol* 3, 117-124 (2008)

169. E. Darai, A.F. Bringuier, F. Walker-Combrouze, et al.: Soluble adhesion molecules in serum and cyst fluid from patients with cystic tumours of the ovary. *Hum Reprod* 13, 2831-2835 (1998)

170. R. Kuefer, M.D. Hofer, J.E. Gschwend, et al.: The Role of an 80 kDa Fragment of E-cadherin in the Metastatic Progression of Prostate Cancer. *Clin Cancer Res* 9, 6447-6452 (2003)

171. S. Shirahama, F. Furukawa, H. Wakita, et al.: E- and P-cadherin expression in tumor tissues and soluble E-cadherin levels in sera of patients with skin cancer. *J Dermatol Sci* 13, 30-36 (1996)

172. A. Sewpaul, J.J. French, T.K. Khoo, et al.: Soluble E-Cadherin: An Early Marker of Severity in Acute Pancreatitis. *HPB Surg* 2009, 6 (2009)

173. H. Jiang, G. Guan, R. Zhang, et al.: Identification of urinary soluble E-cadherin as a novel biomarker for diabetic nephropathy. *Diabetes/Metabolism Research and Reviews* 25, 232-241 (2009)

174. A. Soyama, S. Eguchi, M. Takatsuki, et al.: Significance of the serum level of soluble E-cadherin in patients with HCC. *Hepatogastroenterology* 55, 1390-1393 (2008)

175. H. Streeck, D.S. Kwon, A. Pyo, et al.: Epithelial adhesion molecules can inhibit HIV-1-specific CD8+ T-cell functions. *Blood* 117, 5112-5122 (2011)

176. F. Ryniers, C. Stove, M. Goethals, et al.: Plasmin Produces an E-Cadherin Fragment That Stimulates Cancer Cell Invasion. *Biol Chem* 383, 159-165 (2002)

177. B. Nawrocki-Raby, C. Gilles, M. Polette, et al.: Upregulation of MMPs by soluble E-cadherin in human lung tumor cells. *Int J Cancer* 105, 790-795 (2003)

178. L.J. Inge, S.P. Barwe, J. D'Ambrosio, et al.: Soluble E-cadherin promotes cell survival by activating epidermal growth factor receptor. *Exp Cell Res* 317, 838-848 (2011)

179. T. Maretzky, K. Reiss, A. Ludwig, et al.: ADAM10 mediates E-cadherin shedding and regulates epithelial cell-cell adhesion, migration, and beta-catenin translocation. *Proc Natl Acad Sci U S A* 102, 9182-9187 (2005)

180. S. Hayward, R. Dahiya, G. Cunha, et al.: Establishment and characterization of an immortalized but non-transformed human prostate epithelial cell line: BPH-1. *In Vitro Cell Dev Biol Anim* 31, 14-24 (1995)

181. M. Shoyab, G.D. Plowman, V.L. McDonald, et al.: Structure and function of human amphiregulin: a member of the epidermal growth factor family. *Science* 243, 1074-1076 (1989)

182. M. Rojas, S. Yao, Y.-Z. Lin: Controlling Epidermal Growth Factor (EGF)-stimulated Ras Activation in Intact Cells by a Cell-permeable Peptide Mimicking Phosphorylated EGF Receptor. *J Biol Chem* 271, 27456-27461 (1996)

183. D.R. Emlet, D.K. Moscatello, L.B. Ludlow, et al.: Subsets of Epidermal Growth Factor Receptors during Activation and Endocytosis. *J Biol Chem* 272, 4079-4086 (1997)

184. J.P. Thiery: Epithelial-mesenchymal transitions in tumour progression. *Nat Rev Cancer* 2, 442-454 (2002)

185. E. Slabáková, Z. Pernicová, E. Slavíčková, et al.: TGF-β1-induced EMT of non-transformed prostate hyperplasia cells is characterized by early induction of SNAI2/Slug. *Prostate* 71, 1332-1343 (2011)

186. J.P. Thiery, H. Acloque, R.Y.J. Huang, et al.: Epithelial-Mesenchymal Transitions in Development and Disease. *Cell* 139, 871-890 (2009)

187. X. Wu, J. Wu, J. Huang, et al.: Generation of a prostate epithelial cell-specific Cre transgenic mouse model for tissue-specific gene ablation. *Mech Dev* 101, 61-69 (2001)

188. Y. Wang, M.P. Revelo, D. Sudilovsky, et al.: Development and characterization of efficient xenograft models for benign and malignant human prostate tissue. *Prostate* 64, 149-159 (2005)

189. V. Jeet, P. Russell, A. Khatri: Modeling prostate cancer: a perspective on transgenic mouse models. *Cancer Metastasis Rev* 29, 123-142